Norwegian Meteorological Institute

METreport

No. 3/2024
ISSN 2387-4201
Meteorology

Storms in Sulafjord

Wind, waves and currents

Hálfdán Ágústsson, Birgitte Rugaard Furevik, Jon Albretsen

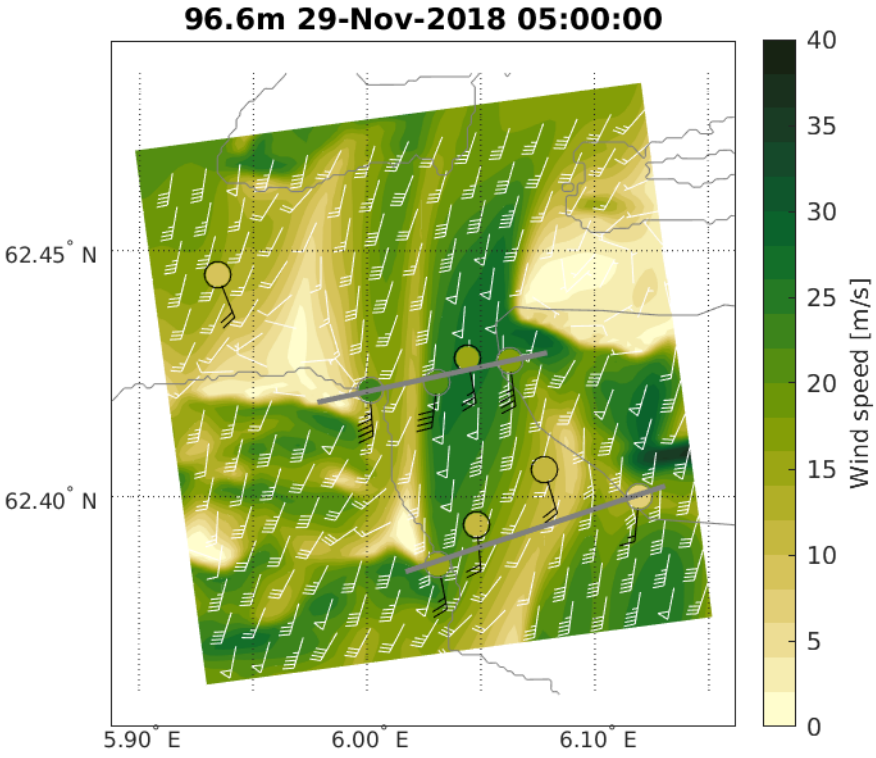

Measured and modelled wind during a southerly storm in Sulafjord, Møre og Romsdal

Norwegian Meteorological Institute

METreport

Title	Date
Storms in Sulafjord - wind, waves and currents	February 15, 2024
Section	**Report no.**
Oceanography and marine meteorology	3/2024
Author(s)	**Classification**
Hálfdán Ágústsson, Birgitte Rugaard Furevik, Jon Albretsen	● Free ○ Restricted
Client(s)	**Client's reference**
Jørn Arve Hasselø, National Public Roads Administration	

Abstract

This report presents an overview of wind, wave and current conditions during storm events in Sulafjorden, Norway. The analysis is based on long series of mesoscale model data, results from a CFD-model, a spectral wave model and a 3D ocean model as well as from a dedicated measurement campaign in Sulafjorden. The measurement campaign includes measurements from buoys, tall masts, scanning and vertical lidars.

Keywords

Observations, numerical models, storms, wind, waves, currents, lidar, WRF, SWAN, ROMS, Simra, coast, Ferje-fri E39

Disciplinary signature	Responsible signature
Øyvind Breivik	Øyvind Breivik

Contents

Nomenclature

CFD Computational fluid dynamics (very fine scale modeling of flow)

HARMONIE-AROME The operational forecasting model at MET Norway

MCP Measure-correlate-predict approach for correlation of time series data

NPRA National Public Roads Administration

ROMS Regional Ocean Modeling System (3D ocean model)

RWS Radial wind speed (wind component along the lidar beam)

SIMRA Computational fluid dynamics (CFD) model developed at SINTEF, Norway

SWAN Simulating WAves Nearshore (numerical phase-averaging wave model)

WRF Weather Research and Forecasting model (mesoscale atmospheric model at Kjeller Vindteknikk)

1 Introduction

Sulafjorden is a 3 – 5 km wide fjord in Møre and Romsdal fylke, between the islands Hareidlandet and Sula. The fjord is about 400 m deep and the islands rise to approximately 600 m. The fjord continues past the island Godøy into Breisundet, as a 200 m deep channel that stretches out into the shelf.

Sulafjorden is one of the fjords where an existing ferry connection is planned to be replaced by a fixed road connection on the road E39 between Kristiansand and Trondheim. Since 2016, the National Public Roads Administration (NPRA) has run a large measurement campaign in the fjord, which is supplemented by numerical model simulations covering atmospheric, oceanic and wave parameters. The long measurement program combined with numerical simulations provides environmental input for the design of the planned fjord crossing.

As a supplement to the standard analyses for design, it was decided to investigate the temporal and spatial development of a number of storms and other relevant situations in the measurement period by the use of atmospheric and CFD model simulations and measurements. The aim of the study was to:

1. to increase the understanding of the local wind phenomena in the fjord, their strength and distribution and how well these are captured by the numerical models. This may also identify relevant phenomena not captured by the measurements in the masts.

2. to map the horizontal and vertical extent of the region of the strongest winds to be able to extrapolate the observations from the masts along the planned crossing and upwards along the bridge towers.

3. to decide if the dataset includes the most severe type of storms in terms of strong winds at the planned fjord crossing

4. to provide a spatial overview of both wind, waves and currents during the storms.

2 Data

2.1 Atmospheric model WRF

The Weather Research and Forecasting (WRF[1]) numerical weather prediction model is run by Kjeller Vindteknikk (KVT)/Norconsult to downscale the global atmospheric re-analysis from the ECMWF down to 500 m grid spacing for areas including the location of the planned bridges in Sulafjorden, Julsundet and Halsafjorden (Harstveit [2018], Christakos et al. [2020]). The WRF-model is a state-of-the-art numerical weather prediction model, widely used for mesoscale and fine scale modelling and operational forecasting of weather. The hindcast dataset produced in the current project currently includes 15 years of simulated wind data. It starts on 1 January 2007 and is continuously updated, with a delay of a few months from the current date. It is forced by atmospheric re-analysis from the ECMWF[2]; the ERA-interim until August 2019, and ERA5 thereafter. A more detailed description of the setup of the model and the dataset are found in Harstveit [2018]. The model domain topography for the innermost domain with 500 m x 500 m horizontal resolution is shown in Fig. 2.

2.2 CFD model Simra

Simra is a computational fluid dynamics (CFD) model developed at SINTEF. The model is set up in a nested system where it receives vertical profiles of wind, temperature and pressure from the mesoscale forecasting model AROME-MEPS (2500 m x 2500 m grid spacing) at the Norwegian Meteorological Institute (MET). Simra has a horizontal resolution of 100 m x 100 m and 51 vertical layers up to 3500 m. The model domain (261 x 261 points) covers Sulafjorden with the topography shown in Fig. 3. The setup for Sulafjorden has been described and validated in Midtbø et al. [2020a].

2.3 Ocean wave and current models

Waves have been simulated using the spectral wave model SWAN at the Norwegian Meteorological Institute (MET Norway) dynamically nested into the hindcast NORA10 but with wind forcing from the WRF simulations. Wave conditions in Sulafjord are discussed in Furevik and Aarnes [2021] and Christakos et al. [2020]. The data set used has a reso-

[1] https://www.mmm.ucar.edu/models/wrf

[2] https://www.ecmwf.int/

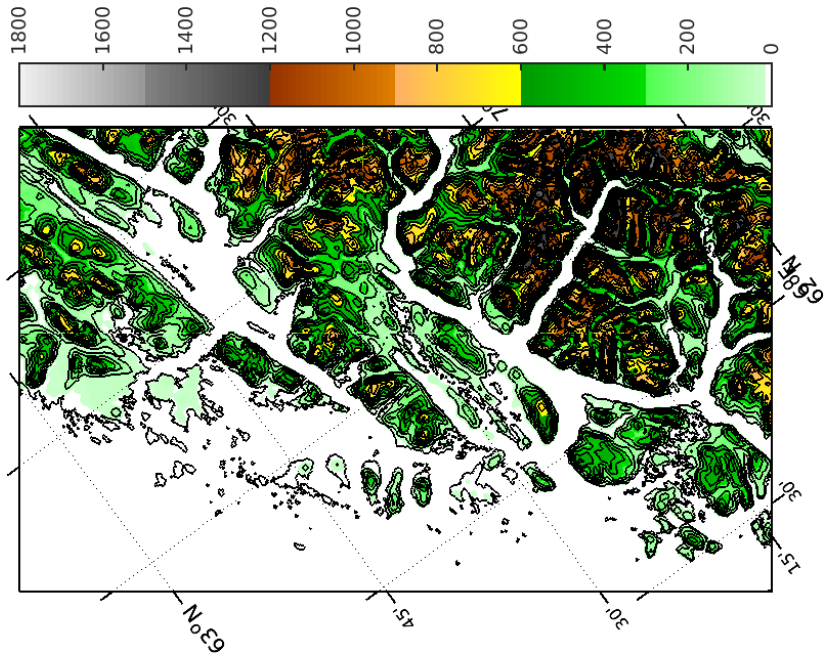

Figure 2: *The innermost domain and model topography for the WRF simulation for Sulafjorden.*

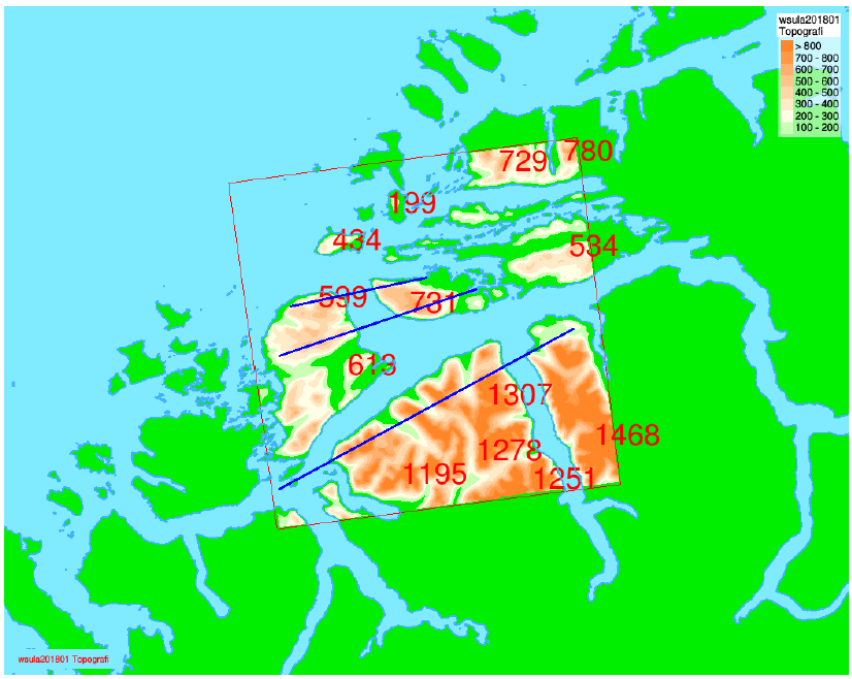

Figure 3: *Map of the Simra model domain and topography Sulafjorden. Maximum terrain elevations are shown in red (metres). Figure reproduced from Midtbø et al. [2020a].*

lution of 250 m x 250 m and covers the period January 2007 to February 2020. In these studies, the wave model SWAN was shown to underestimate the waves at buoy D, model the wave height at A and B relatively well, and overestimate at the inner fjord locations.

It should be noted that SWAN is a phase-averaging wave model and does not include wave diffraction which most certainly occurs in several locations (e.g. at Godøy and Kvitneset) as waves enters from the open sea.

Currents have been modelled using the Regional Ocean Modeling System (ROMS) model[3] at the Norwegian Institute for Marine Research (IMR). Details on the model setup for SWAN and ROMS can be found in Furevik and Aarnes [2021], Harstveit [2018], Ágústsson et al. [2020a] and Ágústsson et al. [2020b].

Results and validation analysis of the nested ocean model system with a coastal model covering the entire Norwegian coast (NorKyst800) and a high resolution (160 m x 160 m) fjord model covering the Møre coast are well explained in several reports (Ágústsson et al. [2019], Ágústsson et al. [2020a], Ágústsson et al. [2020b]).

2.4 Wind and wave hindcast archives NORA10 and NORA3

The NORA3 atmospheric hindcast (Haakenstad et al. [2021]) is produced by MET Norway with the non-hydrostatic HARMONIE-AROME model (Bengtsson et al. [2017]) for a domain of the Nordic Seas and Scandinavia with 3 km horizontal resolution and 65 vertical levels. The model runs consist of 9 hourly forecasts four times a day. Each forecast starts from an assimilated state of the last forecast adapted to surface observations. Model levels are forced with ERA-5 [4]. The last 6 hours of each forecast are used to create the hindcast. The winds force the wave model WAM to provide wave hindcast and boundary conditions (wave spectra) for wave down scaling. Data (1970 - 2023) are available online[5].

NORA3 takes over for the previous hindcast NORA10 (Reistad et al. [2011]) which has a coarser resolution (10 km) and was produced by the hydrostatic atmosphere model HIRLAM. NORA10 data (1959 - 2023) are only available on request.

2.5 Measurements

[3] https://www.myroms.org/

[4] https://climate.copernicus.eu/climate-reanalysis

[5] https://thredds.met.no/thredds/projects/nora3_subsets.html

Land-based meteorological measurements are carried out by Kjeller Vindteknikk in tall masts and with lidars, as previously documented in Haslerud [2021] and Ágústsson [2021]. These include measurements of the 3-dimensional wind at several levels in the masts, with a vertical pointing lidar at the top of the Kvitneset mast and four scanning lidars located in the northern part of Sulafjorden (a summary of available data is given in Furevik et al. [2020]). The dataset used here includes observations of the 10-minute mean wind speed and direction, as well as turbulence intensity. First mast data was available in December 2016 at Kvitneset while first lidar derived wind data at the centre of Sulafjorden was available in November 2018. Mast and lidar locations can be seen in Figs. 4 and 5.

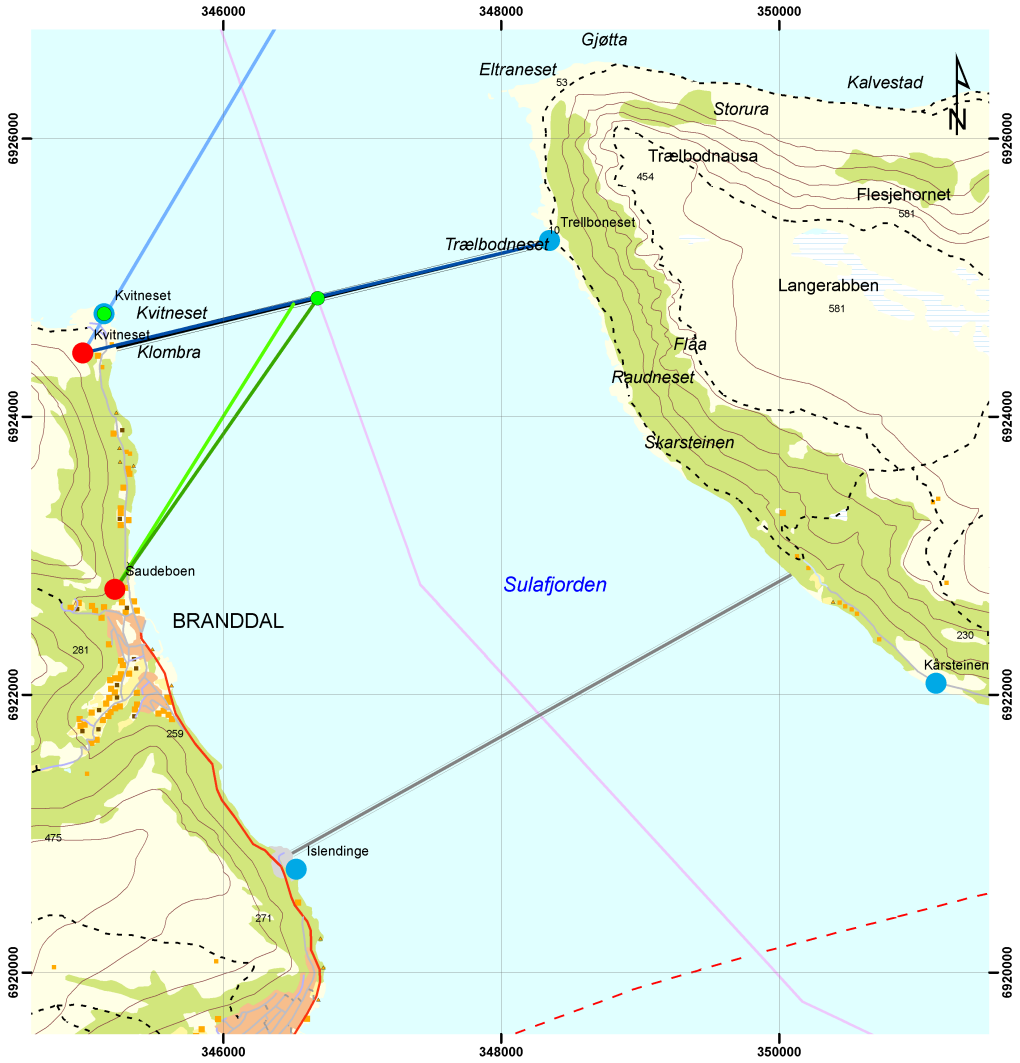

Figure 4: *Map of Sulafjorden indicating the location of masts (blue circles), vertical lidars (green circles) and scanning lidars (red circles). Black lines show approximate locations of possible locations.*

Buoy	Area	Measurement period	Position	Depth
A	Sulafjorden	2016.10.13 -	62.4263 6.0447	375
B	Sulafjorden	2016.10.13 -	62.4038 6.0806	325
B1	Sulafjorden	2019.02.08 - 2021.04.10	62.4051 6.0585	445
C	Sulafjorden	2017.04.27 -	62.3922 6.0509	445
C1	Sulafjorden	2019.02.14 - 2021.04.10	62.3964 6.0459	445
D	Breisundet	2016.10.14 -	62.4464 5.9336	345
F	Vartdalsfjorden	2017.11.29 -	62.2208 5.8994	217
G	Halsafjorden	2016.10.18 - 2020.04.22	63.0856 8.1575	495
G1	Halsafjorden	2017.04.05 - 2018.09.05	63.0872 8.1426	133
G2	Halsafjorden	2017.04.05 - 2018.09.05	63.0898 8.1656	146

Table 1: *Buoy name, area, day of deployment and last day of measurements (- if ongoing), position and depth.*

Wind and wave measurements are carried out by Fugro Oceanor (FOAS) using SEA-WATCH Wavescan buoys. The data are transferred to MET and made available through the MET Norway Thredds Service (DOI: 10.21343/ef2d-jp97). Integrated wave parameters, wind speed and direction (4.1 m height) is available every 10 minutes. Raw wave data are provided in separate files and are used to calculate wave spectra. An overview of the buoys is given in Table 1 and in Fig. 5.

In addition to the observations listed above, regular meteorological weather recordings are taken several places in the area. For wind, we have Vigra airport with a long record started in 1958 which is of particular interest. Ona Lighthouse is situated quite some distance away to the north and only serves as a synoptic reference. The nearby Ørsta-Volda Lufthamn has wind recordings from 2002, but measurements her may have a limited value for Sulafjorden due to the complex local topography.

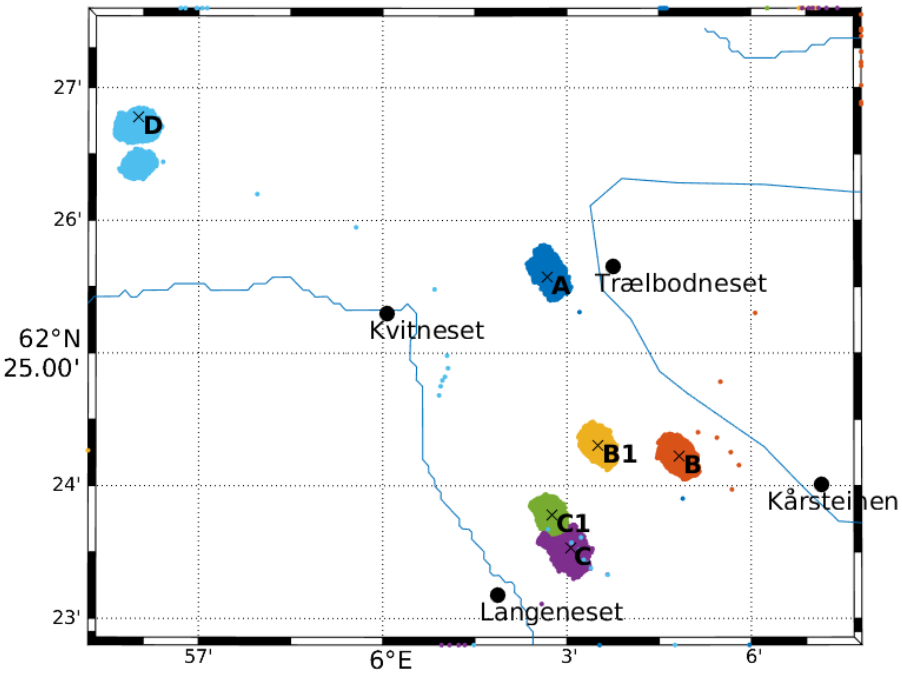

Figure 5: *Map of Sulafjord with location of the buoys marked with x and the recorded position of the buoys 2016-2020 marked with color. Land-based masts are marked with black dots.*

3 Storms

This section provides an overview of selected storms which we believe represent a broad spectrum of strong wind conditions in Sulafjorden. The selection is based on the strongest wind events observed in the measurement campaign, as well as subset of relevant extreme events which have occurred in the region (Table 3).

In order to put storm situations in Sulafjorden into context with the larger scale flow, the section first presents: 1) a model climatology of strong winds, and 2) a discussion on mesoscale effects on flow in mountainous terrain in this part of Norway.

3.1 Model climatology of storms

Due to the short period of available observations and high-resolution model data, we prepare a synthetic model climatology using coarser scale model data and a subset of the observations. Model wind for the period 1970 – 2023 is taken from the NORA3 hindcast at 750 m asl and from the nearest grid point to the centre of the northern crossing (N62.41045, E6.02443). This dataset represents well the synoptic scale flow as well as the large scale topographic effects along the coast. Observations are based on the lidar measurements at the centre of the fjord, as the mast observations are more strongly affected by the nearby terrain. The lidar measurements are valid at 70 m asl and the location is shown in Fig. 4 as a green dot. The lidar series is constructed by combining radial wind data from the lidars at Kvitneset and Saudebøen (cf. Ágústsson [2021]). Using a simple measure-correlate-predict (MCP) approach, a synthetic time series with a length of 50 years in the lidar measurement point is constructed. Based on the hindcast, observed series as well as the synthetic dataset, we analyse the directional distribution of the strongest winds at the centre of the fjord. Noting the limitations of the synthetic dataset, we can provide a first estimate on storm climatology at low-levels in Sulafjorden and its relation to the large-scale flow at mountain top level.

Concurrent data from the hindcast at 750 m and the observed data at 70 m are divided into the following directional sectors using the NORA3 direction at 750 m; north: $300^\circ - 30^\circ$, east: $30^\circ - 120^\circ$, south: $120^\circ - 210^\circ$, west: $210^\circ - 300^\circ$, which are selected based on the fjord orientation. Simultaneous data from the two time series show low correlation and low winds for the easterly sector, while winds from southerly, westerly and northerly directions have a correlation of around 0.8 to the fjord wind (Fig. 6). The distributions

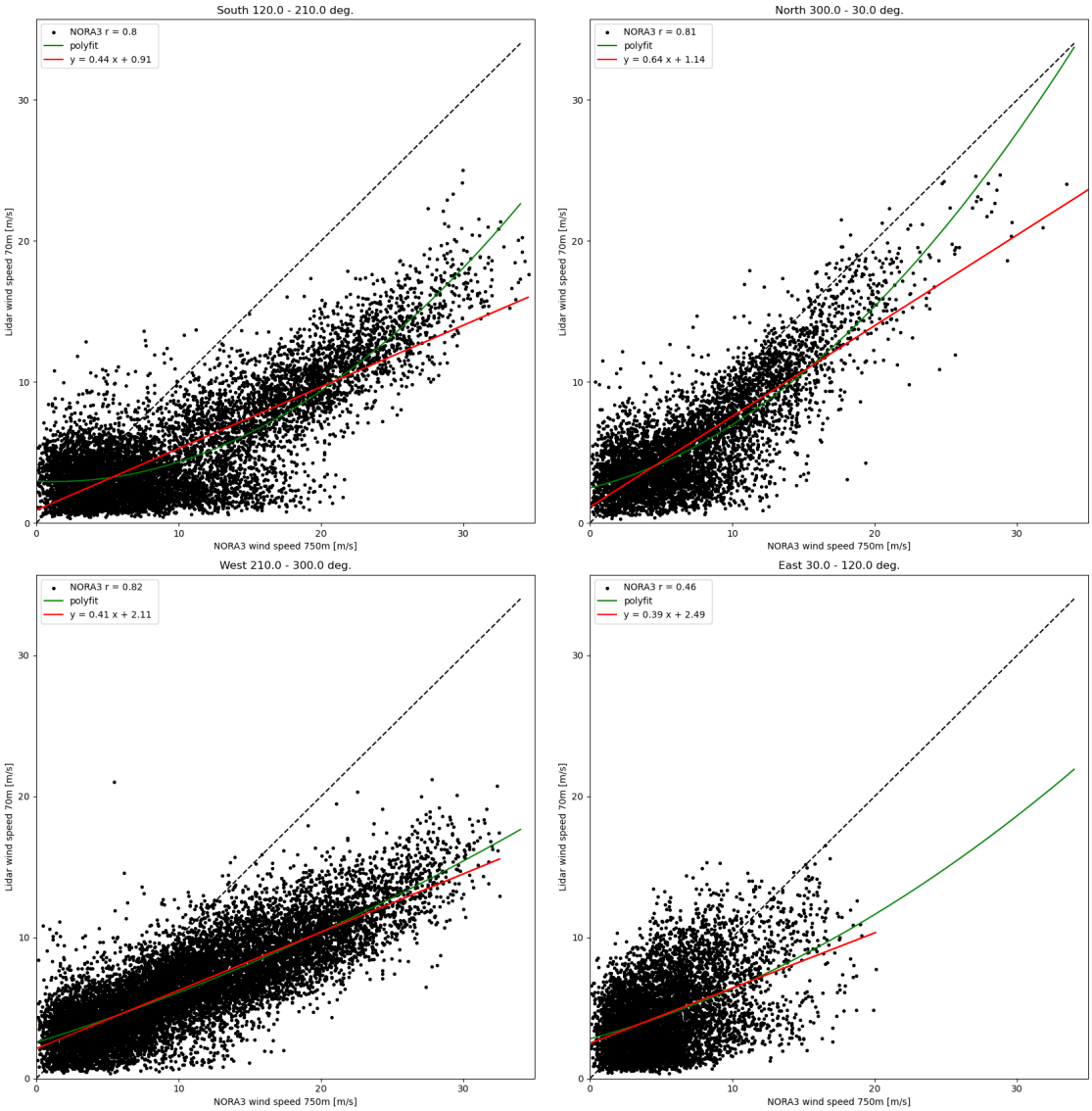

Figure 6: *Scatter plot and correlation of wind speed in 750 m from the hindcast data set NORA3 and lidar measurements at centre of the fjord for four directional sectors based on wind direction in NORA3. The red line is a linear regression line while the green line is a polynomial fit.*

presented in Fig. 6 highlight the the topographic forcing on the low-level flow and that it varies with the direction of the background flow. While weak or easterly low-level flow is presumably often detached from the flow aloft, strong wind at fjord level is well correlated with strong flow aloft. Wind speeds at fjord level are on average 41 % and 44 %, respectively, of the wind speed aloft for southerly and westerly flow. The reduction is on average weaker for northerly flow. The wind shear is often weak during strong

northerly flow, i.e. only northerly storms come close to having a similar wind speed aloft and at low levels.

The above discussion indicates that for the relevant wind directions and for strong winds, the MCP can be employed in the context of the current analysis. Naturally, the majority of the observed data are obtained during low wind speed and the linear regression (red line) is affected by the higher density of these data. In order to account better for high winds, a polynomial fit (green line) is used for making the synthetic time series. The synthetic time series reproduces reasonably well the observed series, with relatively few cases of higher wind than measured.

From the synthetic 50-year wind-series at the centre of the fjord, all storm events with a maximum wind speed exceeding 25 m/s are selected and sorted with regard to wind speed (Table 2). In particular, the strongest storm in the NORA3 dataset on a synoptic scale is the hurricane on 1 January 1992 (46 m/s at 750 m above sea level), but this storm is ranked only second last of the 28 storms in the synthetic wind data at 70 m at the fjord centre. The hurricane had a westerly and southwesterly direction when it was at the strongest in the region, but these directions are however not present in the synthetic dataset at 70 m. Using only data concurrent with synthetic winds stronger than 25 m/s at 70 m, the wind rose at 750 m (NORA3, panel a in Fig. 7) shows that all of these are either south-southwesterly (SSW) or northwesterly (NW) aloft, with the strongest being from SSW. SSW storms at low levels appear to be on average 40 % weaker than the wind aloft while NW winds are reduced much less (panel b in Fig. 7. In other words, the synthetic climatology indicates that storms in Sulafjorden only occur during NW and SSW large-scale flow, that the SSW storms are more reduced in the fjord than NW storms and that the fjord may be sheltered during strong westerly flow aloft.

Year	Month	Max wind speed [m/s]
1989	2	37.9
2022	1	36.3
1975	12	34.1
2016	12	33.5
1985	11	30.2
2015	12	30.1
1994	1	28.9
2000	1	28.9
1988	3	28.5
1995	1	28.4
1991	4	28.3
1987	10	27.8
2008	11	27.3
2004	2	27.2
2019	1	27.2
1997	2	26.2
2018	1	26.1
1997	3	25.6
1981	1	25.5
1977	1	25.4
2016	1	25.3
1976	2	25.2
1973	3	25.2
1972	12	25.1
1993	1	25.0
2016	2	25.0
1992	1	25.0
2013	12	25.0

Table 2: *Rank of storms with wind speed larger than 25 m/s in the synthetic generated time series based on NORA3 at 750 m and lidar data from 70 m asl at the centre of the northerly crossing of Sulafjorden.*

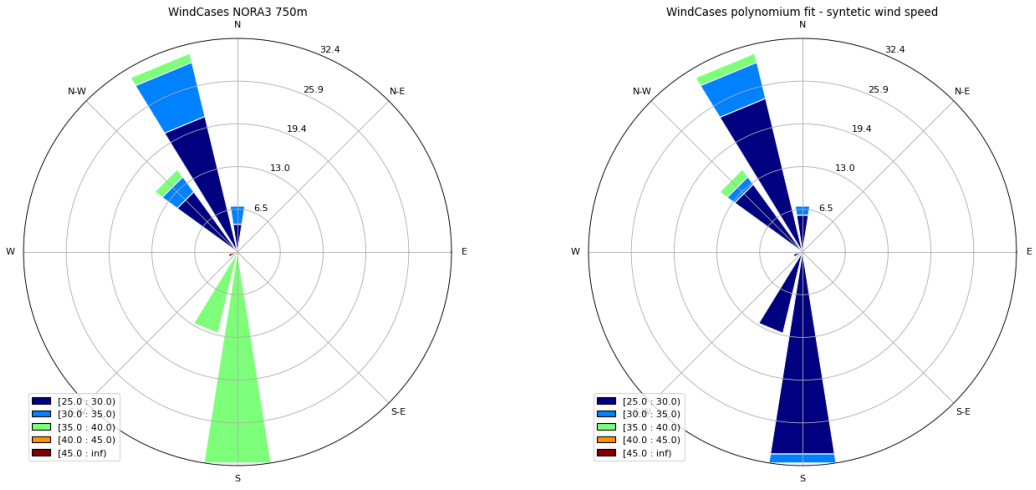

a) b)

Figure 7: *(a) Wind rose for NORA3 at 750 m height, and (b) for the synthetic series at 70 m, for concurrent data when the wind speed at 70 m exceeds 25 m/s.*

3.2 Mesoscale aspects of large-scale flow in mountainous terrain

Before we go on with the individual storms, we provide an overview of the large-scale mountains' effect on the large-scale flow in the region. Sulafjorden is located on the coastline at the northwest part of the large-scale mountains of southern Norway and the terrain has the potential to, at least in part, modulate the flow in this area. Barstad and Grønås [2005] and Barstad and Grønås [2006] describe how the large scale flow may respond to the mountains in this region as the flow turns from south to west. In relation to the task at hand we note that:

- When the large-scale background flow is southerly, and even easterly, the descending air in the lee of the large-scale mountains will generate a low-pressure anomaly in the area. This will in turn draw air out the terrain gaps and fjords and may lead to locally enhanced flow at low level.

- When the large-scale background flow turns from south towards west, the low-pressure anomaly will gradually be removed (less descending air) and the large-scale flow will respond to the coastal mountains with a barrier-like flow, e.g. Overland and Bond [1995]. A low-level jet may occur (e.g. Christakos et al. [2014]). This flow situation seems to be the most frequent among the cases studied here.

- When the large-scale background flow has a strict northerly component, the large-scale mountains may block the flow and subsequent lifting of air will create a high-pressure anomaly which in turn tends to decelerate the flow.

In this area of the North Atlantic, the low pressure systems are often in a mature phase of their development cycle. In such a late phase, the warm air can be wrapped around and be found on the north side of cool air. Among the forecasters, it is known as a "poisonous tail" or a back-bent occluded front which often is associated with a strong wind zone on the south-southwest side of the low pressure core, see Grønås [1995]. The winds have typically a westerly component. If the low pressure has a back-bent occluded front when it passes our area, very strong winds can occur. If the enhancement because of the terrain adds to this, we are set up for an extreme weather situation.

To conclude, in general the strongest winds in the region are typically found for winds with a strong westerly large-scale component. If the low-pressure is late in its development cycle where warm air is cut-off and cool polar air is wrapped around to the south, extreme winds can occur.

The collection of storms which are investigated later in this section have been analyzed with regard to the mesoscale effects on the large-scale flow situations and how they relate to the local wind conditions in Sulafjorden during these events.

Date/hour	Wind spd	Dir.	Observations	Models	Comments	Rank (large-scale)
22 Dec 1988 15	-	S-SW	-	-	Hurricane	3
01 Jan 1992 09	-	SW	-	WRF	*New year storm*, Hurricane	1
25 Dec 2011 21	-	SW	-	WRF	Extreme weather *Dagmar*	2
12 Dec 2013 18	-	S	-	WRF	Extreme weather *Ivar*. Strongest further north	7
14 Mar 2017 21	-	SW-NW	M	WRF	Strong vertical wind	10
29 Nov 2018 05	21 m/s	S	ScL, M, B	WRF, Simra		6
01 Jan 2019 04	27 m/s	NW-N	ScL, M, B	WRF, Simra	Strongest NW storm in obs. period	11
14 Jan 2019 06	23 m/s	NW-N	ScL, M, B	WRF, Simra		12
10 Dec 2019 18	25 m/s	S	M, B, kL	WRF		5
02 Jan 2020 09	21 m/s	S	ScL, M, B, kL	WRF, Simra	Strongest at Trælbodneset	9
07 Jan 2020 17	26 m/s	S	ScL, M, bL, B, kL	WRF, Simra		8
11 Jan 2020 01	27 m/s	S	M, bL, B	WRF, Simra	Strongest S storm	4
12 Apr 2020 18	22 m/s	NW-N	ScL, M, B, kL	WRF		15
22 Sep 2020 20 - 23 Sep 06	26 m/s	S	bL, kL	WRF, Simra	Strong shear and storm aloft	14
19 Nov 2020 09	26 m/s	NW	ScL, M, bL, B, kL	WRF, Simra	Sudden increase in wind speed	13

Table 3: *The strongest storms observed in Sulafjorden 2017 - 2020 and four historical storms listed with the approximate date, time and value of maximum 10-minute wind speed observation, the overall wind direction, available observations (M=Masts, B=buoys, ScL=Scanning Lidar, kL=vertical Lidar on Kvitneset, bL=vertical Lidar on buoy) and models (WRF 500 m and Simra 100 m). The ranking is relative to the storms in the table and based on numerical model data from the NORA3 dataset (Haakenstad et al. [2021]).*

3.3 The storm of 22 December 1988

3.3.1 General overview

A strong westerly storm hit the west coast of Norway on 22 and 23 of December 1988. It was associated with a very deep, relatively small scale and fast moving low pressure system coming in from the west. The two synoptic weather stations Vigra and Ona recorded the strongest winds at 13 UTC the 22nd with 27.8 m/s and 34.5 m/s respectively (not shown). The wind directions were 240 degrees for both stations.

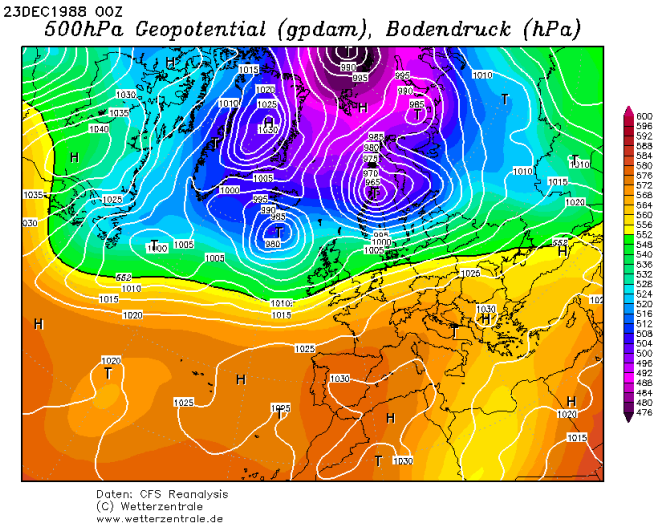

Figure 8: *The analysis from CFS (Climate Forecast System) showing surface pressure and 500 hPa geopotential. Figure is retrieved from Wetterzentale (http://wetterzentrale.de).*

The storm is not discussed further here as no observational or high-resolution model data is available for the flow in Sulafjorden. The storm could potentially be investigated using using synoptic observational data and coarser scale model datasets, but that is beyond the scope of this work.

3.4 The New Year's day storm of 1 January 1992

3.4.1 General overview

The strongest storm to hit mainland Norway occurred on New Year's day 1992, see a published study on this event in Grønås [1995].

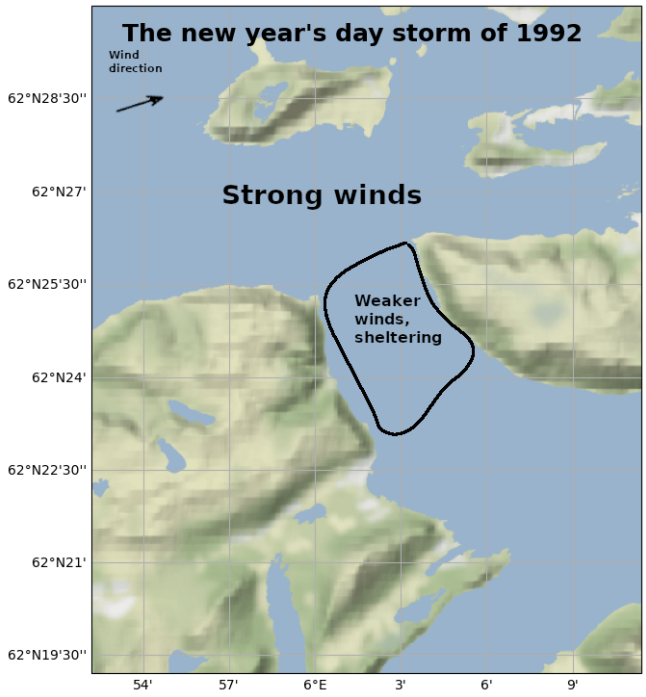

Figure 9: *A schematic summary of important aspects of the storm.*

The synoptic picture was associated with a deep and fast moving low pressure system coming in towards the area from the west. It had a relatively small scale, see Fig. 10. The storm was strongest along the Møre and Romsdal coast. Mean winds was reported to 46 m/s at Svinøy and Skalmen light houses. The storm has been estimated to have a return period of 200 years and the storm caused the largest natural disaster in Norway in modern times.

No observations are available in Sulafjorden during the storm but it has however been simulated with WRF at 500 m horizontal resolution.

3.4.2 Simulated flow

The WRF simulations indicate the storm was strong and southwesterly in Sulafjorden, see an overview in Fig. 9. The simulations indicate that the 10-minute mean wind ex-

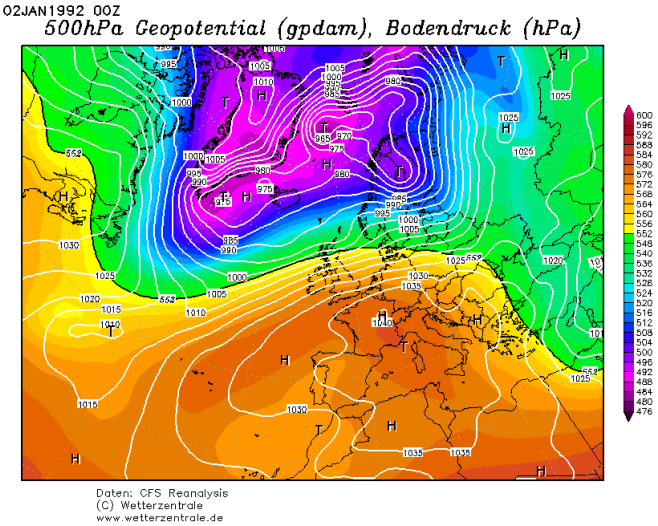

Figure 10: *The analysis from CFS (Climate Forecast System) showing surface pressure and 500 hPa geopotential. Figure is retrieved from Wetterzentale.*

ceeded 32 m/s at 75 m at the mast sites, and 40 m/s at the top of the planned towers. The simulations indicate a considerable lee-side sheltering by the upstream mountains in Sulafjorden, resulting in weaker winds at Kvitneset than Trælbodneset. The location of the size and extent of the sheltered region varies in time.

The resolution of WRF is somewhat limited in such complex terrain, and it would be valuable to have higher resolution Simra data available for the storm. However, since the availability of observations is limited in the area, it has not been prioritized in this report.

According to the model, the Hareid mountains give a strong sheltering effect for Sulafjorden. Trælbodneset however, seems to be excluded from the sheltering effect and has very strong winds in the model, Fig. 11. A small shift in the background wind direction has the potential of casting the wind shadow onto a different places and to expose others.

It is also worth noticing that such steep hills which are found in the lee of the Hareid mountains can potentially create strong and violent rotors. Studies from the Owens Valley, California, USA (see literature on the T-Rex campaign, e.g. Doyle et al. [2009]) show that gravity waves over mountains can generate a reversed pressure gradient on the lee side which in turn produces a return airflow near the ground. Such violent rotors are known to cause aviation hazards. In T-Rex, it was proven hard to accurately model such rotors and we should not expect these features to be resolved on a general basis in mesoscale models. Figs. 12 and 13 show the shadowing effect of the Hareid mountains, with a large horizontal variability and vertical shear. As expected, we have no details in Sulafjorden.

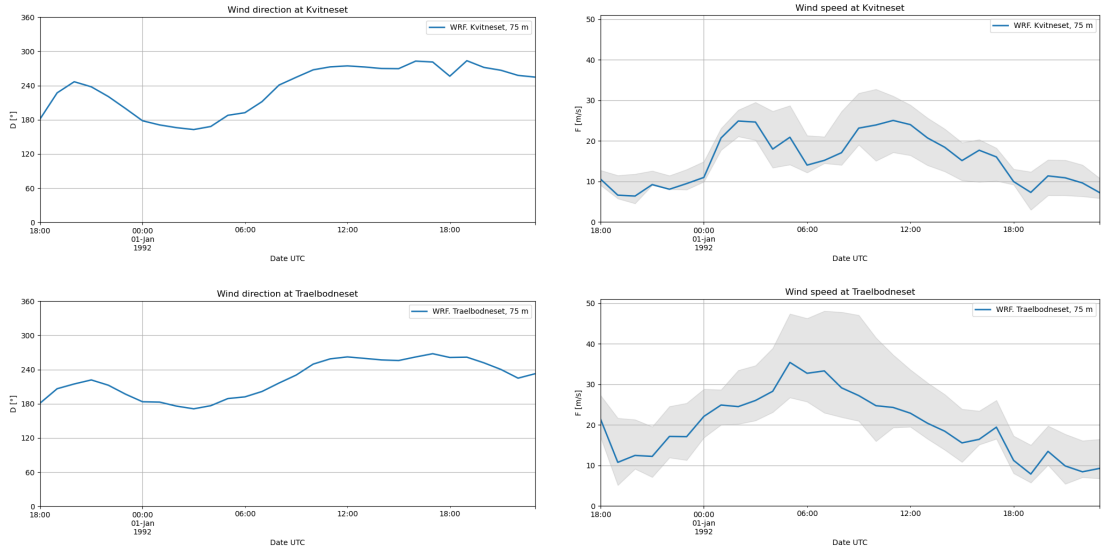

Figure 11: *Simulated (solid lines) wind direction (left) and wind speed (right) from the WRF-model. The grey envelope indicates the range of the simulated wind speed in the 9 nearest grid points (eq. 1 km x 1 km area).*

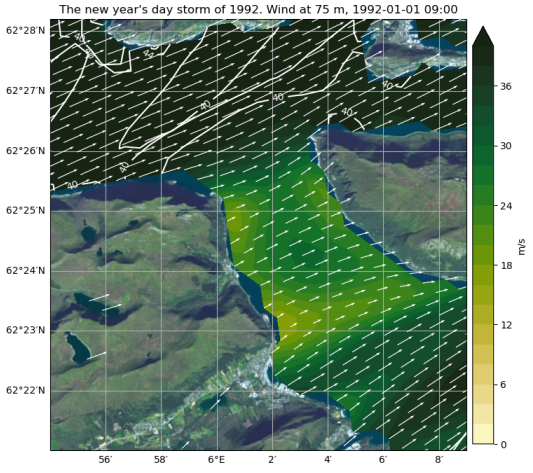

Figure 12: *Simulated wind from WRF at 75 m above sea level, valid when the storm is strongest. Contour lines with a 4 m/s division are shown for wind exceeding 40 m/s.*

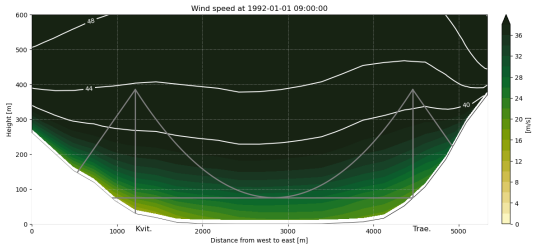

Figure 13: *Simulated wind from WRF in a section along the planned crossing. Bridge location is indicated with grey lines. Contour lines with a 4 m/s division are shown for wind exceeding 40 m/s.*

3.5 The extreme weather *Dagmar* of 26 December 2011

3.5.1 General overview

The extreme weather *Dagmar* hit the the west coast of Norway late on 25 December 2011. It was in many aspects similar to the New Year's storm of 1992 (Fig. 14), but winds speeds were weaker than in 1992. However, the storm surge and waves were higher.

As for the New Year's day storm , it was associated with a deep and fast moving low pressure system moving in from the west towards the area (Fig. 15). The storm was strongest along the coast of Sogn and Fjordane, Møre and Romsdal as well as in Trøndelag. The 10-minute westerly winds were reported to exceed 45 m/s at some exposed coastal locations.

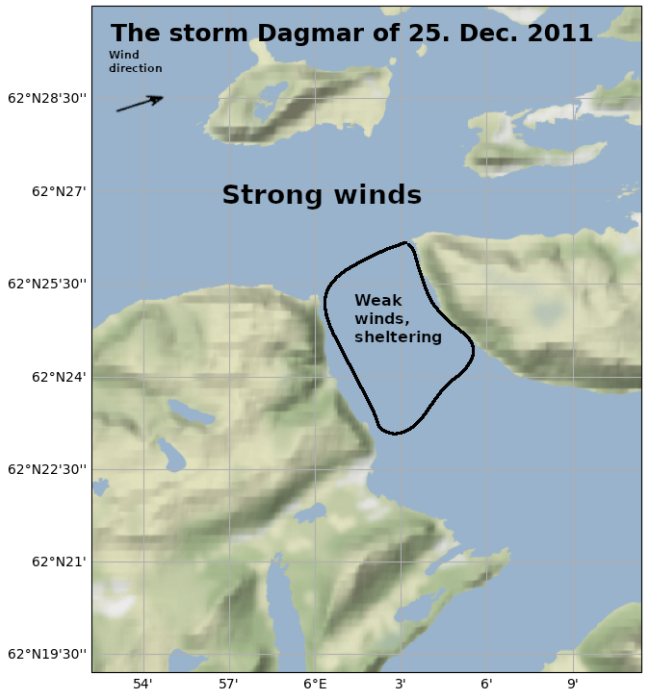

Figure 14: *A schematic summary of important aspects of the storm*

No observations are available in Sulafjorden during the storm but it has however been simulated with WRF at 500 m horizontal resolution. The WRF simulations indicate the storm was strong and southwesterly in Sulafjorden (Fig. 14).

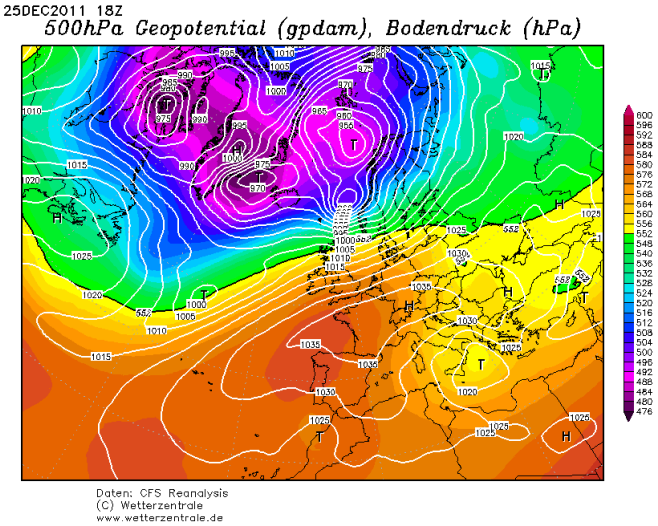

Figure 15: *The analysis from CFS (Climate Forecast System) showing surface pressure and 500 hPa geopotential. Figure is retrieved from Wetterzentale.*

3.5.2 Simulated flow

The simulations indicate that the 10-minute mean wind at the mast sites was a little over 20 m/s (Fig. 16), but with far stronger winds (+30 m/s) in the immediate vicinity (Fig. 17), including at the top of the planned bridge towers (Fig. 18). The simulations indicate a considerable lee-side sheltering by the upstream mountains in Sulafjorden, resulting in weaker winds at Kvitneset than at Trælbodneset, see Fig. 17. The location of the size and extent of the sheltered region varies in time, both in the horizontal and the vertical. We note that with the current model resolution, the mesoscale models may note resolve the low level flow well.

3.5.3 Waves

The waves during *Dagmar* reached 14 m with 18 s peak period offshore from Sulafjorden. In the fjord at location A we simulate Hs of 3.8 – 4.4 m with peak period of around 16 s (Fig. 19). During this storm, we simulate the highest waves at location A the last 20 years, i.e. higher than the New Year Storm on 1 January 1992, down-scaled from the NORA10 data [Furevik and Aarnes, 2021], even if the wind speed was higher in the 1992-hurricane. The local winds naturally play a significant role in building local waves on top of the ocean waves (swell) entering through Breisundet in both cases. But slower passage of the low and a more westerly wind direction during *Dagmar* are factors that lead to higher waves

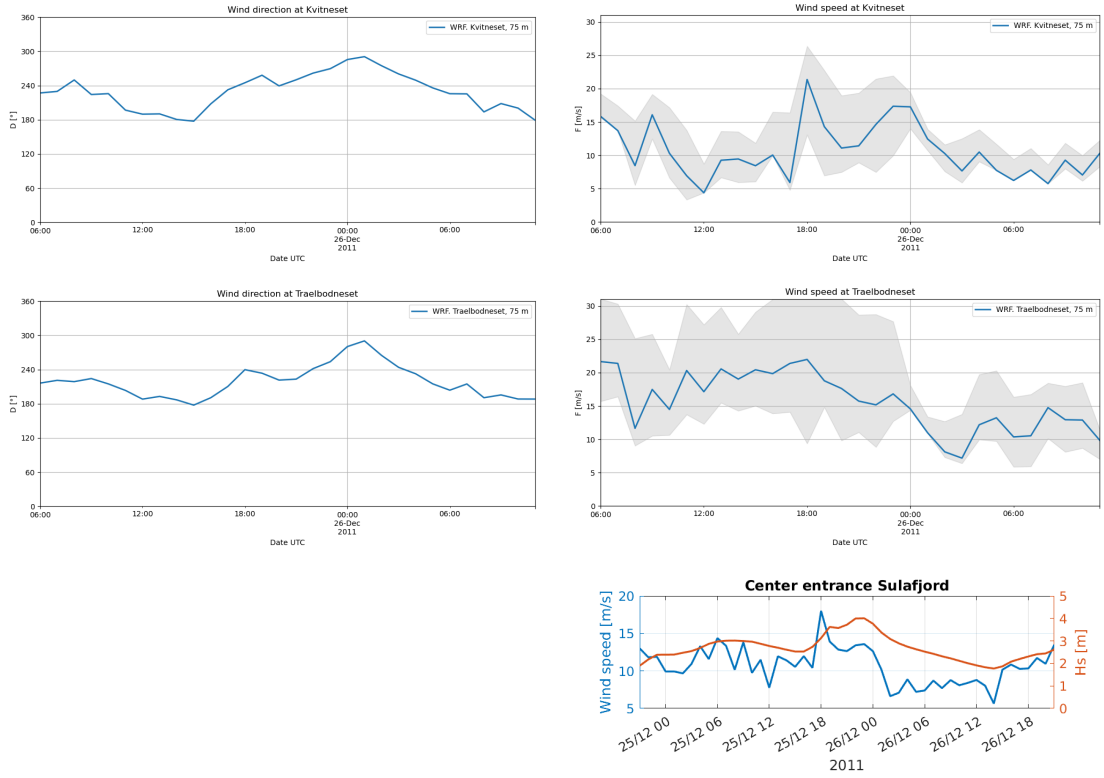

Figure 16: *Simulated (solid lines) wind direction (left) and wind speed (right) from the WRF-model. The grey envelope indicates the range of the simulated wind speed in the 9 nearest grid points (eq. 1 km x 1 km area). Lower right panel shows WRF wind speed in blue (10 m) and significant wave height (red line) at the center of the outer crossing.*

than during the new year's storm.

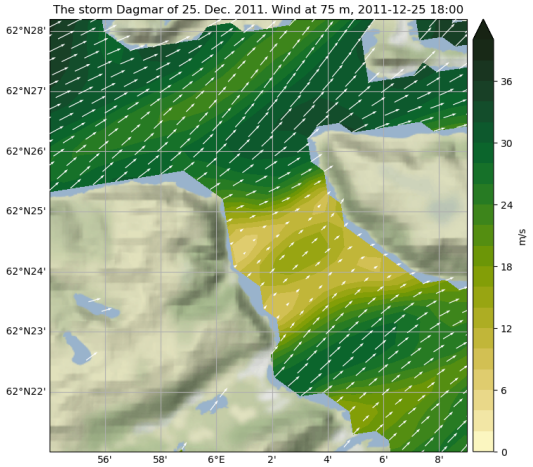

Figure 17: *Simulated wind from WRF at 75 m above sea level, valid when the storm is strongest.*

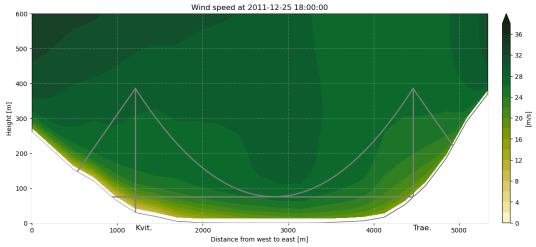

Figure 18: *Simulated wind from WRF in a section along the planned crossing. Bridge location is indicated with grey lines.*

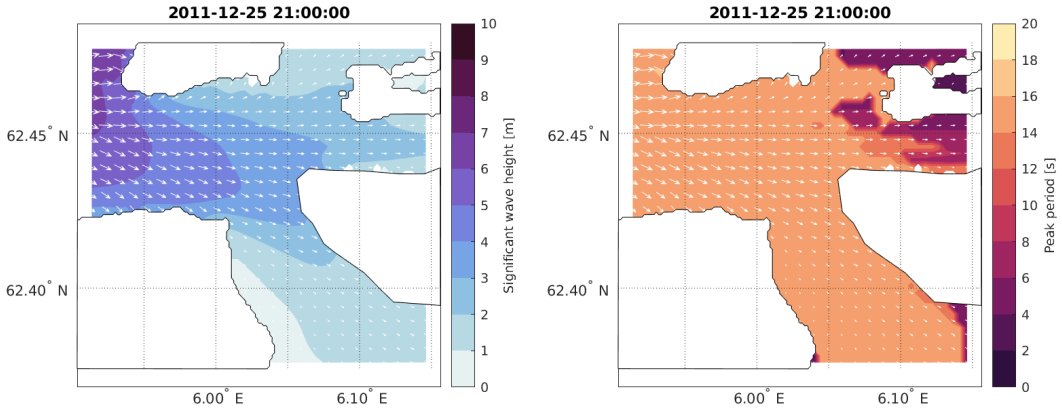

Figure 19: *Significant wave height [m] (left panel) and peak period (right panel) from SWAN and observations at the storm peak.*

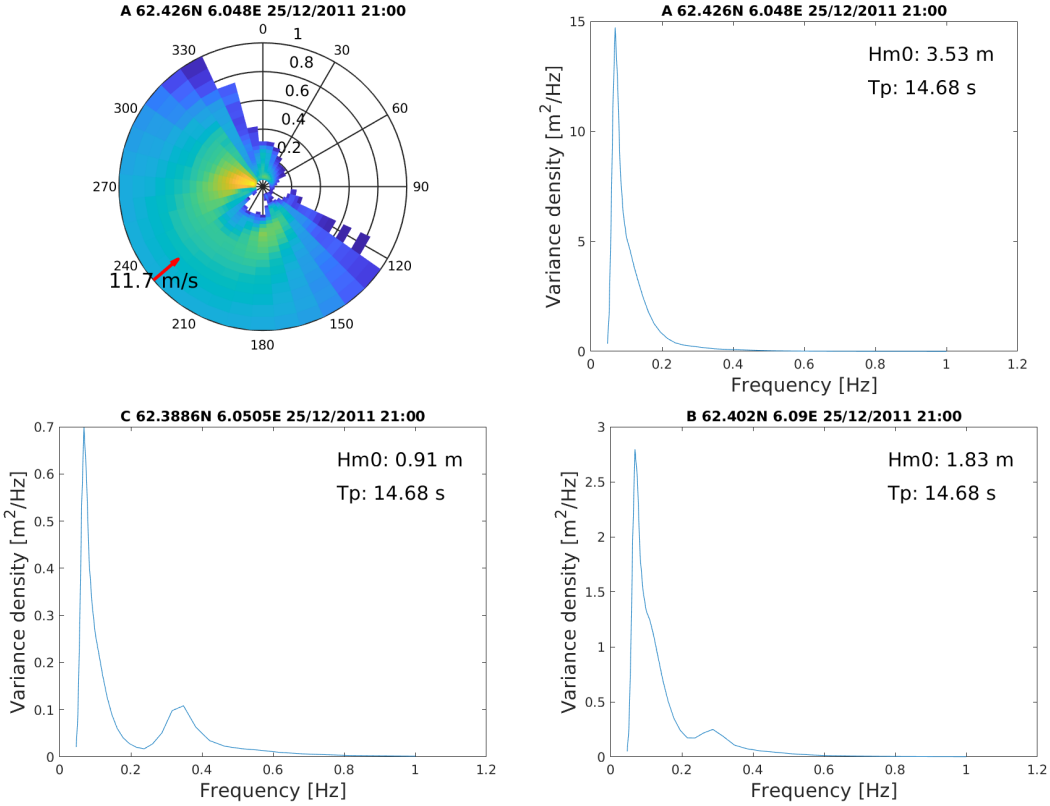

Figure 20: *2D (direction-frequency) wave spectrum from location A (top left panel) and 1D (frequency) wave spectra from locations A (top right panel), B (lower right panel) and C (lower left panel) from SWAN at the storm peak. Please note the different scale on the y-axes. Wind speed and direction (from WRF) is shown in the 2D spectrum. The energy is plotted in the direction the waves come from. Significant wave height (Hm0 or Hs) and peak period (Tp) is indicated for each location in the 1D plots.*

3.6 The extreme weather Ivar of 12 December 2013

3.6.1 General overview

On the evening of December 12 2013, a short and intense northwesterly windstorm hit Møre and Romsdal, as well as Trøndelag. The event is referred to as the extreme weather Ivar. It was associated with a rapidly deepening low which came in from the northwest (see Fig. 22). The 10-minute winds were reported to exceed 30 m/s at some locations.

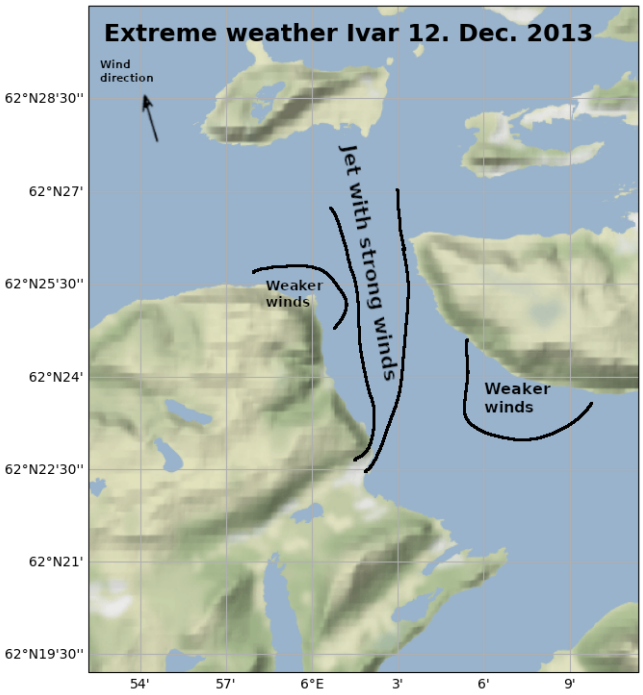

Figure 21: *A schematic summary of important aspects of the storm*

No observations are available in Sulafjorden but the event has however been simulated with the WRF-model. The simulations indicate that the storm itself did not impact Sulafjorden, as simulated winds were weak and northerly when the storm was strongest further to the north (Fig. 21). However, strong southerly winds were simulated in Sulafjorden, 12-24 hours in advance of the extreme weather Ivar.

3.6.2 Simulated flow

The simulations indicates transient jet like structures emanating from the valleys on the western flank of Sulafjorden, in particular near the village of Hareid, see Fig. 21. Furthermore, lee-side sheltering is simulated below the high mountains and upstream of the

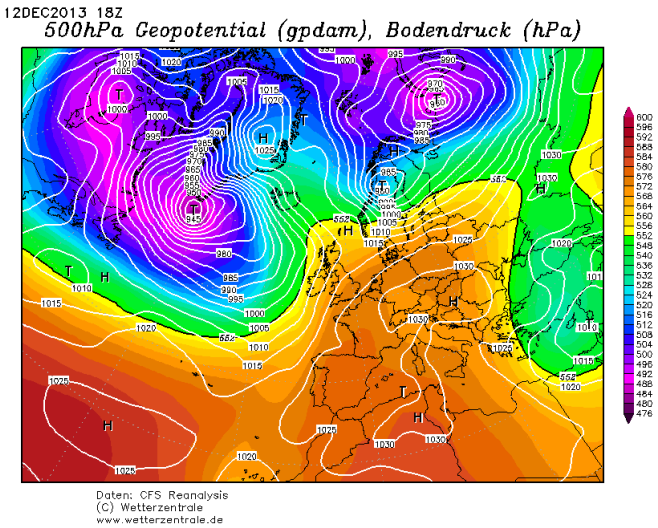

Figure 22: *The analysis from CFS (Climate Forecast System) showing surface pressure and 500 hPa geopotential. Figure is retrieved from Wetterzentale.*

mountains on the island of Sula, Fig. 24. The strongest winds were simulated at the site of the mast at Trælbodneset (32 m/s) and were from the south, well before the storm had turned to northwesterly and had its maximum at other locations in the region.

3.6.3 Waves

During this storm wave heights up to 2-3 m with a peak period of 10-12 s (Figure 25 was simulated with SWAN at location A. The wave height increases rather quickly when the wind direction turns from south over west to north (Figure 23 lower right panel) due to the much longer fetch and increased wind. The wave spectra at A and B at 18 UTC (26) has only one peak due to the incoming sea (combined wind sea and swell). After the wind turns north, Godøy causes a wind shadow and both wind speed as well as Hs in the fjord center decreases.

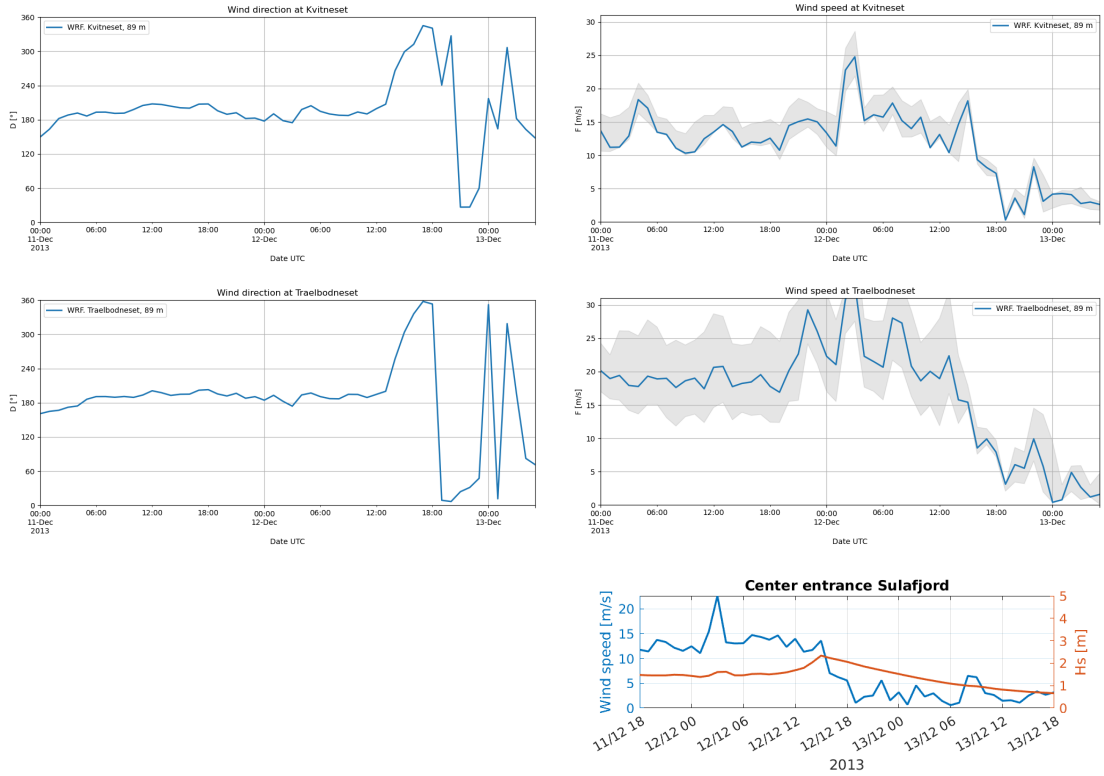

Figure 23: *Simulated (solid lines) wind direction (left) and wind speed (right) from the WRF-model. The grey envelope indicates the range of the simulated wind speed in the 9 nearest grid points (eq. 1 km x 1 km area). Lower right panel shows wind speed in blue (10 m) and significant wave height (red line) at the center of the outer crossing.*

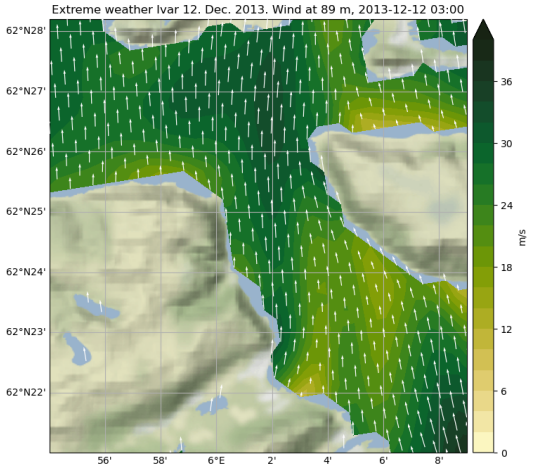

Figure 24: *Simulated wind from WRF at 89 m above sea level, valid when the storm is strongest.*

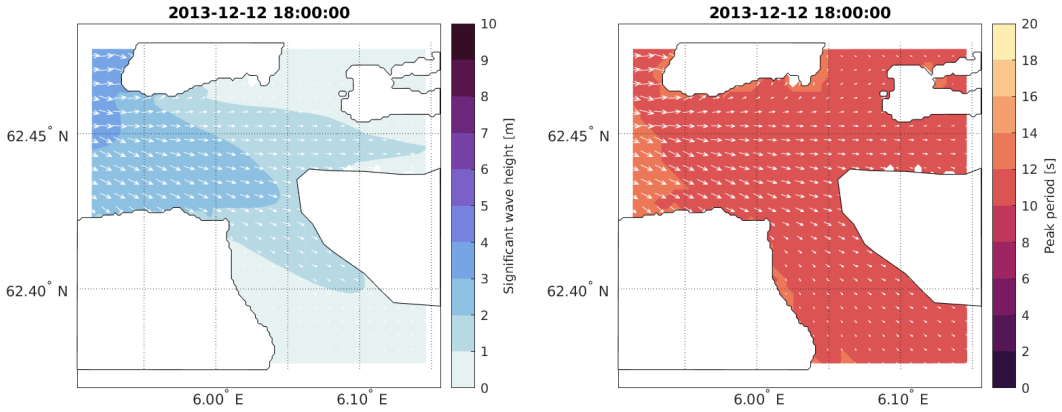

Figure 25: *Significant wave height [m] (left panel) and peak period (right panel) from SWAN and observations at the storm peak.*

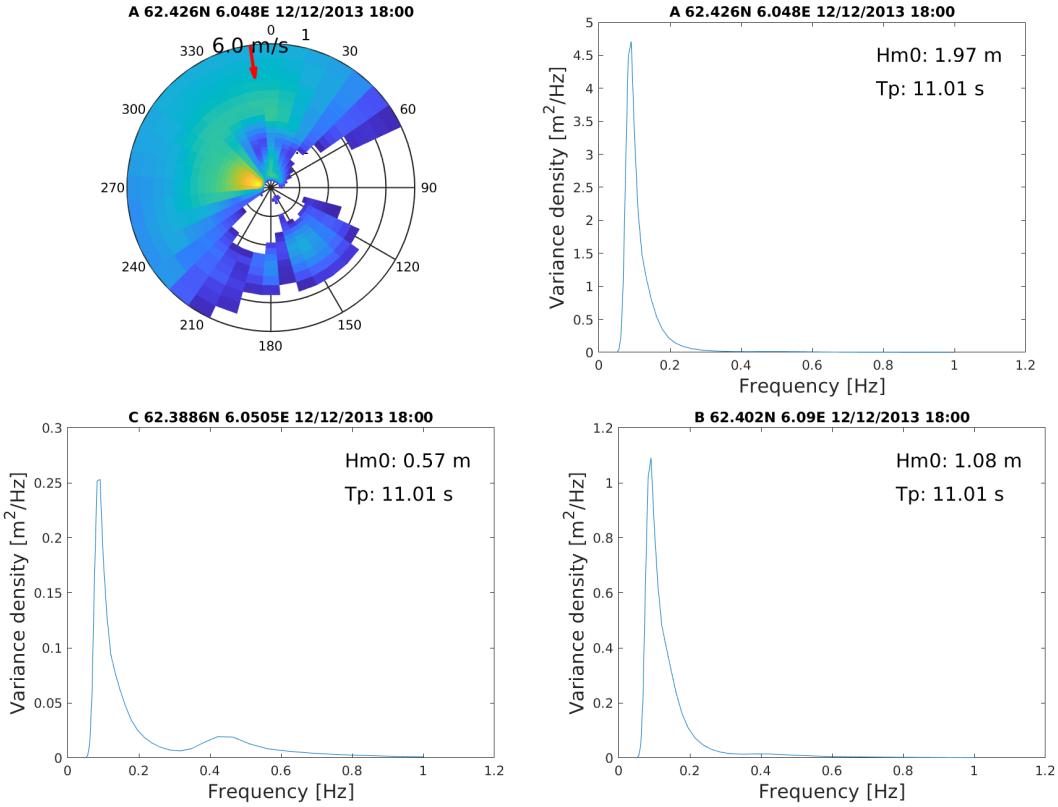

Figure 26: *2D (direction-frequency) wave spectrum from location A (top left panel) and 1D (frequency) wave spectra from locations A (top right panel), B (lower right panel) and C (lower left panel) from SWAN at the storm peak. Please note the different scale on the y-axes. Wind speed and direction (from WRF) is shown in the 2D spectrum. The energy is plotted in the direction the waves come from. Significant wave height (Hm0 or Hs) and peak period (Tp) is indicated for each location in the 1D plots.*

3.7 The storm of 14 March 2017

3.7.1 General overview

The storm of 14 March 2017 is the first storm in our collection where we are able to compare with data recorded in Sulafjorden. For this event, there are observational data available from the mast at Kvitneset and buoys A, B and D in Sulafjorden. The winds at Kvitneset were associated with strong vertical gusts and a weak wind shadow radiated out from Langeneset towards east, see overview in Fig. 27.

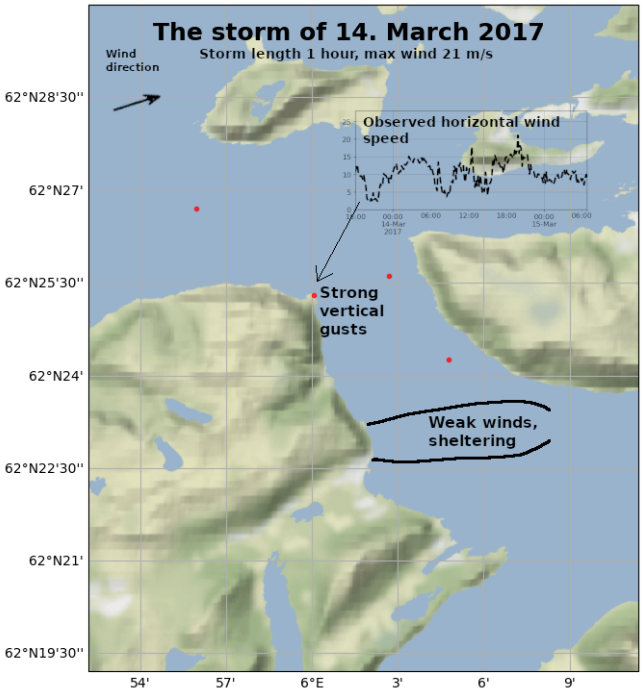

Figure 27: *A schematic summary of important aspects of the storm*

The event is associated with a high pressure system over the bay of Biscay and a broad low pressure system between northern Norway and Iceland, resulting in strong westerly winds, see Fig. 28.

The atmospheric flow during the event has been simulated with both the WRF and the Simra models. Simulated wave and current data are also available.

3.7.2 Model validation at observation sites

The data from Kvitneset show that the WRF-model does a reasonable job simulating the wind speed, perhaps with the exception of the afternoon wind enhancement, see Fig. 29.

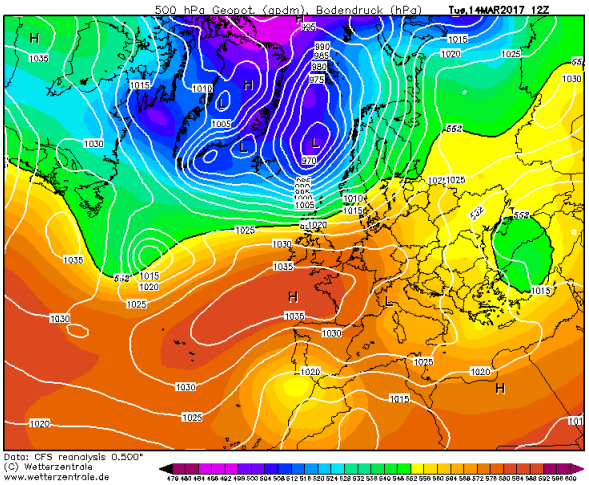

Figure 28: *The analysis from CFS (Climate Forecast System) showing surface pressure and 500 hPa geopotential. Figure is retrieved from Wetterzentale.*

The wind direction is not as well captured at Kvitneset, but very well reproduced at the Breisundet buoy. This may come from insufficient terrain resolution of the mesoscale model near Kvitneset. The observed 10-minute winds reached up to 20 m/s at Kvitneset and 17 m/s at the buoy (4 m asl) in Breisundet.

3.7.3 Simulated flow - horizontal structure

Simulated wind from both models indicate two wakes in Sulafjorden close to each of the proposed crossings (Fig. 30 upper panels). The wakes are more pronounced in Simra as a result of the higher spatial resolution. We also see from observations at Kvitneset that Simra has more topographic steering than simulated by WRF. There are few observations available at this time, but the wind direction is confirmed by the buoys. The simulated wind speed in the wakes of Simra is the same or lower than measured by the buoys at A and B (4 m), which indicates that Simra wind speed may be too low in these wakes.

The wakes are associated regions of high turbulence intensity, and most affected is the outer crossing (Fig. 30 lower left panel). This event is included as an example of a case with strong and turbulent vertical winds (recorded at Kvitneset, not shown here). The simulated vertical wind velocity from Simra (Fig. 30 lower right panel) shows an area of downdraft (less than 1 m/s) over most of the fjord. There are no indications of lee waves or very strong vertical winds at this time in the simulation.

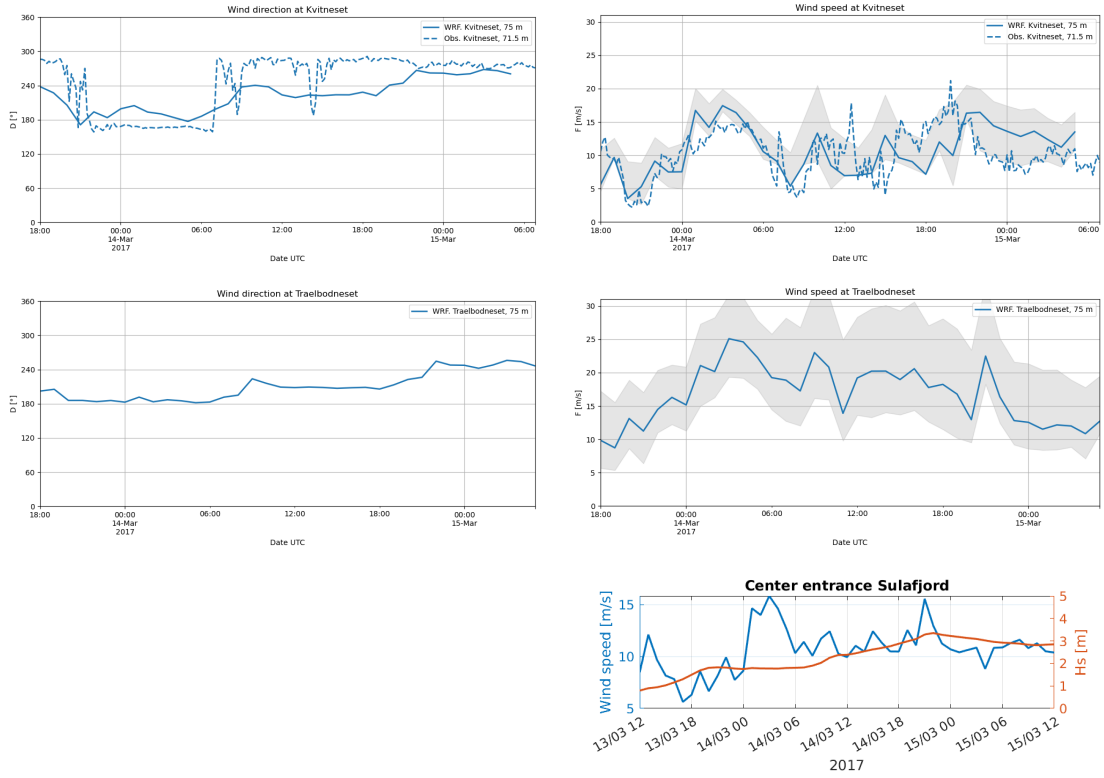

Figure 29: *Simulated (solid lines) and observed (dashed) wind direction (left) and wind speed (right) from the WRF-model. The grey envelope indicates the range of the simulated wind speed in the 9 nearest grid points (eq. 1 km x 1 km area). Lower right panel shows WRF wind speed in blue (10 m) and significant wave height (red line) at the center of the outer crossing.*

3.7.4 Simulated flow - vertical structure

The vertical structure from WRF along the northern section is relatively homogeneous with steady increase in wind speed with height (Fig. 31 upper left). The corresponding simulation from Simra has much lower wind speed and two jumps, at 1100 m and 3000 m on the x-axis. We have not been able to rule out the possibility that these jumps are from numerical failure. The pattern is also seen in the simulated turbulence intensity (lower right).

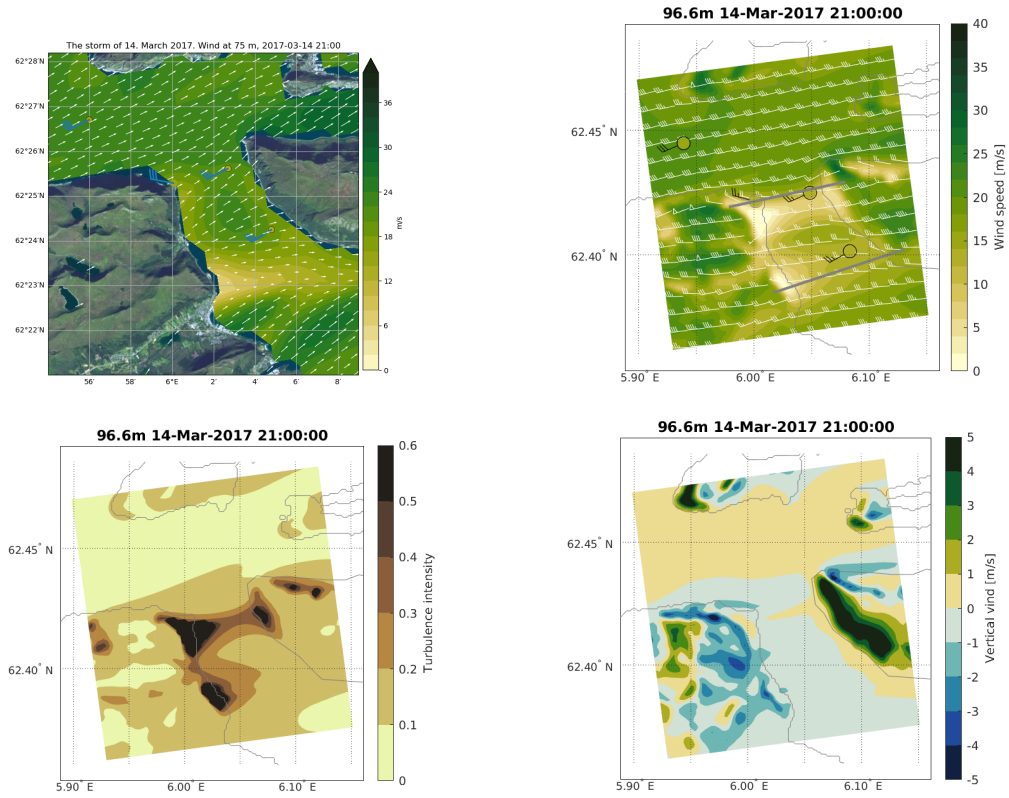

Figure 30: *Simulated wind from WRF at 75 m above sea level (upper left) and from Simra at 97 m (upper right), valid when the storm is strongest. Also shown are the observed wind and direction using traditional wind barbs and coloured circles based on the same colour map as the contour plot. Each flag is 5 m/s and a triangle is equivalent to 25 m/s. The direction of the barbs shows the observed horizontal direction. Buoy measurements at 4 m indicated with black outline. The grey lines indicate the northern and southern sections. Lower panels: Turbulence intensity and vertical wind velocity from Simra at 97 m asl.*

3.7.5 Waves

This storm produced waves in the SWAN simulation of 2-3 m at location B and A, respectively (Fig. 32). This is the first storm case included here where we have observations from the buoys. These are included in the maps as colored points in the same scale as the SWAN contour plot and with black arrows. We see from the two panels that at the peak of the storm the wave observations of both Hs and Tp were slightly lower than the simulations. The directional wave spectra at the location buoy A (Fig. 33) show a swell coming from Breisundet and a broad wind sea from Sulafjord. The wind sea and the swell is clearly visible in the 1D spectra at buoy location B and C.

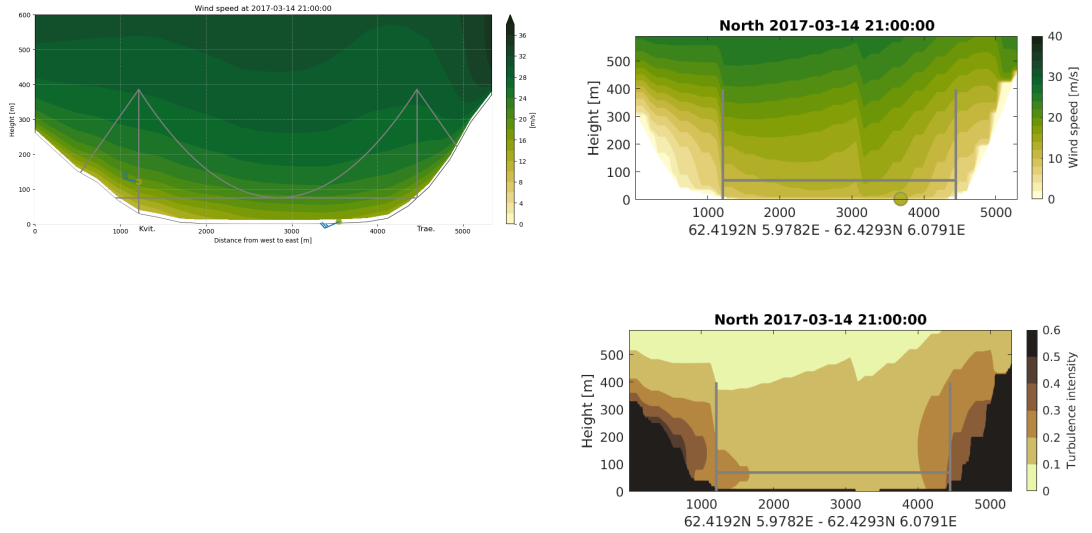

Figure 31: *Simulated wind from WRF (left) and from Simra (right) in a section along the planned crossing. Bridge location is indicated with grey lines. Also shown are the observed wind and direction using traditional wind barbs and coloured circles based on the same colour map as the contour plot. Each flag is 5 m/s and a triangle is equivalent to 25 m/s. The direction of the barbs shows the observed horizontal direction. Turbulence intensity from Simra at the northern crossing (lower right).*

3.7.6 Currents

Model snapshots of surface currents from the storm show that the response of strong winds from the southwest, west and northwest are strong currents from the west in the southern part of Breisundet and a southward surface flow in Sulafjorden with sharp gradients related to wake effects of land (Figure 34). The maximum current speed is found in Sulafjorden with velocities as high as 70 cm/s at buoy location B. The time series where observation and model data are compared show that the current speed and direction correspond well most of the time during the main storm event.

Since the long-term average current direction in Sulafjorden is toward the north, the strong, surface currents from the north alter the current pattern in the entire water column (Figure 35). Instead of a 10 - 15 m thick surface layer with a northward flow and southward currents below down to approximately 100 m, the model sets up a southward flow from the surface down to about 50 - 100 m and northward currents below.

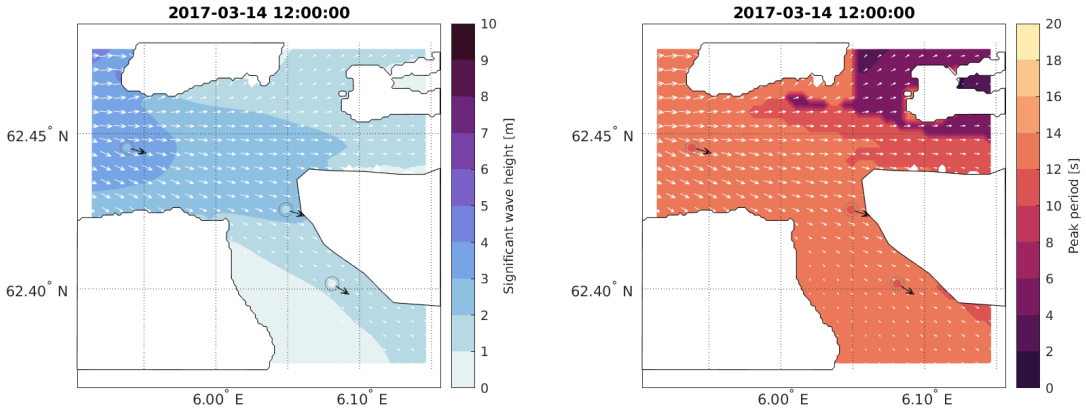

Figure 32: *Significant wave height [m] (left panel) and peak period (right panel) from SWAN and observations at the storm peak. Buoy observations are included as colored points in the same scale as the SWAN contour plot and with black arrows for the peak direction.*

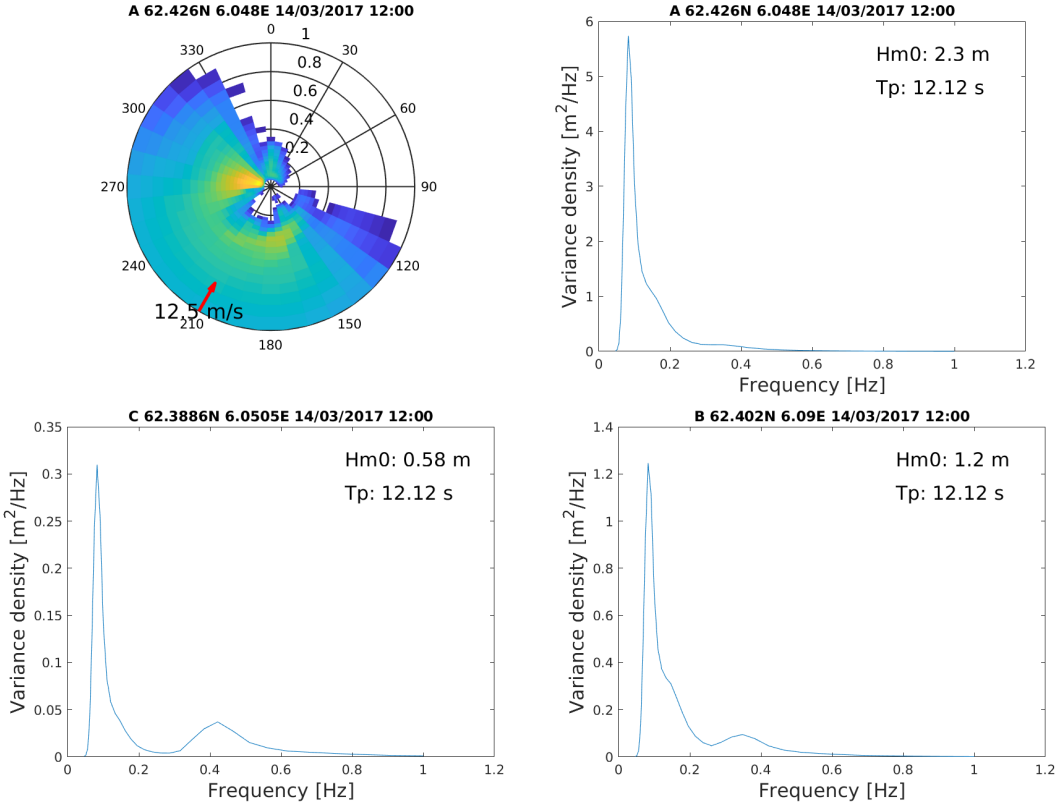

Figure 33: *2D (direction-frequency) wave spectrum from location A (top left panel) and 1D (frequency) wave spectra from locations A (top right panel), B (lower right panel) and C (lower left panel) from SWAN at the storm peak. Please note the different scale on the y-axes. Wind speed and direction (from WRF) is shown in the 2D spectrum. The energy is plotted in the direction the waves come from. Significant wave height (Hm0 or Hs) and peak period (Tp) is indicated for each location in the 1D plots.*

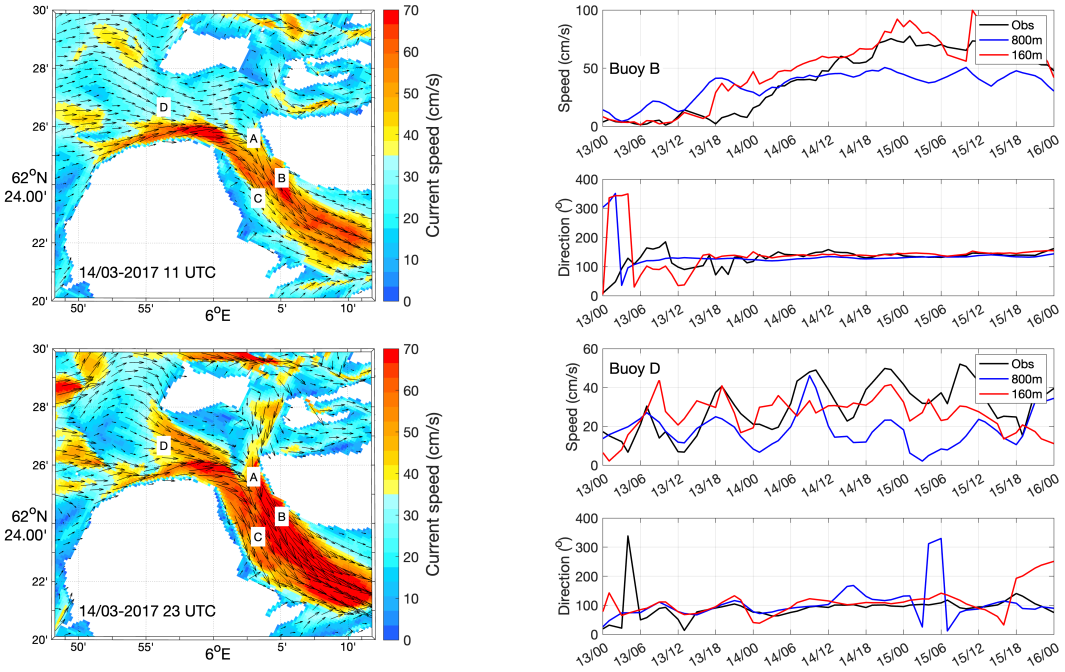

Figure 34: *The maps show instantaneous surface currents from the 160m-model valid at the times indicated in the map (left panels). The observational buoy locations A, B, C and D are denoted in the maps. The graphs to the right show current speed and direction at 1m depth from the two buoy locations B (upper two panels) and D (lower two panels) based on measurements (black line), NorKyst800 (blue) and 160m-model (red). The time stamps are written as day/hour.*

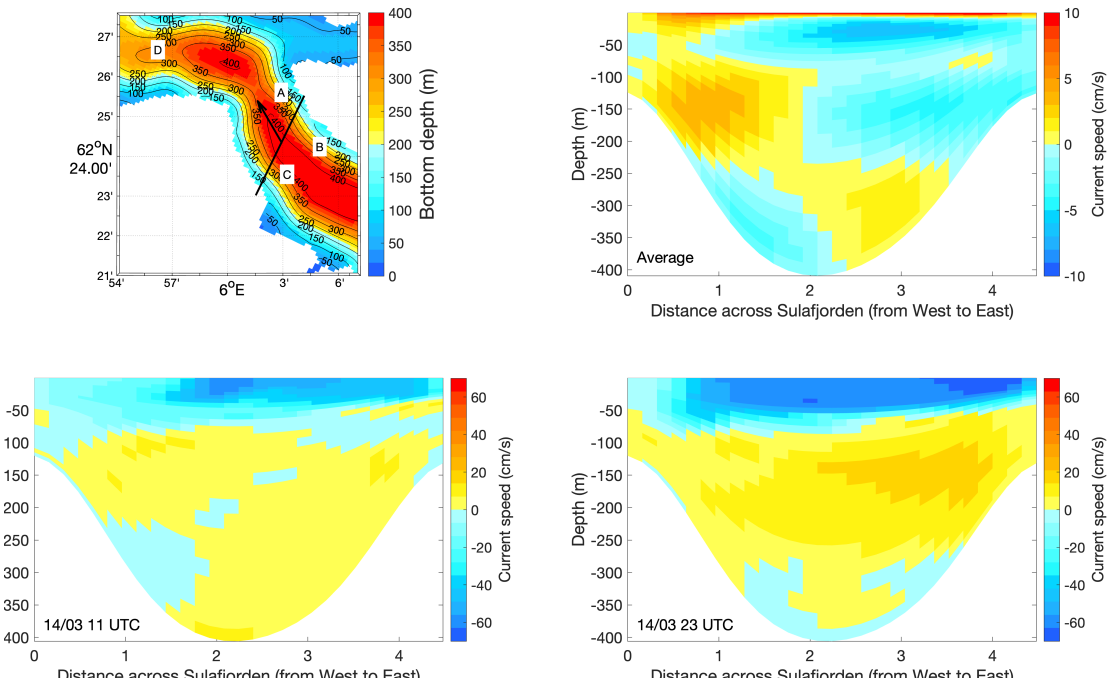

Figure 35: *The upper right panel is retrieved from Ágústsson et al. [2020a] and shows long-term average current speed normal to the transect crossing Sulafjorden denoted as a black line in the bathymetric map (upper left). The lower panels show two snapshots of current speed over the same transect. Red and yellow colors denote currents toward the north in the direction of the arrow in the map, while blue colors denote the opposite southerly currents.*

3.8 The storm of 29 November 2018

3.8.1 General overview

The storm of 29 November, 2018 brought strong southerly winds in Sulafjorden, Fig. 36.

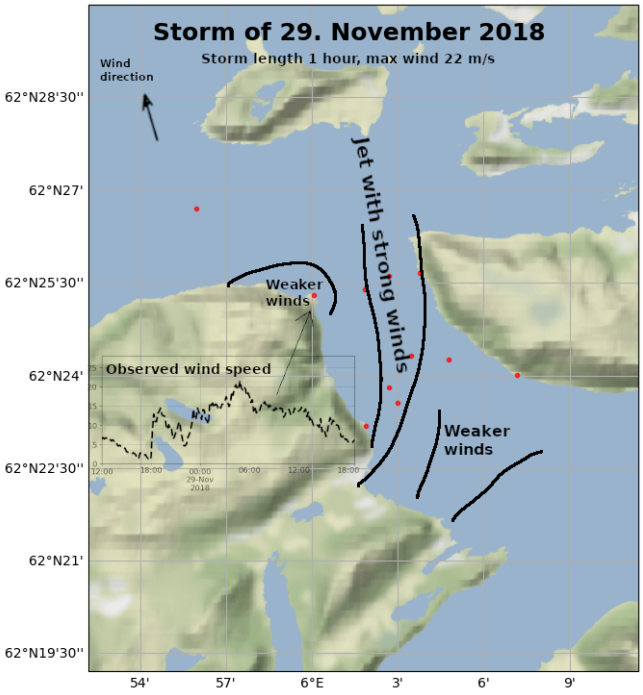

Figure 36: *A schematic summary of important aspects of the storm.*

The event is associated with a deep low pressure system between Iceland and Ireland, and a high pressure system centred over Belarus, resulting in strong east-west pressure gradient over most of Europe, and along the west coast of Norway, see Fig. 37.

During the storm, there are observational data available from the 4 masts in Sulafjorden, and Kvitneset and Trælbodneset are particularly exposed in the fjord. Data is also available from the buoys in Sulafjorden and Breisundet, but only at 4 m asl. The WRF 500 m x 500 m dataset and the Simra 100 m x 100 m datasets are both available for the event. Data is also available from wave and current model.

3.8.2 Model validation at observation sites

Observed 10-minute winds were from the south and west and up to 20 m/s at Kvitneset and 17 m/s at the buoy in Breisundet, see Fig. 38. The observed wind is well reproduced by WRF at Kvitneset as well as by lidar observations at the centre of the fjord, but

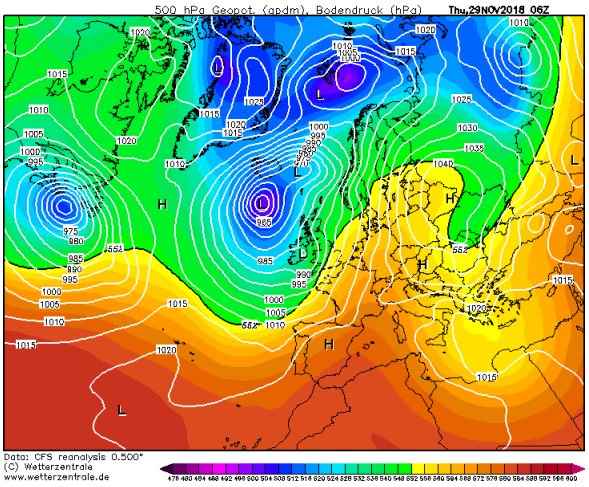

Figure 37: *The analysis from CFS (Climate Forecast System) showing surface pressure and 500 hPa geopotential. Figure is retrieved from Wetterzentale.*

overestimated at Trælbodneset (25 m/s).

The limited resolution of WRF may result in the model not being able to reproduce the correct conditions for the observed gustiness (large wind speed variations over short time period) at Kvitneset. The higher resolution Simra model is more likely to better reproduce the conditions near Kvitneset.

3.8.3 Simulated flow - horizontal structure

In WRF we see reduced wind in the inner part of the Sulafjorden and between Langeneset and Kvitneset (Fig. 39 left panel). Less relevant to the bridge crossing, there is also a signature of wind reduction between Kvitneset and Godøy and north of Sula. In Simra (right panel) the signatures of wakes and enhanced wind is very pronounced with sharp gradients and confirms the main picture we see in WRF. The wind direction in Simra is slightly too much to the west when we compare with the buoy winds at 4 m, but we note that Simra model performs worse near the surface than aloft. The enhanced wind speed (jet) radiating from south of Langeneset towards Trælbodneset is a feature that is seen during all the southerly wind events. In the present case, the wind speed in Kvitneset is higher than at Trælbodneset which the models do not reproduce. The local response at these two stations seems to be very sensitive to the background flow so perhaps if the wind direction in Simra was more southerly, the wakes and enhanced wind in Simra would agree better with observations.

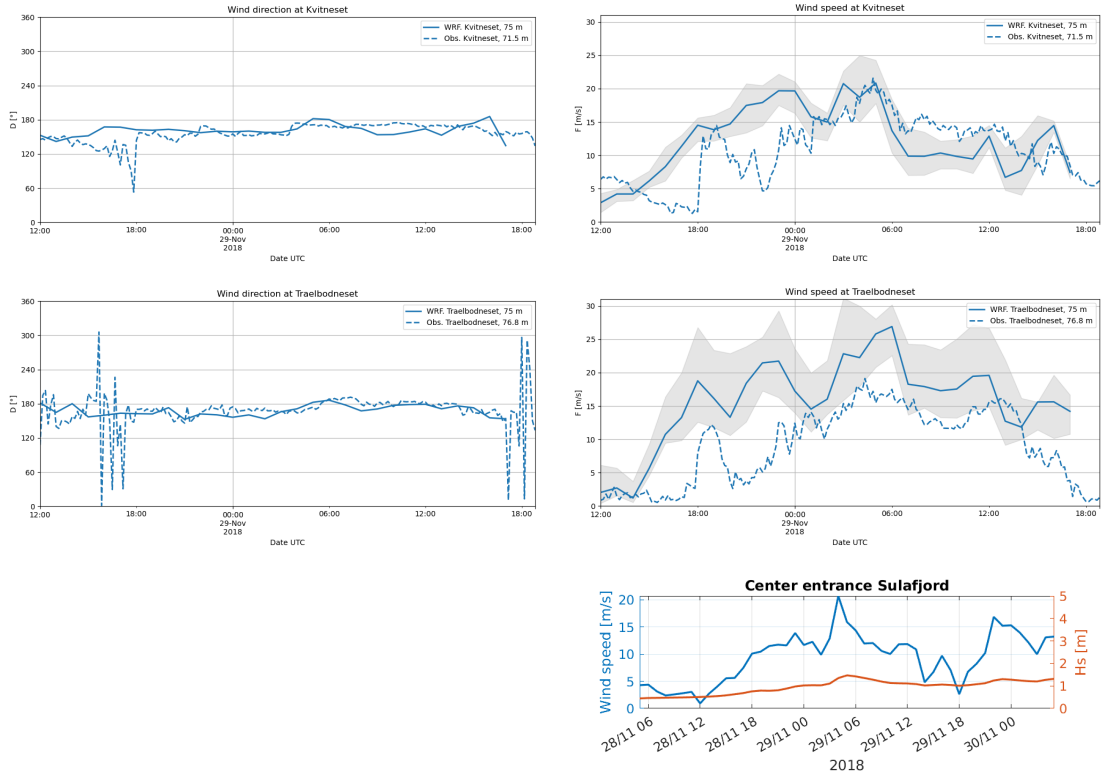

Figure 38: *Simulated (solid lines) and observed (dashed) wind direction (left) and wind speed (right), from the WRF-model. The grey envelope indicates the range of the simulated wind speed in the 9 nearest grid points (eq. 1 km x 1 km area). Lower right panel shows wind speed in blue (10 m) and significant wave height (red line) at the center of the outer crossing.*

3.8.4 Simulated flow - vertical structure

Transects of wind speed are extracted from the models and shown along the northern section in Fig. 40 at the same time and overlaid with lines indicating a suspension bridge. WRF has higher wind speed in the eastern part, and this is also the case in Simra. We attribute this to the jet radiating out from Langeneset towards Trælbodneset mentioned earlier. There is however no confirmation by measurements in this case. Simra indicates that the wake close to Kvitneset extends to more than 600 m height. The simulated turbulence intensity is moderate across the fjord, but higher at Kvitneset. This is not confirmed by the observations at the mast.

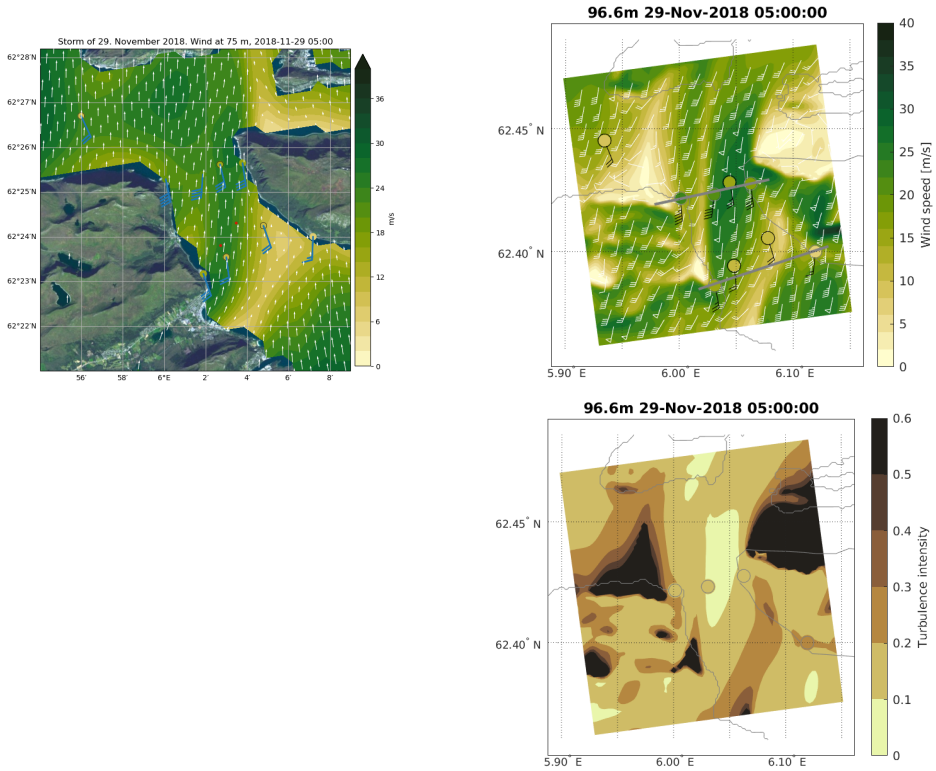

Figure 39: *Simulated wind from WRF at 75 m above sea level (left), and simulated wind from Simra at 97 m above sea level (right), valid when the storm is strongest. Also shown are the observed wind and direction using traditional wind barbs and coloured circles based on the same colour map as the contour plot. Each flag is 5 m/s and a triangle is equivalent to 25 m/s. The direction of the barbs shows the observed horizontal direction. Buoy measurements at 4 m indicated with black outline. The grey lines indicate the northern and southern sections. Turbulence intensity from Simra at 97 m (lower right panel).*

3.8.5 Waves

The southwesterly wind direction along the Norwegian coast is subject to topographic steering which results in southerly winds in the fjord as shown in the WRF and Simra simulations. The wave height increases to 1 - 1.5 m as the wind speed increase in the morning of the 29th. The wave simulations are confirmed by the buoy observations at the peak of the storm (Figure 41), even if Hs is slightly high at locations A, B, and D in SWAN. The right panel and the spectra in figure 42 shows how the outer part of the fjord is dominated by 14 s swell while the winds in the inner part of the fjord makes the wind sea (4 - 6 s) the most dominating.

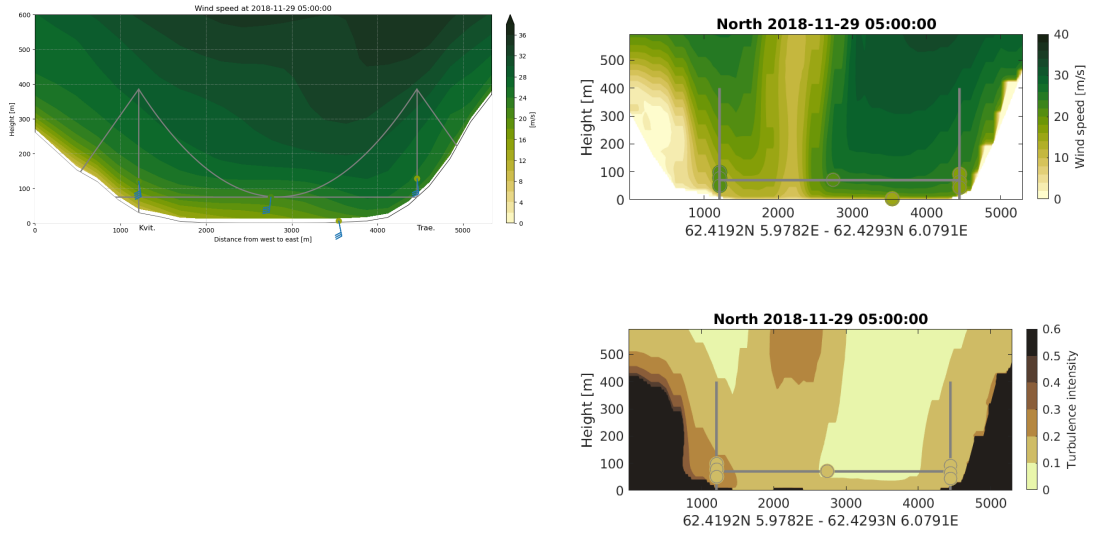

Figure 40: *Simulated wind from WRF (left) and from Simra (right) in a section along the planned crossing. Bridge location is indicated with grey lines. Also shown are the observed wind and direction using traditional wind barbs and coloured circles based on the same colour map as the contour plot. Each flag is 5 m/s and a triangle is equivalent to 25 m/s. The direction of the barbs shows the observed horizontal direction. Turbulence intensity from Simra along the northern section (lower right).*

3.8.6 Currents

Model snapshots of surface currents from the storm show that the response of strong winds from the south are not particularly visible in the surface current pattern in the Sulafjorden area (Figure 43). The maximum current speeds are below 50 cm/s during the entire storm event. The time series where observation and model data are compared show that the current speed and direction correspond well most of the time during the main storm event.

Since the long-term average surface current direction in Sulafjorden is toward the north, winds from the south will not have a large impact on the current pattern across Sulafjorden (Figure 44). During the storm there is at first a surface layer with northward currents less than 5 m thick, with southward currents below down to 50m depth and northward currents below. After the storm has weakened, we see that currents from the west in the southern part of Breisundet alters the direction of the thin surface layer in Sulafjorden from northward to southward.

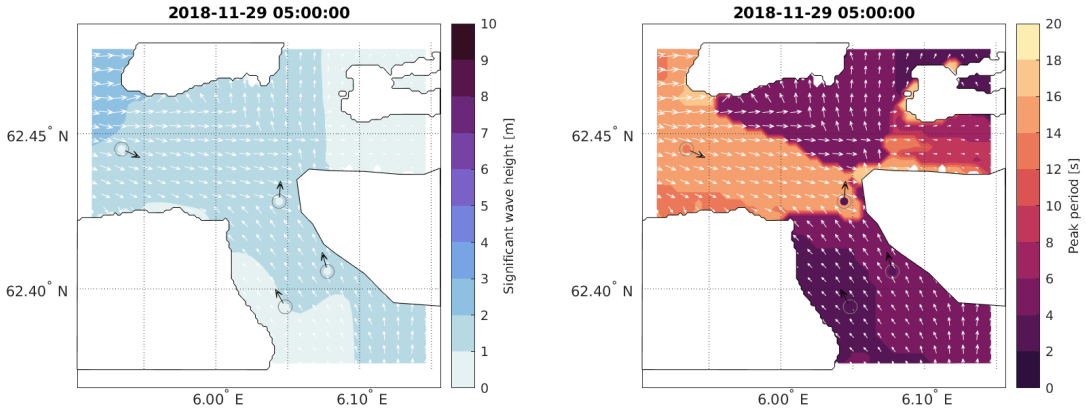

Figure 41: *Significant wave height [m] (left panel) and peak period (right panel) from SWAN and observations at the storm peak. Buoy observations are included as colored points in the same scale as the SWAN contour plot and with black arrows for the peak direction.*

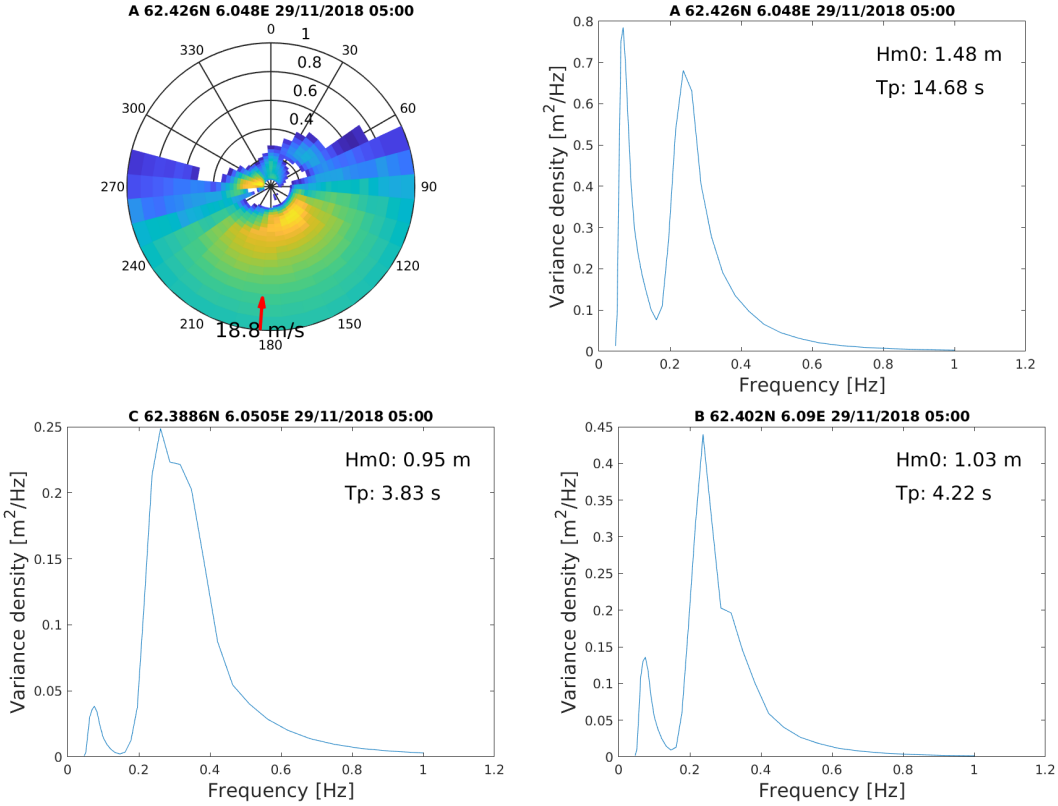

Figure 42: *2D (direction-frequency) wave spectrum from location A (top left panel) and 1D (frequency) wave spectra from locations A (top right panel), B (lower right panel) and C (lower left panel) from SWAN at the storm peak. Please note the different scale on the y-axes. Wind speed and direction (from WRF) is shown in the 2D spectrum. The energy is plotted in the direction the waves come from. Significant wave height (Hm0 or Hs) and peak period (Tp) is indicated for each location in the 1D plots.*

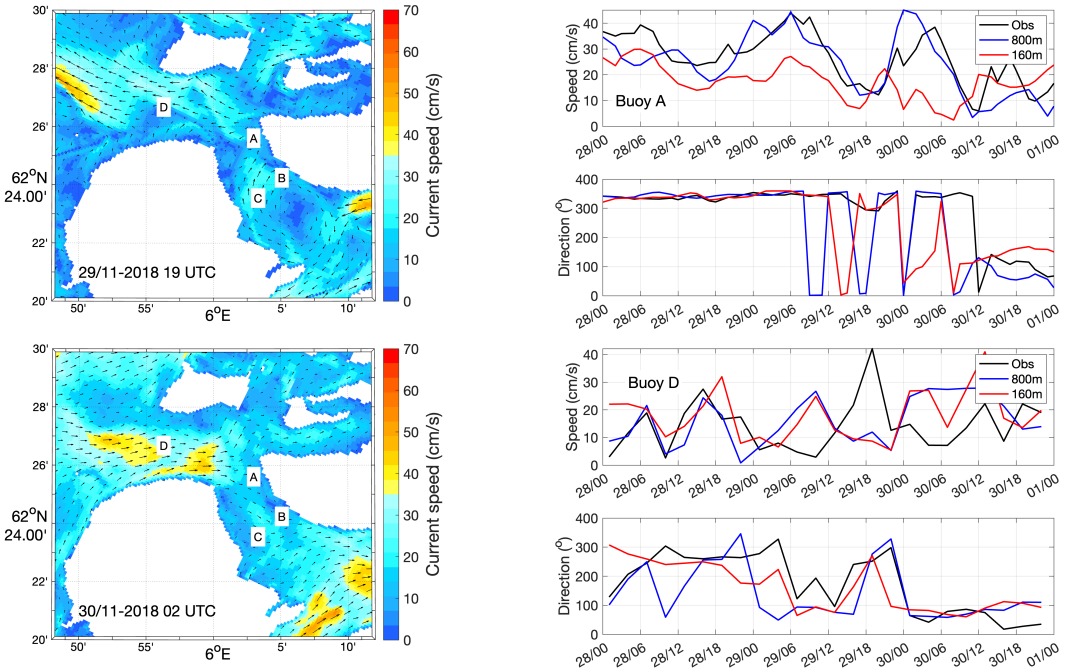

Figure 43: *The maps show instantaneous surface currents from the 160m-model valid at the times indicated in the map (left panels). The observational buoy locations A, B, C and D are denoted in the maps. The graphs to the right show current speed and direction at 1m depth from the two buoy locations A (upper two panels) and D (lower two panels) based on measurements (black line), NorKyst800 (blue) and 160m-model (red). The time stamps are written as day/hour.*

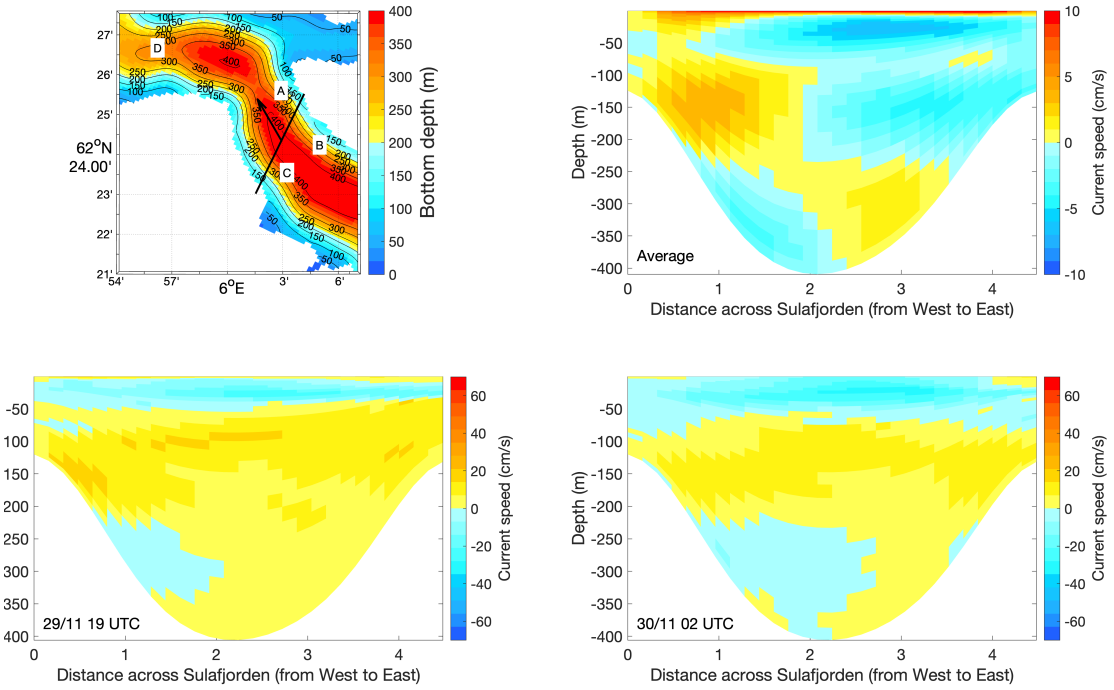

Figure 44: *The upper right panel is retrieved from Ágústsson et al. [2020a] and shows long-term average current speed normal to the transect crossing Sulafjorden denoted as a black line in the bathymetric map (upper left). The lower panels show two snapshots of current speed over the same transect. Red and yellow colors denote currents toward the north in the direction of the arrow in the map, while blue colors denote the opposite southerly currents.*

3.9 The storm of 1 January, 2019

3.9.1 General overview

The event is the strongest northwesterly storm observed during the campaign in Sulafjorden. See Fig. 45, and occurred in relation to a broad and deep low over the gulf of Bothnia and a ridge extending from Iceland to the British isles see Fig. 46.

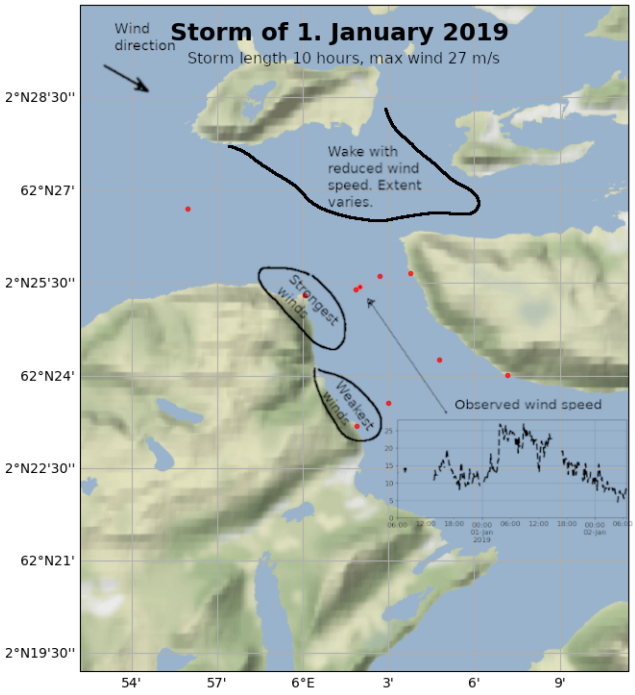

Figure 45: *A schematic summary of important aspects of the storm*

The northwesterly flow caused a wake behind Godøya and a wind speed enhancement at west side of Sulafjorden, in particular at Kvitneset (Fig. 45).

Regular weather observations at Vigra, Ørsta og Volda airport and Eitrefjell had weak winds, mostly below 15 m/s the whole day. In the morning at 07 UTC, the exposed mountain station Eitrefjell had 21.2 m/s and the Ørsta/Volda airport had 5.8 m/s at the same time. Vigra had 13.8 m/s.

Four masts reported in Sulafjorden during the storm and we look at Kvitneset and Trælbodneset. Observations of wind at the centre of the fjord are also available from the scanning lidars. The buoys recorded data in the fjord at 4 m asl.

The WRF 500 m x 500 m and the Simra 100 m x 100 m simulated the event. Data is also available from wave and current model.

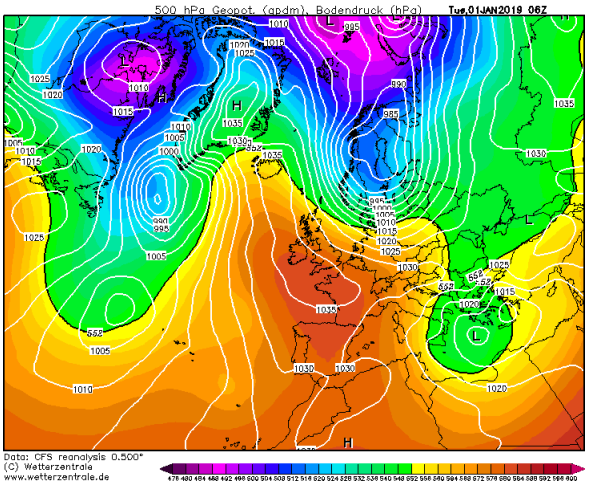

Figure 46: *The analysis from CFS (Climate Forecast System) showing surface pressure and 500 hPa geopotential. Figure is retrieved from Wetterzentale.*

3.9.2 Model validation at observation sites

Observed 10-minute winds were strongest at Kvitneset (27 m/s) but only slightly weaker at both Trælbodneset and at the centre of Sulafjorden, see Fig. 47. The observed wind speed and direction are reasonably well reproduced by the WRF-model, except that the wind speed before the storms onset is overestimated at Trælbodneset. The Simra model also performs reasonably well, in particular it is better at Trælbodneset than WRF 48.

3.9.3 Simulated flow - horizontal structure

The models show a wake in the lee of Godøya; more pronounced in the Simra model and less in WRF, see Fig. 48. The winds in the wake are weak and the spatial extent and direction of the wake varies greatly. The Simra model indicates that it reaches as far as Trælbodneset, while this is not seen in the WRF-data, explaining the better behaviour in the Simra model.

Between 03 and 04 UTC the wind speed increased from 15 to 25 m/s. Simulated and observed wind speed is shown at 04 UTC in the upper panels of Figure 49, where we notice the very strong wind at Kvitneset, Trælbodneset and the lidar in the observations. The buoy (A) measuring at 4 m is around 5 m/s lower. Simulated wind speed with Simra agree relatively well with the observations, while the wind speed from WRF at this time is too low. Both simulations indicate the wake behind Godøy and a region of increased wind speed around Kvitneset.

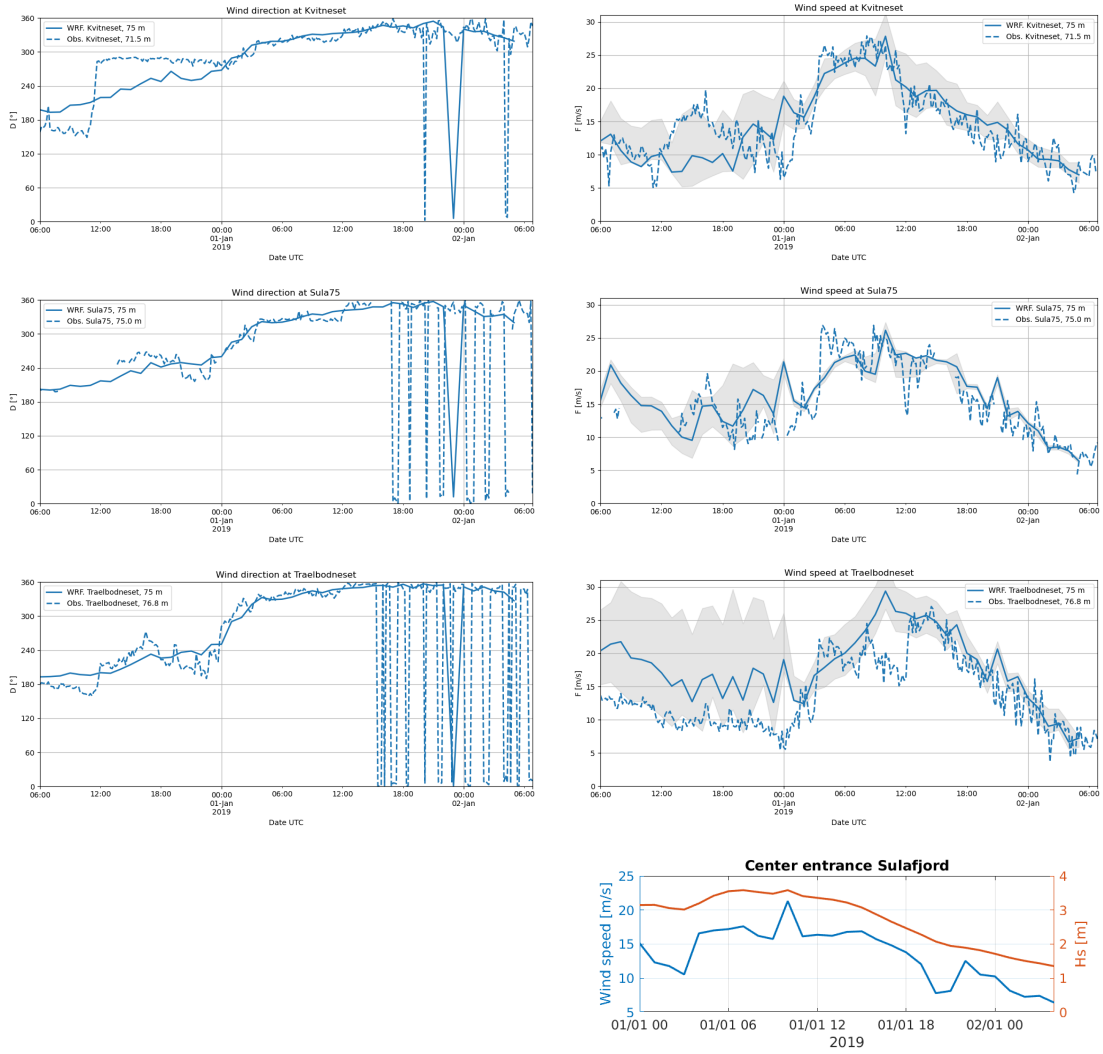

Figure 47: *Simulated (solid lines) and observed (dashed) wind direction (left) and wind speed (right) from the WRF-model. The grey envelope indicates the range of the simulated wind speed in the 9 nearest grid points (eq. 1 km x 1 km area). Lower right panel shows wind speed in blue (10m) and significant wave height (red line) at the center of the outer crossing.*

The wind is coming straight into Sulafjorden from the ocean with very little turbulence, but turbulence is generated at the tip of Kvitneset, propagating down to the southern section in Sulafjorden (Figure 49 lower right). There is also a sign of this wake when comparing the wind speed from buoys B and C (upper right).

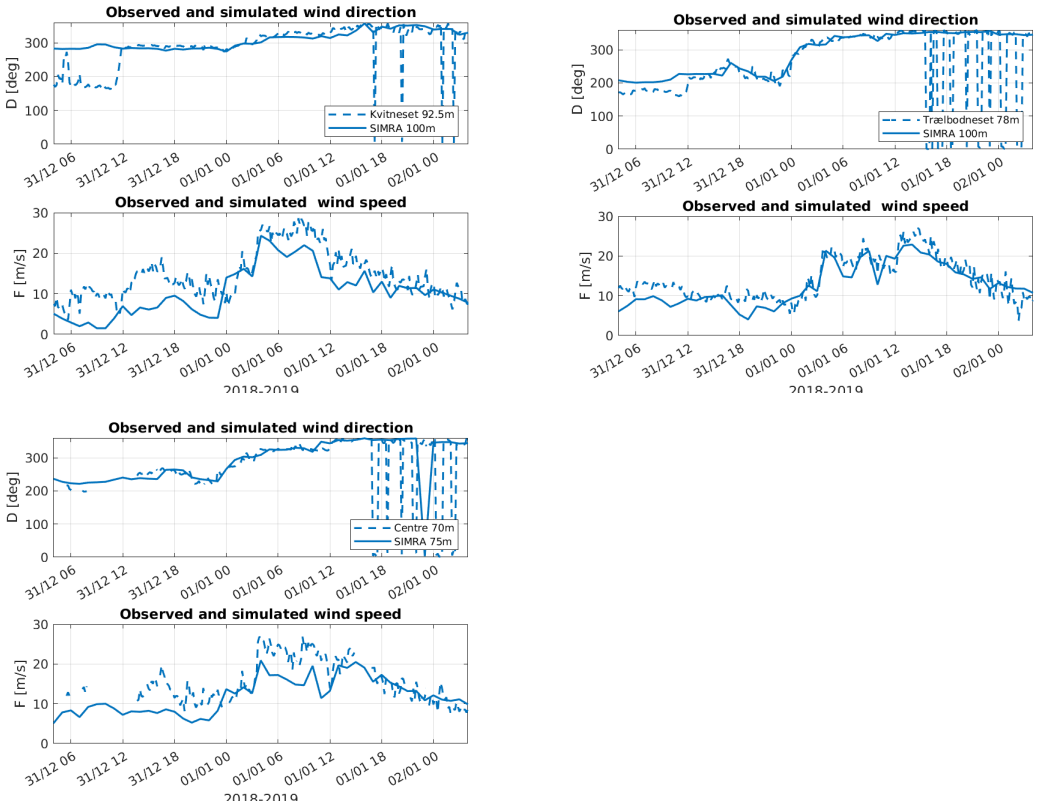

Figure 48: *Observed (dashed lines) and simulated (solid lines) wind direction and wind speed from Kvitneset (upper left), Trælbodneset (right), and at the centre of the fjord (lower left) from 100 m in the Simra-model.*

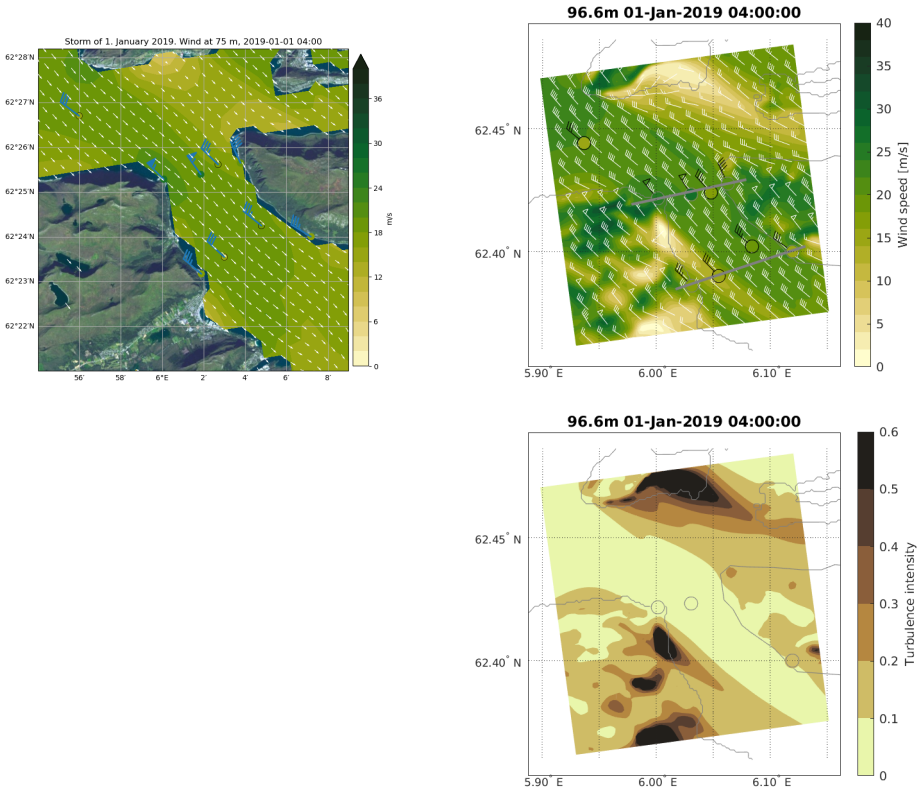

Figure 49: *Simulated wind from WRF at 75 m above sea level (left), and simulated wind from Simra at 97 m above sea level (right), valid when the storm is strongest. Also shown are the observed wind and direction using traditional wind barbs and coloured circles based on the same colour map as the contour plot. Each flag is 5 m/s and a triangle is equivalent to 25 m/s. The direction of the barbs shows the observed horizontal direction. Buoy measurements at 4 m indicated with black outline. The grey lines indicate the northern and southern sections. Lower right: Turbulence intensity from Simra at 97 m asl.*

3.9.4 Simulated flow - vertical structure

The transect along the northern proposed crossing shows strong winds increasing with height in the simulation with Simra (Figure 50). The wind speed is highest on the west side at the northern section but at the southern section (lower left panel) the strong wind speed is found on the eastern side of the fjord and the gradient in wind speed is larger due to the wake at Langeneset (described above).

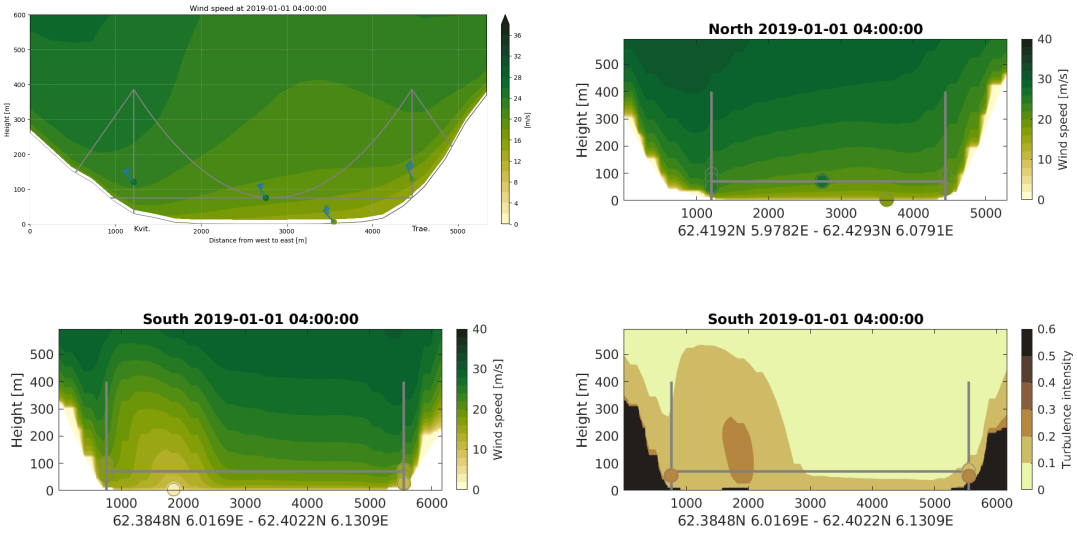

Figure 50: *Upper panels: Simulated wind from WRF (left) and from Simra (right) in a section along the northern planned crossing. Bridge location is indicated with grey lines. Also shown are the observed wind and direction using traditional wind barbs and coloured circles based on the same colour map as the contour plot. Each flag is 5 m/s and a triangle is equivalent to 25 m/s. The direction of the barbs shows the observed horizontal direction. Lower panels: Simulated wind (left) and turbulence intensity (right) from Simra over the southern section.*

3.9.5 Waves

With northwesterly wind, waves penetrate from the coast through Breisundet and into Sulafjord. Local wind sea in Sulafjord/Breisundet is generated on top of the swell. The simulated Hs is above 3 m at location A during the morning of 1 January 2019 (Figure 47 lower right panel). The wave height is confirmed by the observations at 04 UTC (Figure 51 but the peak period is overestimated. However, this case was also treated in Furevik and Aarnes [2021] where is was found that the maximum simulated waves at location A is lower than observed (3.4 m versus 4.1 m). Maximum observed peak period was 15.8 s at buoy A. The directional wave spectrum at A show how the wind sea and the swell is nearly aligned. At locations B and C, the wind sea turns up like a "shoulder" to the swell peak, more than a separate peak.

3.9.6 Currents

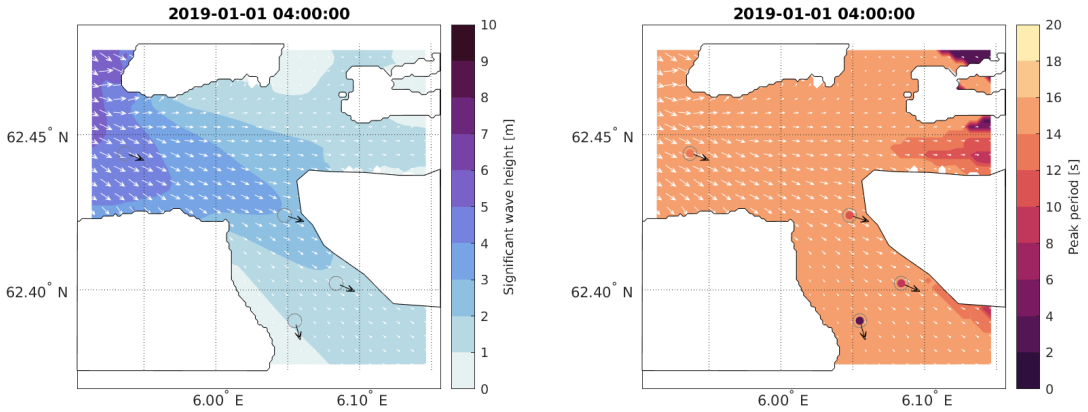

Figure 51: *Significant wave height [m] (left) and peak period (right) from SWAN and observations at the storm peak. Buoy observations are included as colored points in the same scale as the SWAN contour plot and with black arrows for the peak direction*

Model snapshots of surface currents from the storm show that the response of strong winds from the northwest are strong currents into Breisundet and Sulafjorden from the same direction with sharp gradients related to wake effects of land (Figure 53). After the storm has weakened, the water masses that have been pushed into the fjord system return offshore with relatively high velocities. The time series where observation and model data are compared show that the current speed and direction correspond well most of the time during the main storm event. We may particularly notice that the transition from eastward to westward currents in Breisundet (location D) is reproduced very well in the model.

Since the long-term average current direction in Sulafjorden is toward the north, the strong surface currents from the north alter the current pattern in the entire water column (Figure 54). Instead of a 10 - 15 m thick surface layer with a northward flow and southward currents below down to approximately 100 m, the model sets up a southward flow from the surface down to about 100 m and northward currents below. However, the outflowing waters after the storm event (2 January 2019 00 UTC) is clearly visible in the eastern part of Sulafjorden down to approximately 50 m depth.

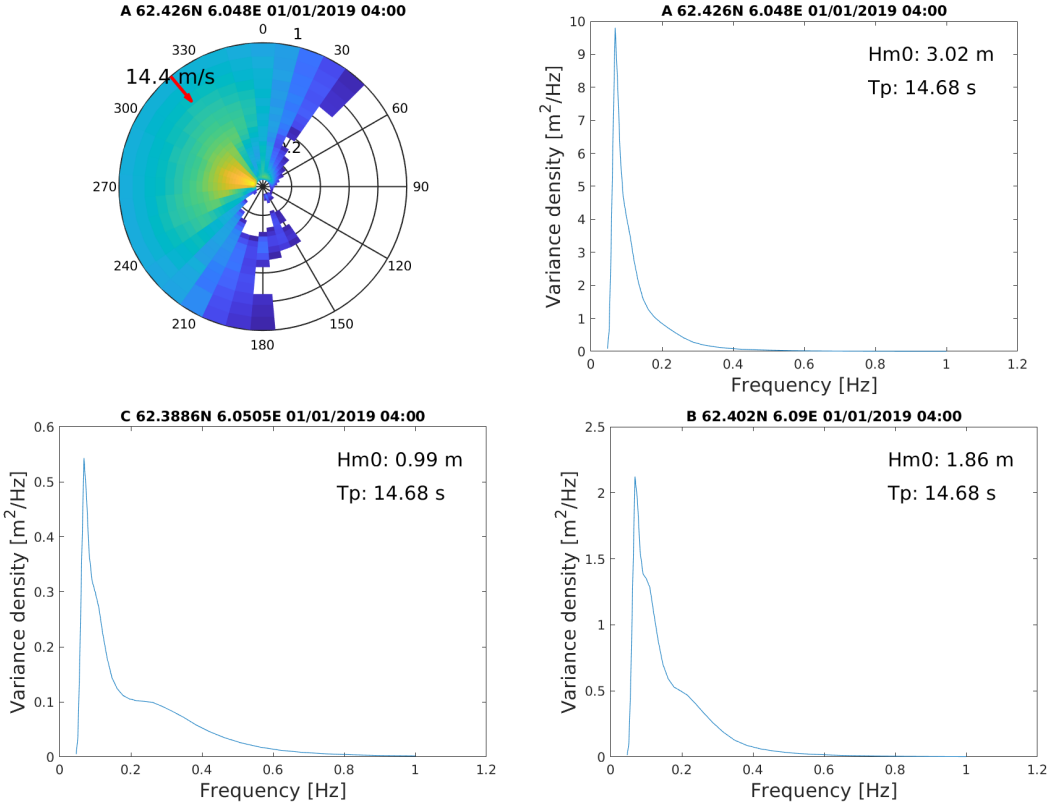

Figure 52: *2D (direction-frequency) wave spectrum from location A (top left panel) and 1D (frequency) wave spectra from locations A (top right panel), B (lower right panel) and C (lower left panel) from SWAN at the storm peak. Please note the different scale on the y-axes. Wind speed and direction (from WRF) is shown in the 2D spectrum. The energy is plotted in the direction the waves come from. Significant wave height (Hm0 or Hs) and peak period (Tp) is indicated for each location in the 1D plots.*

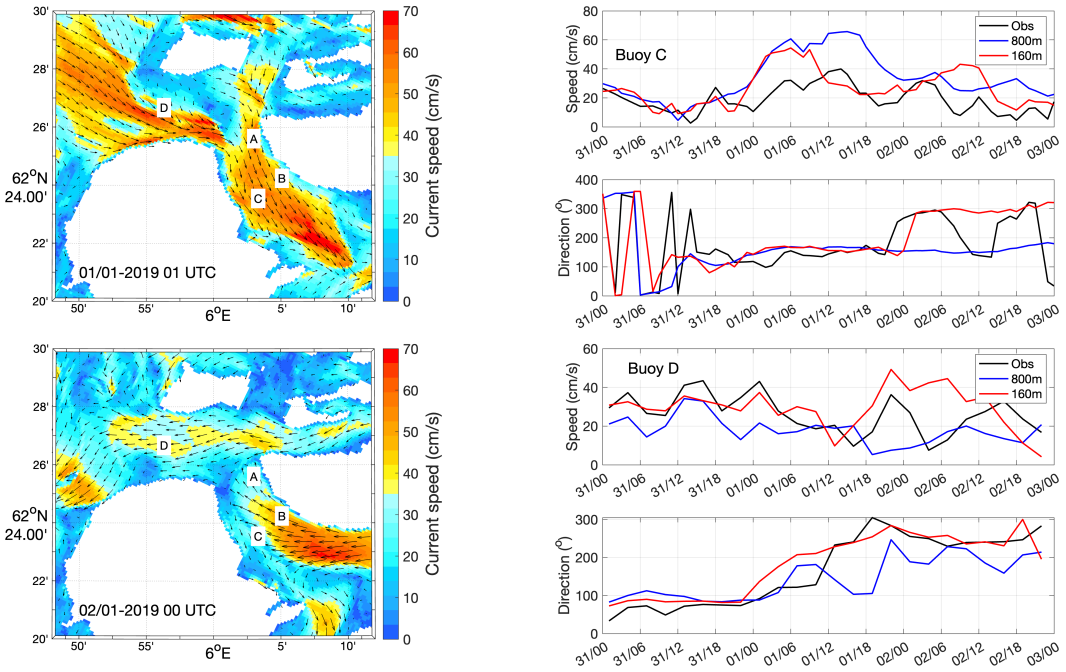

Figure 53: *The maps show instantaneous surface currents from the 160m-model valid at the times indicated in the map (left panels). The observational buoy locations A, B, C and D are denoted in the maps. The graphs to the right show current speed and direction at 1m depth from the two buoy locations C (upper two panels) and D (lower two panels) based on measurements (black line), NorKyst800 (blue) and 160m-model (red). The time stamps are written as day/hour.*

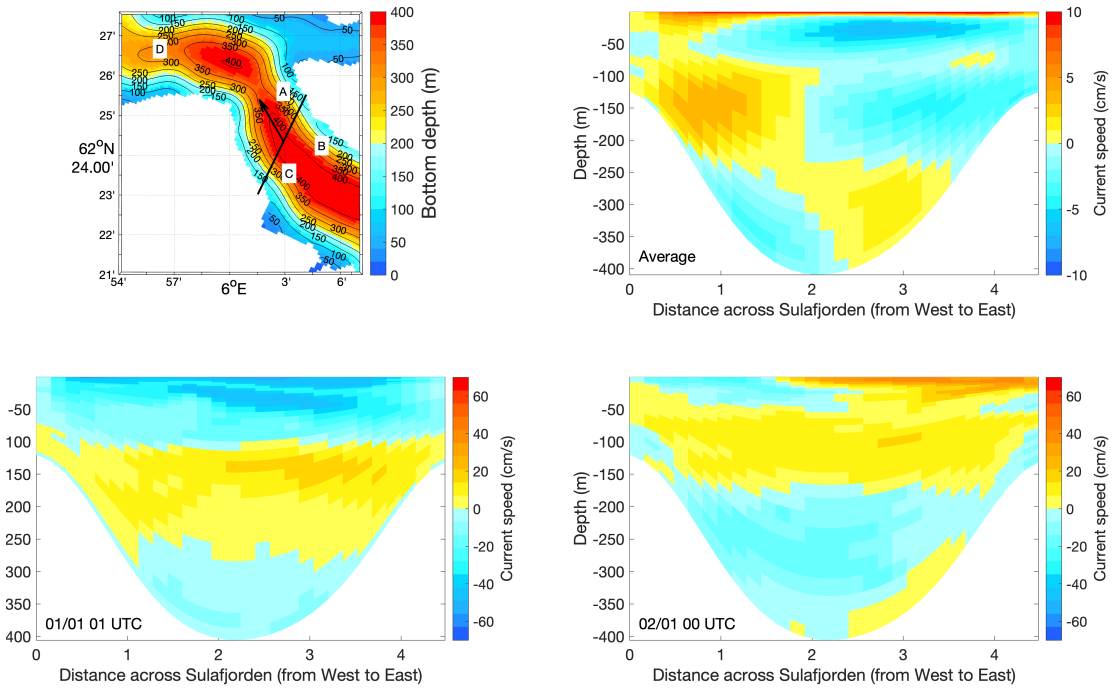

Figure 54: *The upper right panel is retrieved from Ágústsson et al. [2020a] and shows long-term average current speed normal to the transect crossing Sulafjorden denoted as a black line in the bathymetric map (upper left). The lower panels show two snapshots of current speed over the same transect. Red and yellow colors denote currents toward the north in the direction of the arrow in the map, while blue colors denote the opposite southerly currents.*

3.10 The storm of 13 – 14 January 2019

3.10.1 General overview

A northwesterly storm occurred in Sulafjorden on 13 – 14 January 2019. The maximum mean wind speed was not particularly high (∼25 m/s), and the wind direction was more or less constant throughout the storm, see Fig. 55.

Simulations of the flow as well as lidar observations and satellite based observations indicate a variable wake on the southern side of Godøya, extending towards Trælbodneset. The wake is associated with weak and varying winds, and the vertical extent may be on the order of several hundred metres near Godøya. At time the wake appears to extend to the tip of the island Sula, and the easternmost part of the crossing, in particular towards the end of the storm. It would in that case contribute to enhancing the horizontal wind shear across the fjord.

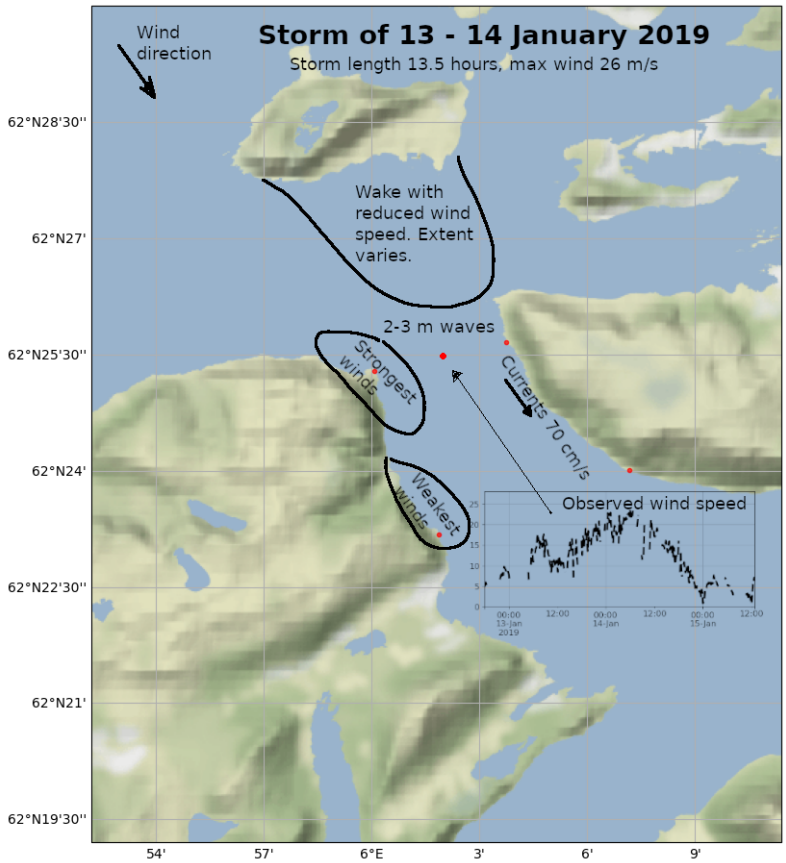

Figure 55: *A schematic summary of important aspects of the storm*

At the northerly planned crossing, the winds were strongest on the Kvitneset side,

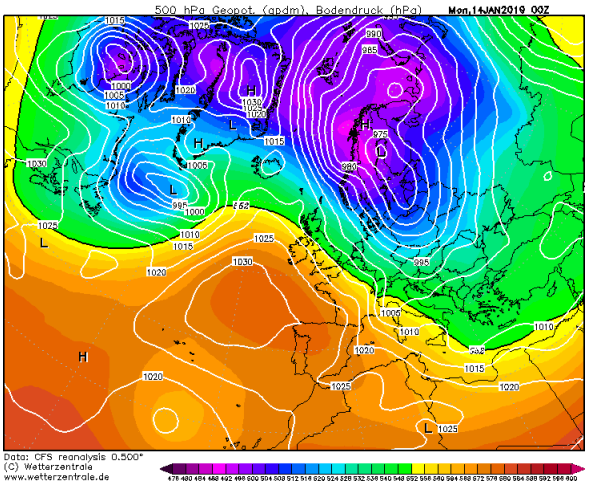

Figure 56: *The analysis from CFS (Climate Forecast System) showing surface pressure and 500 hPa geopotential. Figure is retrieved from Wetterzentale.*

were the horizontal wind shear also was strongest. Winds were slightly weaker near the centre of the fjord and on the eastern side, see Fig. 55.

The storm is associated with a cold air out break which lasts for a couple of days, see Fig. 56. In this cold air outbreak a small polar low is formed, but it makes landfall just north of our area.

The storm had a relatively sudden onset in the late afternoon of 13 January and a gradual weakening in the morning of the following day. The storm length was 13.5 hours, defined as the largest number of 10-minute observations of wind of at least 20 m/s at any of the available observation sites. Vigra airport reported its 10-minute wind speed maximum at 05 UTC, 14 January having 16.5 m/s, which is not a particularly strong wind.

3.10.2 Model validation at observation sites

The WRF simulations (Fig. 57) reproduce relatively well the observed 10-minute wind speed and direction at the masts, and especially at the lidar location at the centre of the fjord. The abrupt wind direction change at the masts at the start of the storm, and some of the short term wind speed variations, are not reproduced. The max wind from the model is similar to what is observed, $\sim$26 m/s. Simra (Fig. 58) is somewhat low in wind speed at the peak of the storm at both masts. The model reproduces the wind direction well, except the sudden veering of the observed wind at the start of the storm.

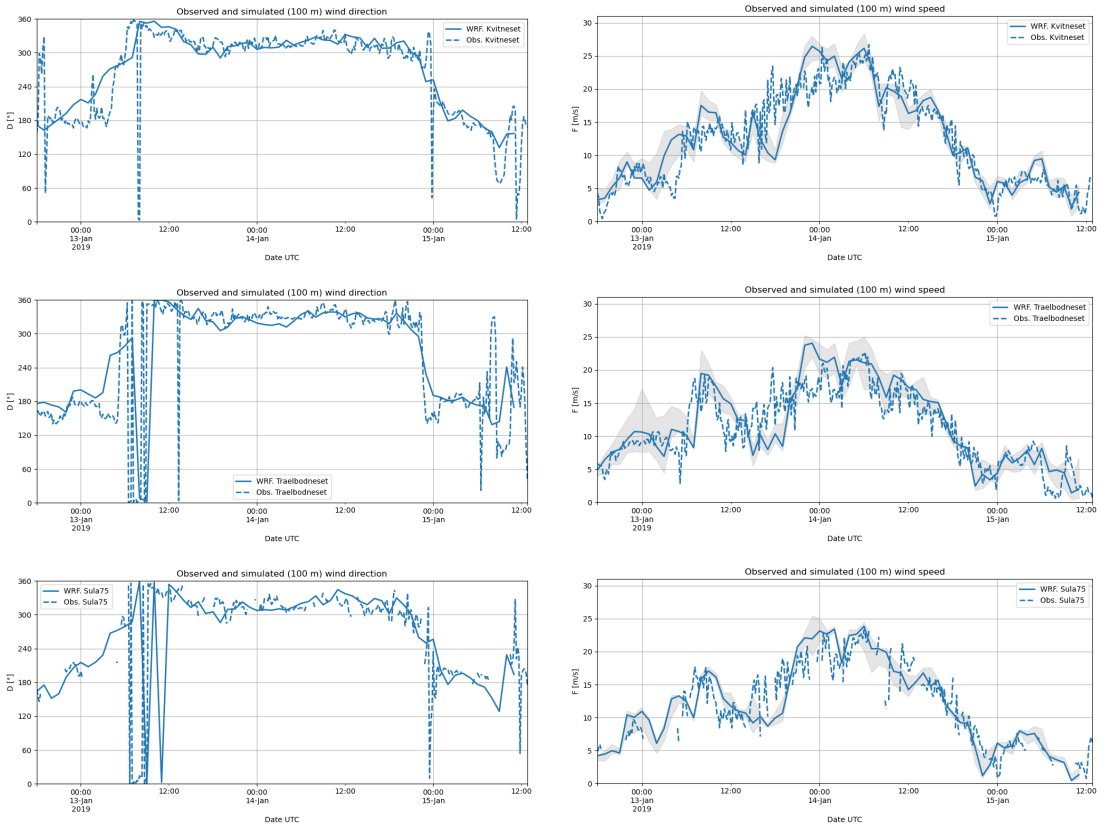

Figure 57: *Observed (dashed lines) and simulated (solid lines) wind direction (left) and wind speed (right) using WRF. The grey envelope indicates the range of the simulated wind speed in the 9 nearest grid points (eq. 1 km x 1 km area).*

Figure 58: *Observed (dashed lines) and simulated (solid lines) wind direction and wind speed from Kvitneset (left), Trælbodneset (right), and at the bridge deck location in the centre of the fjord (below) using simulated data at 100 m from the Simra-model.*

3.10.3 Simulated flow - horizontal structure

The simulated flow at 100 m asl from both WRF and Simra (Fig. 59) indicates that the strongest winds are observed along the western coast at the mouth of Sulafjorden, in particular at the Kvitneset mast. Simra has a region of weak wind near Langeneset which is not seen in WRF. The available wind observations are in general well reproduced. As the wind direction is more or less constant during the storm, then the temporal and spatial variability in the flow is not particularly large at Kvitneset. The variability is higher elsewhere, e.g. near Trælbodneset, presumably partly related to the wake in the lee of Godøy. The simulated wake varies in strength and extent, and is more pronounced in the simulations with Simra than with WRF. The stronger wake in Simra is probably related to differences in model resolution, i.e. Godøy is higher and better reproduced in Simra than in WRF. In Simra, the wake is at times close to reaching Trælbodneset. Such wakes are likely to be frequent during northerly and northwesterly flow and will have a considerable impact on the flow structure at the site of the planned crossing when reaching that far.

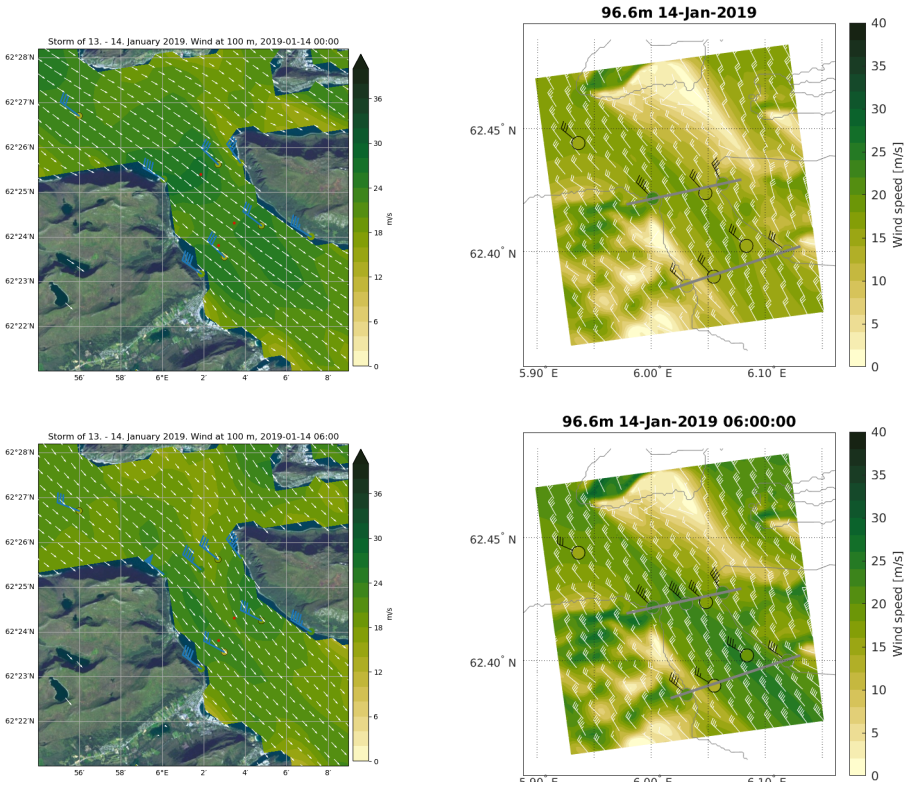

Figure 59: *Simulated wind from WRF at 75 m above sea level (left) and Simra (right) at 100 m over sea level during the peak of the storm. Also shown are available wind observations, from top of masts, at 75 m asl at the centre of the fjord and from the buoys (4 m asl. marked with black circles).*

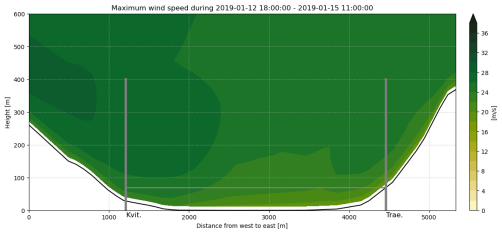

Figure 60: *The strongest simulated wind speed with WRF in a section along the planned crossing. Bridge tower and deck locations are indicated with grey lines.*

3.10.4 Simulated flow - vertical structure

The vertical structure of the simulated flow is shown in Figs. 60 and 61. The models indicate that the strongest winds are shown at and above the mast at Kvitneset, and that the weakest wind are found near Trælbodneset. The observed wind speeds are generally reproduced in WRF but Simra tends to underestimate the wind speed especially at 00 UTC.

Turbulence intensity (TI) is available from Simra and has been validated in Midtbø et al. [2020a] and Midtbø et al. [2020b]. Even if the wind speed from Simra is relatively low compared to the measurements, the level of the turbulence intensity from the model compares well to observations. Figure 62 shows maps of turbulence intensity at 100 m above sea surface and sections from Simra, depicting the increased turbulence (and reduced wind speed) due to topography. Note in particular the wake behind Godøya. In Simra, this wake reaches Trælbodneset (Figs. 63 and 64) with a depth of up to 300 m. The time series in Figure 64 show higher TI at Trælbodneset, than at Kvitneset and the centre position, during most of the storm. Increased turbulence is seen in the western part of the southern section (Figure 63) reaching up to 300-500 m, which is a result of a wake downstream of Kvitneset.

3.10.5 Horizontal flow structure from lidar observations

Fig. 65 shows lidar observations of the radial wind speed (RWS, i.e. the wind speed component along the lidar beam, which is equivalent to the projection of wind speed vector on the lidar beam) as well as a comparison with WRF simulated wind projected on the lidar beam. WRF fails to reproduce the weak radial wind speeds in the lee of Godøy, while the lidar observations indicate that Simra reproduces the wake (cf. Fig. 59). However, we note that a reduction in the radial wind speed may be caused by changes in

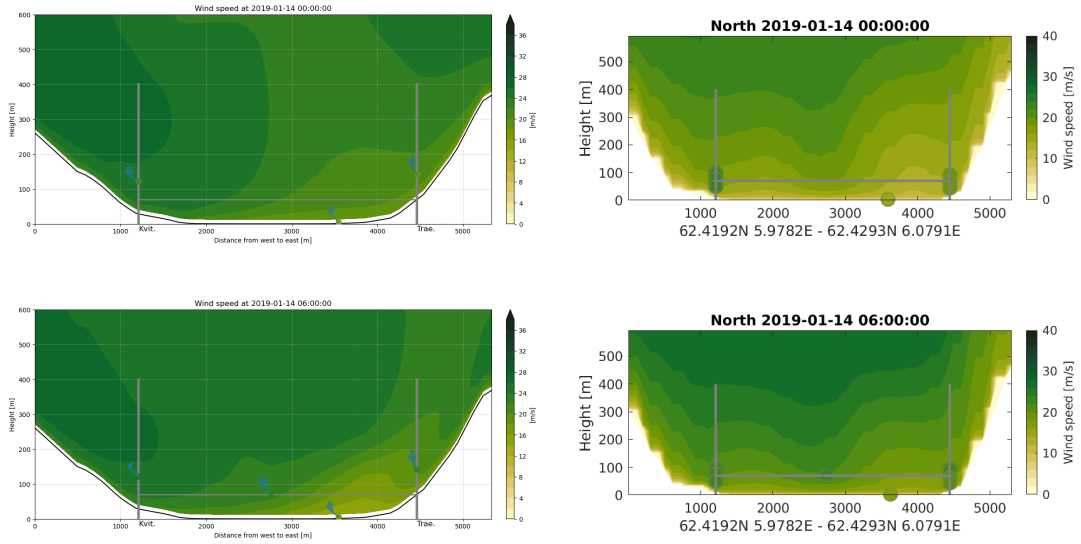

Figure 61: *The simulated wind speed with WRF (left) and Simra (right) in a section along the planned crossing. Bridge tower and deck locations are indicated with grey lines. Also shown are the observed wind and direction using traditional wind barbs and coloured circles based on the same colour map as the contour plot. Each flag is 5 m/s and a triangle is equivalent to 25 m/s. The direction of the barbs shows the observed horizontal direction.*

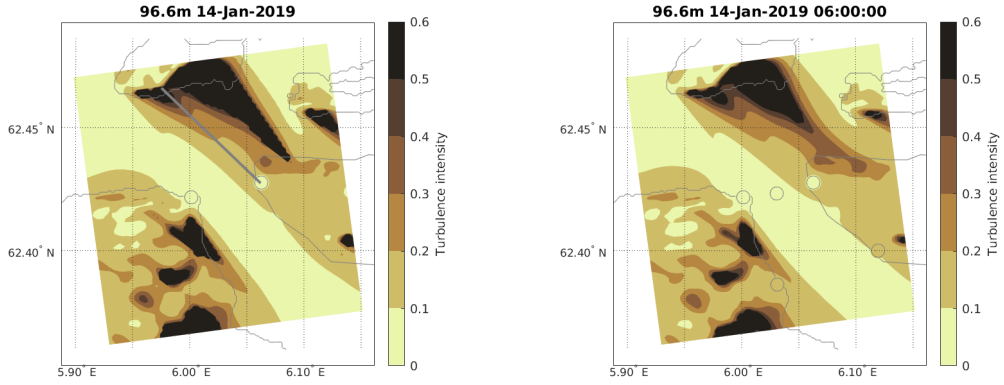

Figure 62: *Turbulence intensity from Simra at 97 m asl. The grey line indicates the location of the transect in Fig. 63.*

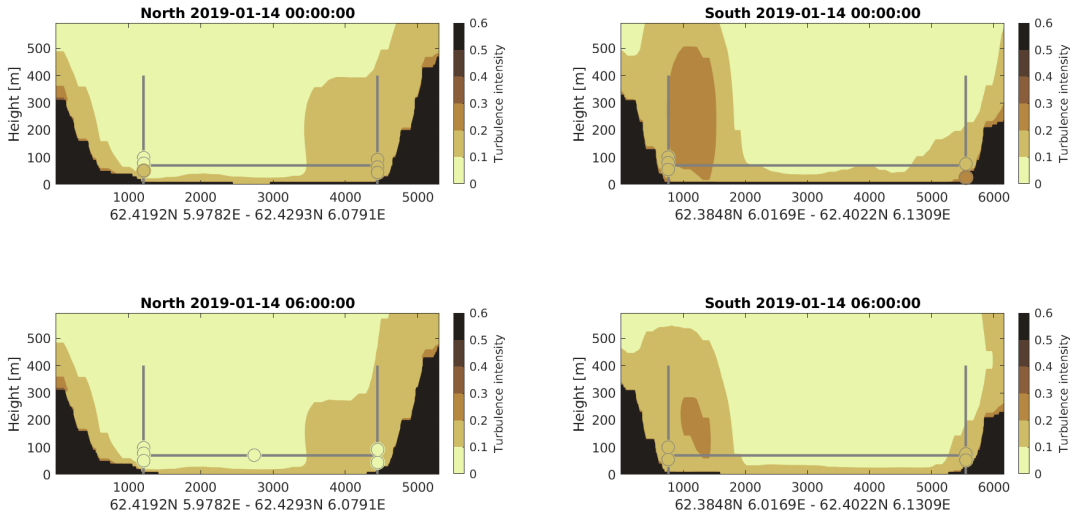

Figure 63: *Turbulence intensity from Simra at the northern (left) and southern crossing (right). Bridge tower and deck locations are indicated with grey lines.*

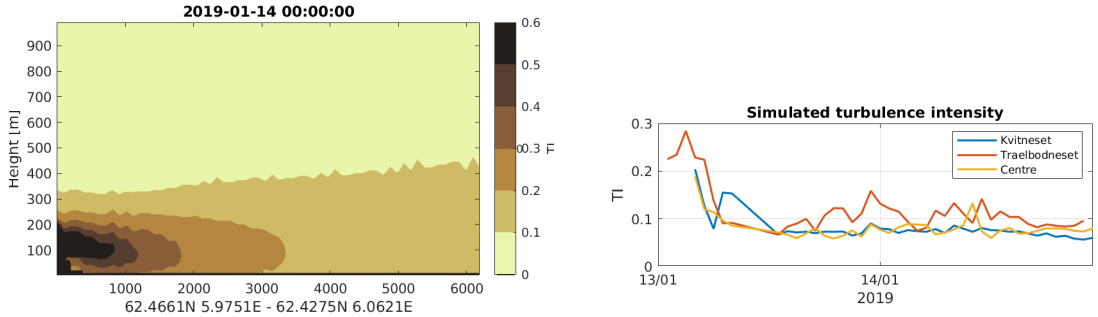

Figure 64: *Section of simulated turbulence intensity from Simra from Godøya to Trælbodneset (left) and from Simra at Kvitneset, Trælbodneset and the center of the fjord, during the storm (right).*

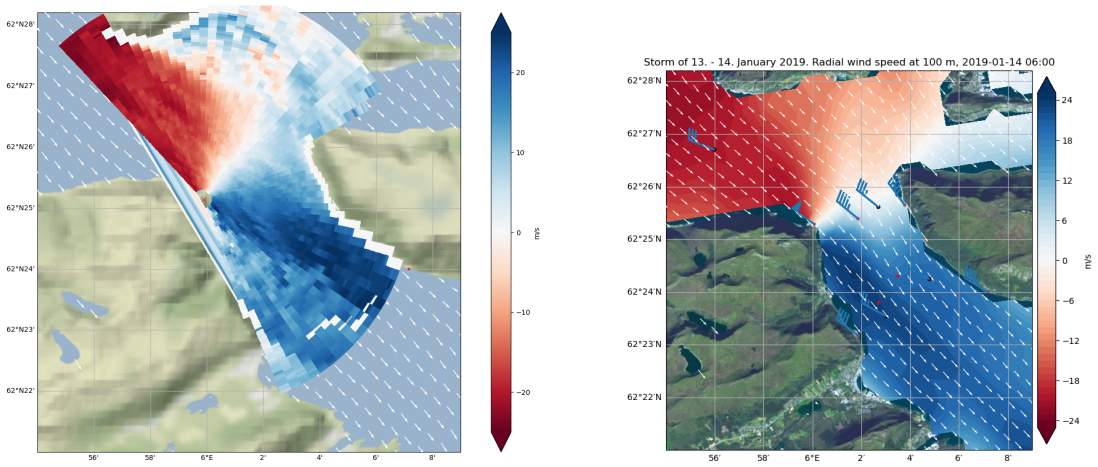

Figure 65: *Near instantaneous radial wind speed from the lidar at Kvitneset, based on 2 minutes of lidar observations (left) and on WRF simulated flow (right).*

wind direction or/and reduced wind speed, i.e. the rotation of the wind vector to more perpendicular to the lidar beam will give lower radial wind speeds. It is typically not possible to separate these two effects with RWS data from a single lidar.

3.10.6 Satellite observations of sea surface winds

The Sentinel-1A satellite with the instrument Advanced Synthetic Aperture Radar (ASAR) onboard had a passing over Sulafjorden in the morning of 14 January 2019. The radar back-scatter recording by the ASAR is converted to wind speed using using Openwind[6] i.e. an empirical relation and wind direction information from the atmospheric forecast model, in this project from the European Centre for Medium-Range Weather Forecasts (ECMWF). The quality of the wind speed from the satellite image is strongly dependent of the accuracy of the input wind direction from the model. The wind speed image in Figure 66 shows increased wind speed at Kvitneset and in the center of the fjord and a wake behind Godøy all of which resembles the spatial overview provided by Simra at 6 UTC (Figure 59). The wind quality flag from the OCN level 3 ESA product estimates the wind speed from this image to be good (dark blue - value equal to 0) in the Sulafjorden area (right).

[6]https://github.com/nansencenter/openwind

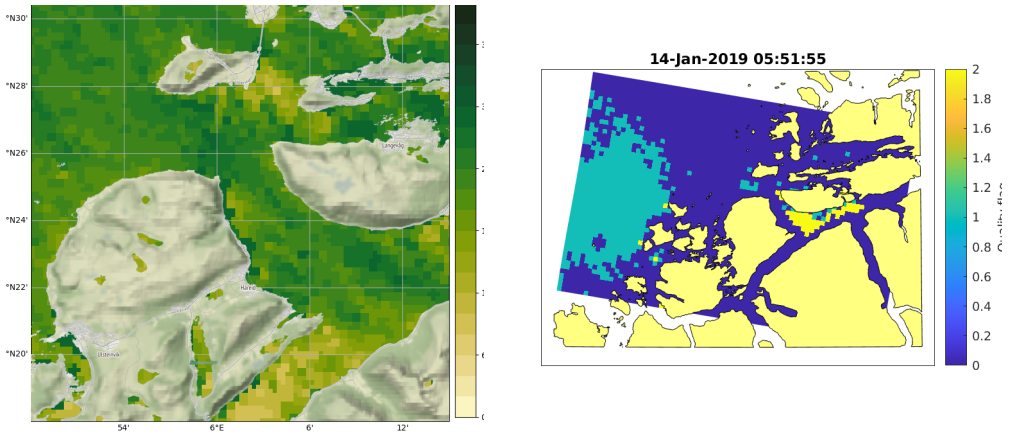

Figure 66: *Wind speed [m/s] at 10 m height from Sentinel1 ASAR satellite image (left). Wind quality flag for the same image: 0 (high quality), 1 (medium quality), 2 (low quality) or 3 (bad quality).*

3.10.7 Waves

During this storm on 13-14 January 2019 the significant wave height was 3 - 4 m at the outer crossing (Figures 58 and 67) which agree well with buoy A. Further inside the fjord, simulations of both Hs and Tp are higher than observed. The recorded peak period is reduced from 12-14 s at D to 10-12 s at A and C. It was earlier documented that the model has too little dissipation of swell in the fjord [Furevik and Aarnes, 2021], but for snapshot-comparisons like here, it should also be noted that the observed peak period naturally may vary considerably in a combined swell and wind sea condition, as in Sulafjorden. The spectra in figure 68 shows the combined wind sea and swell at all locations. A small amount of wind sea from the north is seen in the directional spectrum.

3.10.8 Currents

Model snapshots of surface currents from the storm show that the response of strong winds from the northwest are strong currents from the north offshore Godøy and in Sulafjorden with sharp gradients related to wake effects of land (Figure 69). The maximum current speed is found in the centre of Sulafjorden with velocities around 70 cm/s. The time series where observation and model data are compared show that the current directions are similar most of the time during the main storm event. The deviation in currents at buoy location C where the model overestimates the speed is probably due to a minor inconsistent positioning of the sharp gradient in this area where the waters near Hareid

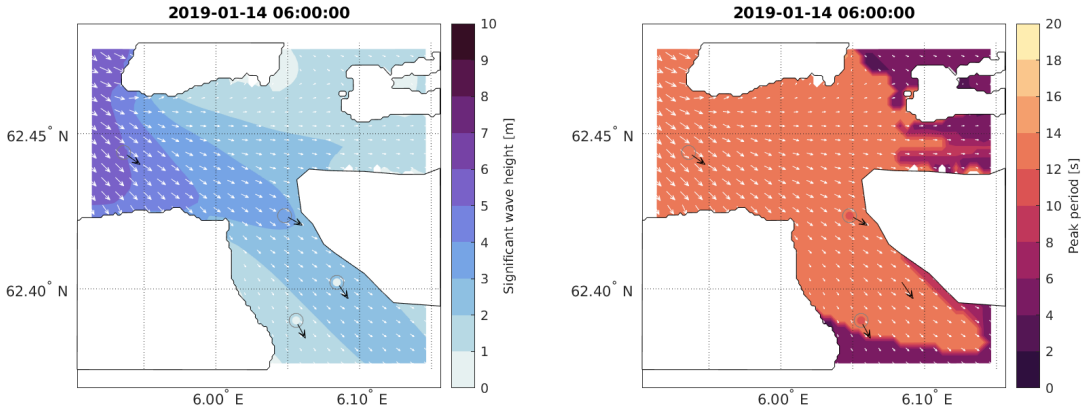

Figure 67: *Significant wave height [m] and peak direction from SWAN and observations at the peak of the storm.*

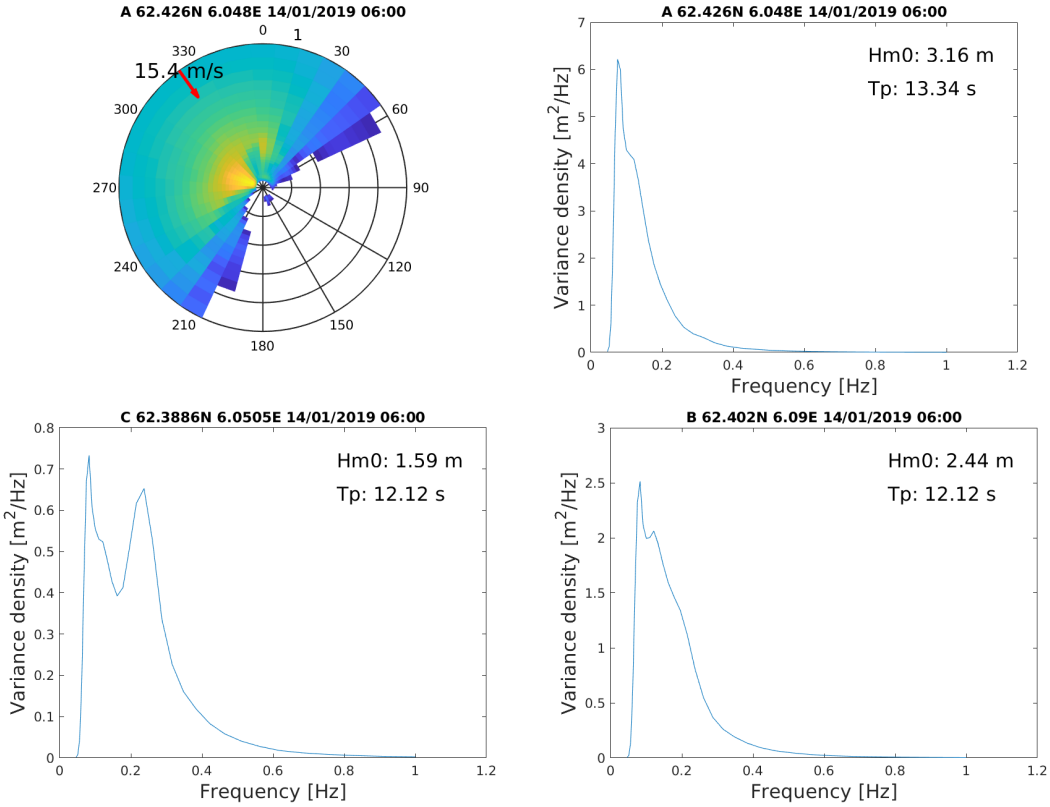

Figure 68: *2D (direction-frequency) wave spectrum from location A (top left panel) and 1D (frequency) wave spectra from locations A (top right panel), B (lower right panel) and C (lower left panel) from SWAN at the storm peak. Note the different scale on the y-axes. Wind speed and direction (from WRF) is shown in the 2D spectrum. The energy is plotted in the direction the waves come from. Significant wave height (Hm0 or Hs) and peak period (Tp) is indicated for each location in the 1D plots.*

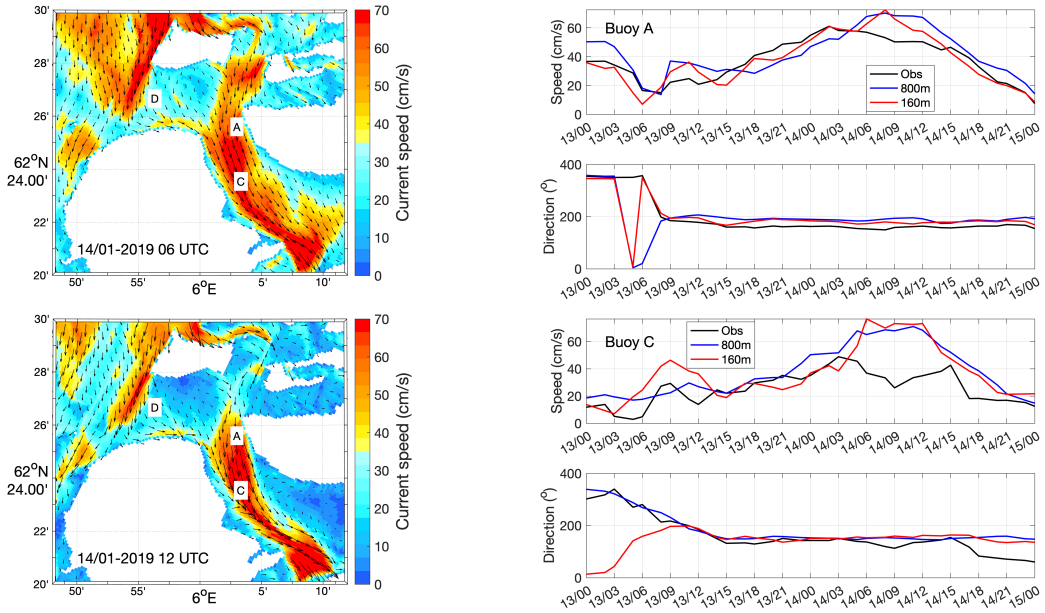

Figure 69: *The maps show instantaneous surface currents from the 160m-model valid at the times indicated in the map (left panels). The observational buoy locations A, C and D are denoted in the maps. The graphs to the right show current speed and direction at 1m depth from the two buoy locations A (upper two panels) and C (lower two panels) based on measurements (black line), NorKyst800 (blue) and 160m-model (red). The time stamps are written as day/hour.*

has much lower velocities than the central areas of Sulafjorden due to wake effects.

Since the long-term average current direction in Sulafjorden is toward the north, the strong winds from the northwest alter the current pattern in the entire water column (Figure 70). Instead of a 10 - 15 m thick surface layer with a northward flow and southward currents below down to approximately 100 m, the model sets up a southward flow from the surface down to about 50 m and northward currents below.

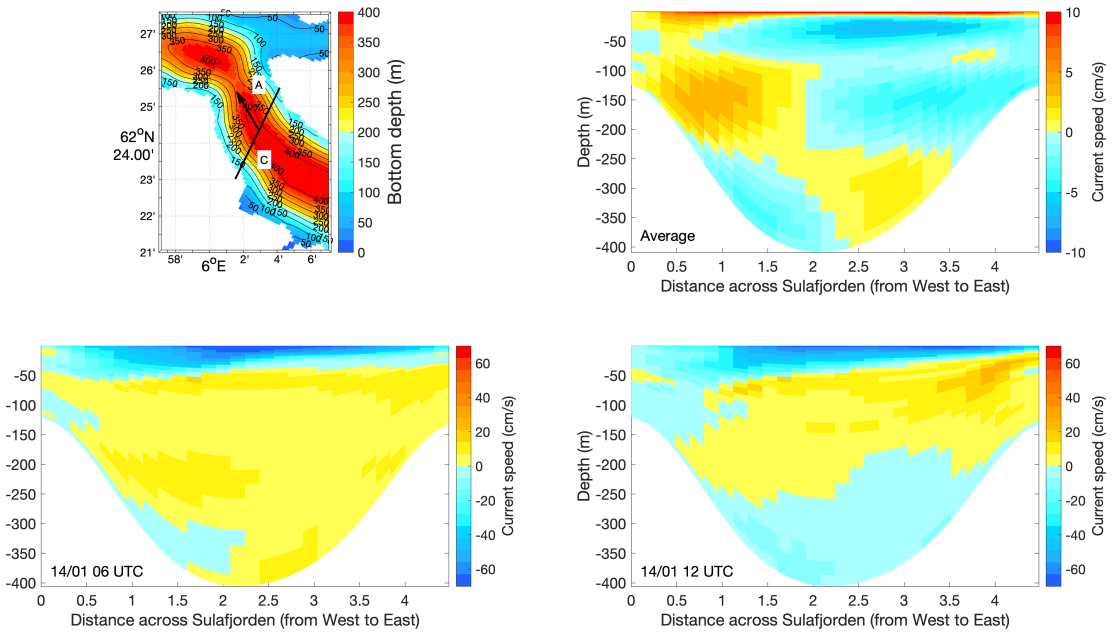

Figure 70: *The upper right panel is retrieved from Ágústsson et al. [2020a] and shows long-term average current speed normal to the transect crossing Sulafjorden denoted as a black line in the bathymetric map (upper left). The lower panels show two snapshots of current speed over the same transect. Red and yellow colors denote currents toward the north in the direction of the arrow in the map, while blue colors denote the opposite southerly currents.*

3.11 The storm of 10 December 2019

3.11.1 General overview

A southerly storm occurred in Sulafjorden on 10 December 2019. Observed 10-minute winds were from the south and reached 25 m/s at Kvitneset (18UTC) and 20 m/s at the fjord centre, see overview in Fig. 71. A classical broad low pressure system moves up from the mid-Atlantic prior to the event in Sulafjorden. The low centre is located over Iceland with an occluded front off the west coast of western Norway, see Fig. 72, at the time of strongest winds in Sulafjorden.

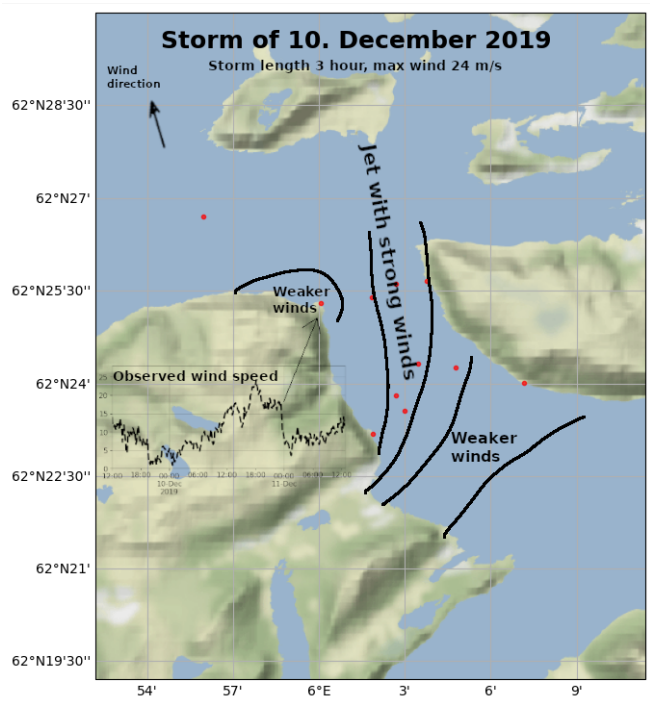

Figure 71: *A schematic summary of important aspects of the storm*

The observed wind speed and direction are reasonably well reproduced at Kvitneset by the WRF-model. They are likely to be over-estimated at the fjord centre. The WRF model shows a jet of strong winds emanating from the valleys at Hareid, on the west side of Sulafjorden, with the maximum wind speed over the eastern half of the planned crossing. The direction of the jet varies, and the simulated maximum wind speed value moves from the west to the east across the fjord.

During the storm, there are observational data available from 3 masts in Sulafjorden, but Trælbodneset was not operational. Observations of wind are also available at the fjord

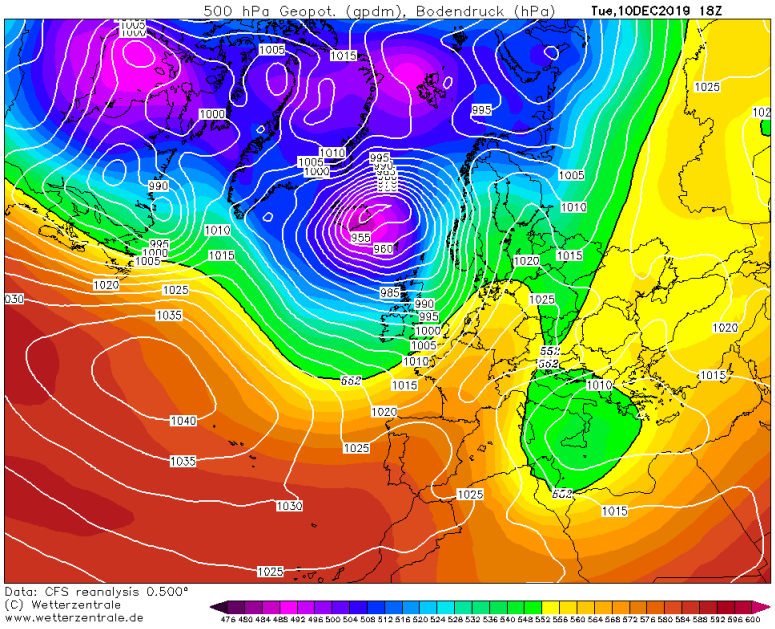

Figure 72: *The analysis from CFS (Climate Forecast System) showing surface pressure and 500 hPa geopotential. Figure is retrieved from Wetterzentale.*

centre from the scanning lidars. Data is also available from the buoys in Sulafjorden and Breisundet, but only at 4 m asl.

The WRF 500 m x 500 m dataset is available for the event. Data is also available from wave and current model.

3.11.2 Model performance and flow features

Although simulating the winds reasonably well, the WRF-model seems to have too high winds compared to Kvitneset and at the planned bridge deck at the fjord centre in the afternoon the 10th, see Fig. 73. This happens at the time when the occluded front is passing. It seems like there are two disturbances in the model while the observations have a mere single peak at 18 UTC. In Fig. 74 showing plan view of the winds in Sulafjorden also indicate that the model has problems with getting the direction correct (too westerly in the model) which may indicate that there are problems with the frontal passage. A section across the fjord, from Kvitneset to Trælbodneset shows the extent of the planned wind speed maxima at the fjord centre, while weaker winds are found at the towers (Fig. 75).

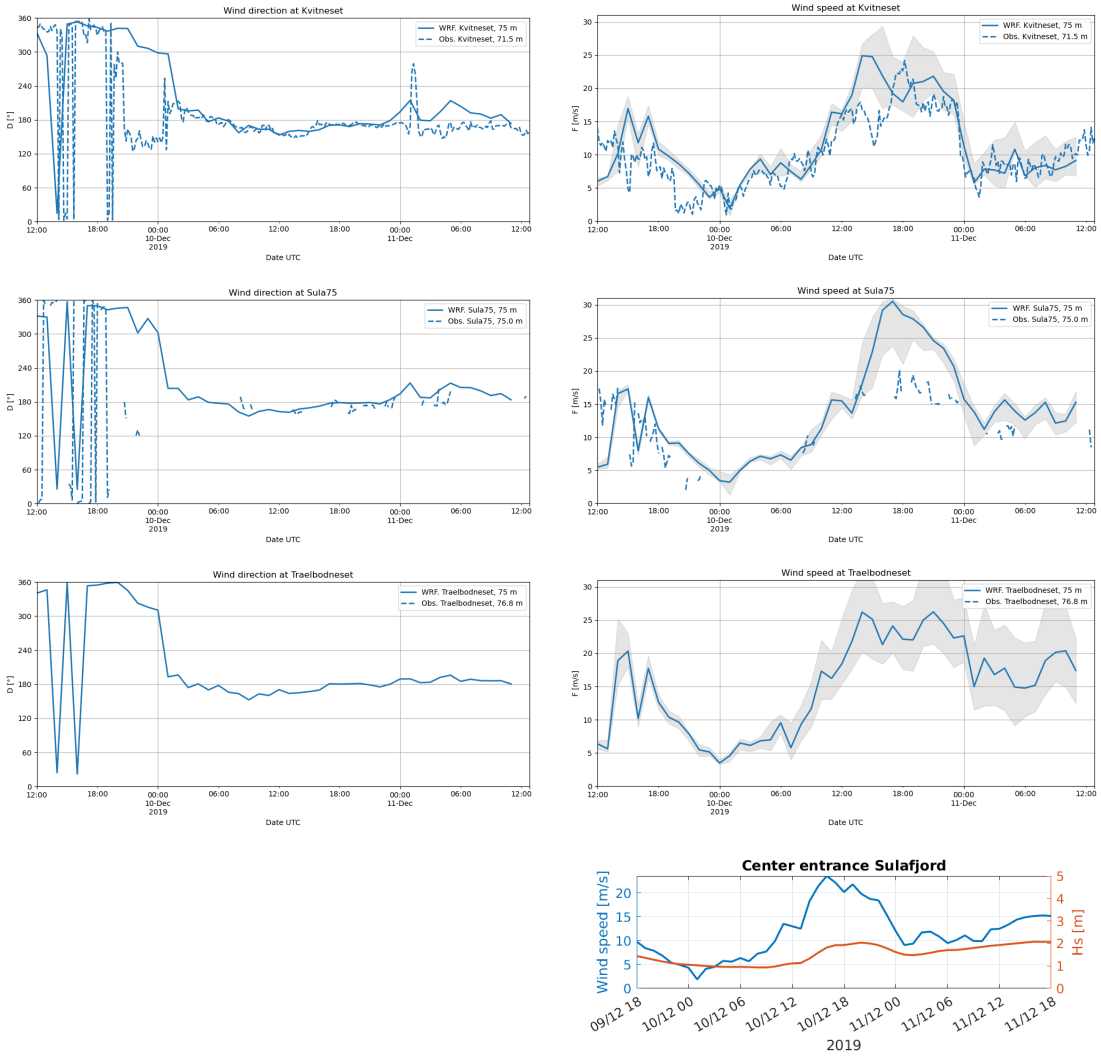

Figure 73: *Simulated (solid lines) and observed (dashed) wind direction (left) and wind speed (right) from the WRF-model. The grey envelope indicates the range of the simulated wind speed in the 9 nearest grid points (eq. 1 km x 1 km area). Lower right panel shows wind speed in blue (10 m) and significant wave height (red line) at the center of the outer crossing.*

3.11.3 Waves

The situation is similar to 29 November 2019 although the wind is somewhat stronger giving higher waves in this case. Hs is around 2 m in Sulafjord, dominated by wind sea in the inner part of the fjord and incoming waves/swell in the outer part (location D and A). The simulated wave height seems slightly overestimated when comparing to

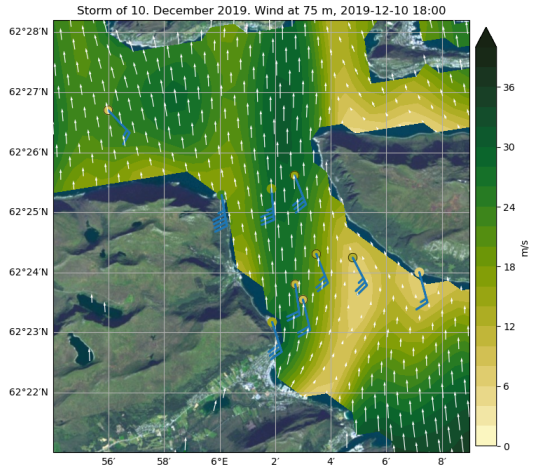

Figure 74: *Simulated wind from WRF at 75 m above sea level, valid when the storm is strongest. Also shown are the observed wind and direction using traditional wind barbs and coloured circles based on the same colour map as the contour plot. Each flag is 5 m/s and a triangle is equivalent to 25 m/s. The direction of the barbs shows the observed horizontal direction. Buoy observations at 4 m are marked with a black circle.*

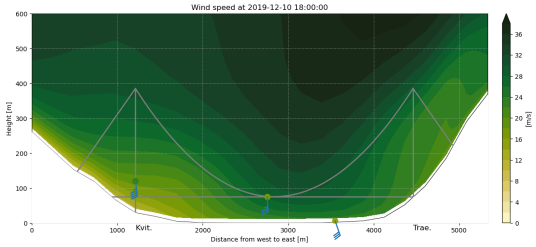

Figure 75: *Simulated wind from WRF in a section along the planned crossing. Bridge location is indicated with grey lines. Also shown are the observed wind and direction using traditional wind barbs and coloured circles based on the same colour map as the contour plot. Each flag is 5 m/s and a triangle is equivalent to 25 m/s. The direction of the barbs shows the observed horizontal direction.*

the observations and the incoming waves are too strong compared to the wind sea in the central part (at B and B1), but the general picture is confirmed (figure 76). The spectra in figure 77 clear show the two wave systems at all three buoy locations.

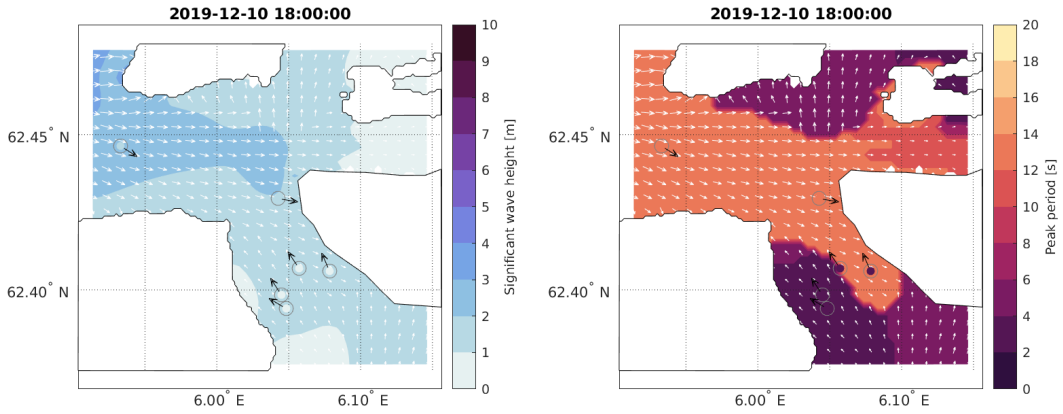

Figure 76: *Significant wave height [m] (left) and peak period (right) from SWAN and observations at the storm peak. Buoy observations are included as colored points in the same scale as the SWAN contour plot and with black arrows for the peak direction*

3.11.4 Currents

Model snapshots of surface currents from the storm show that the response of strong winds from the south are visible in the entire Sulafjorden fjord system with northward currents with sharp gradients related to wake effects of land (Figure 78). The maximum current speed is about 50 cm/s in location A, and this location also corresponds to the area with the highest velocities toward the north. The time series where observation and model data are compared show that the current speed and direction correspond well most of the time during the main storm event.

The long-term average surface current direction in Sulafjorden is toward the north, and the winds from the south extend the layer with northward currents down to approximately 100m depth (Figure 79). During the last part of the storm event (10 December 2019, at 15 UTC), we see a horizontal separation of the surface circulation in Sulafjorden with strong, northward currents in the eastern part and southward currents in the western part.

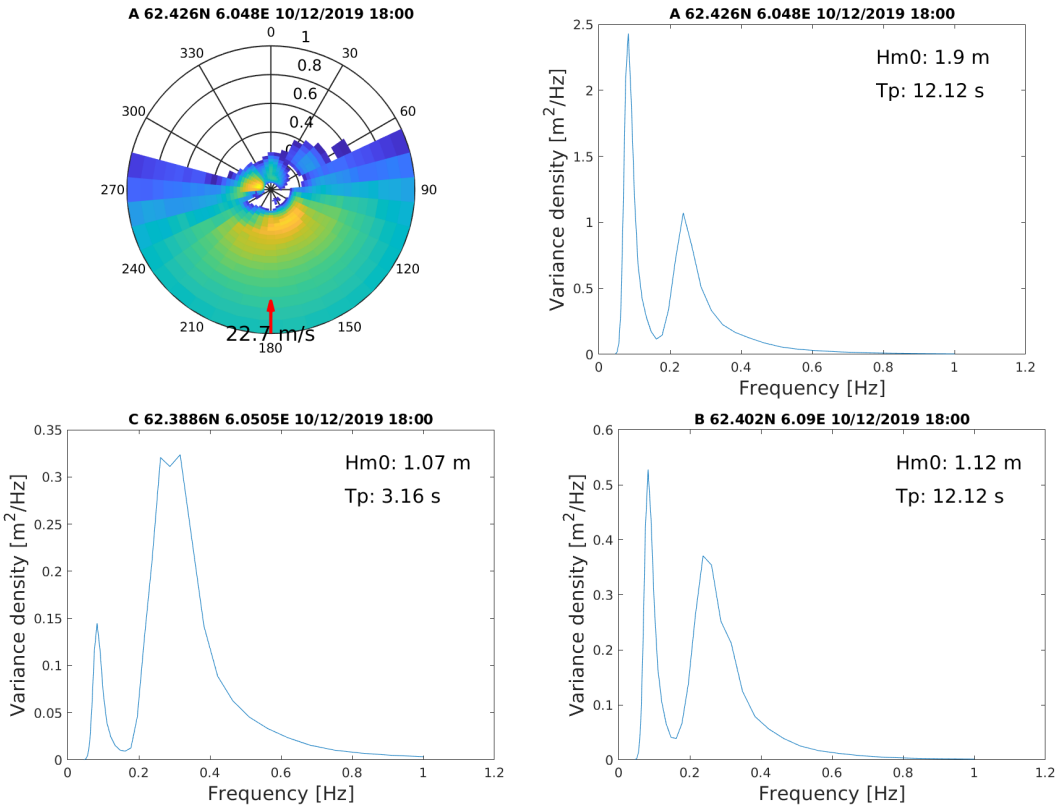

Figure 77: *2D (direction-frequency) wave spectrum from location A (top left panel) and 1D (frequency) wave spectra from locations A (top right panel), B (lower right panel) and C (lower left panel) from SWAN at the storm peak. Please note the different scale on the y-axes. Wind speed and direction (from WRF) is shown in the 2D spectrum. The energy is plotted in the direction the waves come from. Significant wave height (Hm0 or Hs) and peak period (Tp) is indicated for each location in the 1D plots.*

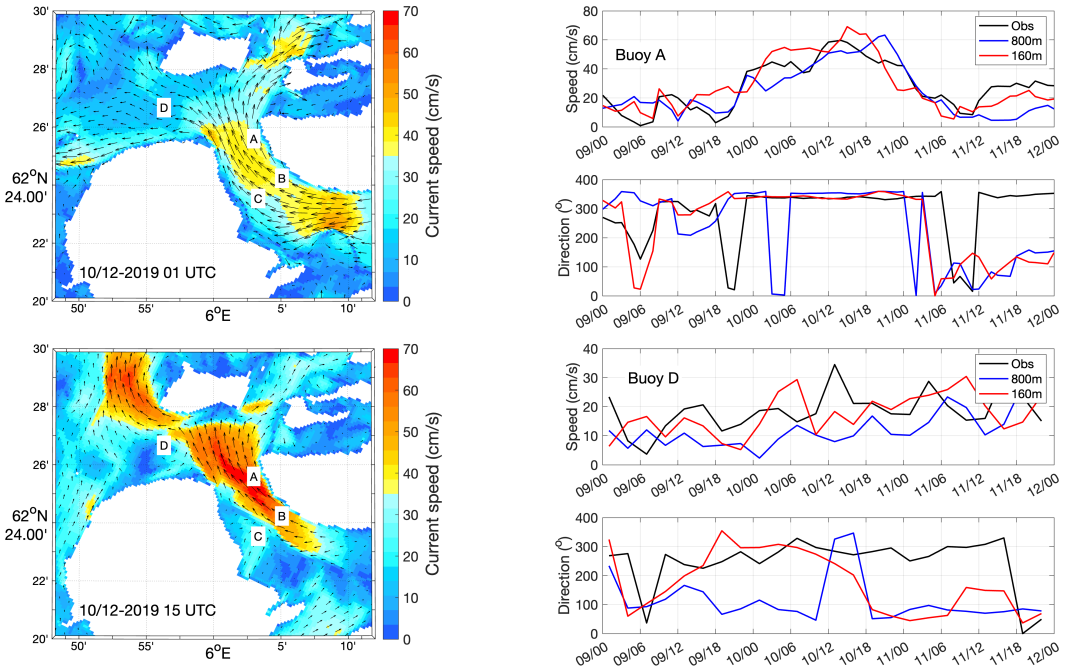

Figure 78: *The maps show instantaneous surface currents from the 160m-model valid at the times indicated in the map (left panels). The observational buoy locations A, B, C and D are denoted in the maps. The graphs to the right show current speed and direction at 1m depth from the two buoy locations A (upper two panels) and D (lower two panels) based on measurements (black line), NorKyst800 (blue) and 160m-model (red). The time stamps are written as day/hour.*

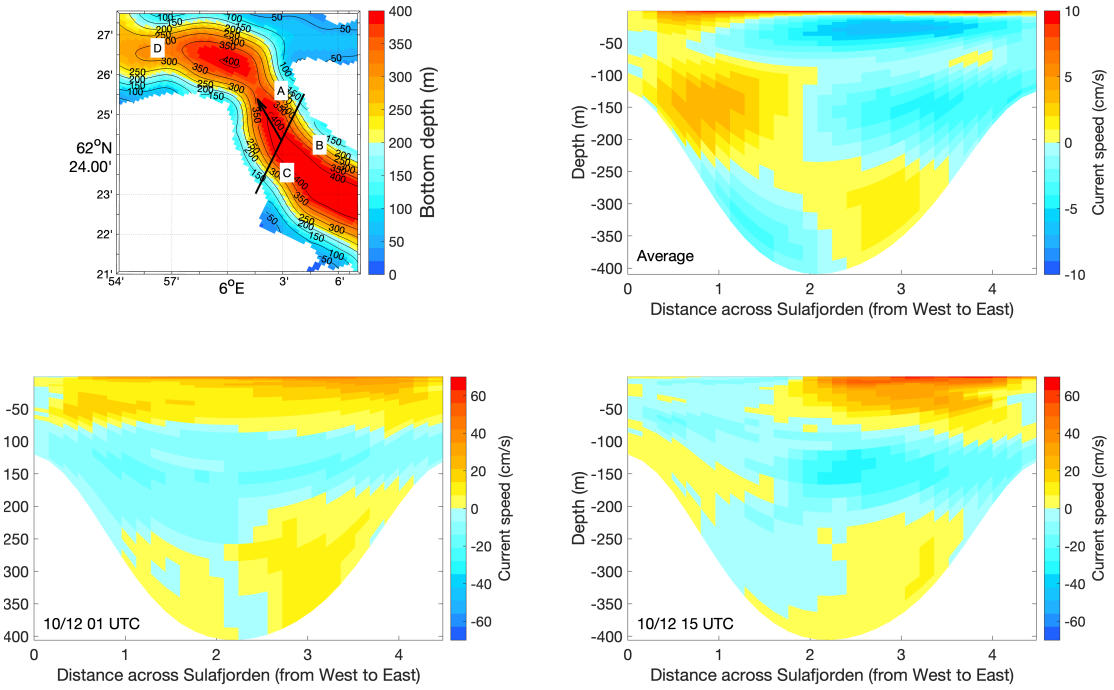

Figure 79: *The upper right panel is retrieved from Ágústsson et al. [2020b] and shows long-term average current speed normal to the transect crossing Sulafjorden denoted as a black line in the bathymetric map (upper left). The lower panels show two snapshots of current speed over the same transect. Red and yellow colors denote currents toward the north in the direction of the arrow in the map, while blue colors denote the opposite southerly currents.*

3.12 The storm of 2 January 2020

3.12.1 General overview

In early January 2020, a series of southerly storms appeared in Sulafjorden. The storm of 2 January is the first in this series.

Observed 10-minute winds were from the south turning westerly and reached up to 22 m/s at Trælbodneset, where the strongest winds were observed, see schematic overview in Fig. 80. The wind was only slightly weaker at the centre of the fjord, and 16 m/s at Kvitneset. The WRF simulations indicated stronger winds at Trælbodneset (25 m/s). The observed wind speed and direction are well reproduced by the WRF-model, except that the wind speed is overestimated at Trælbodneset. The model shows transient jets of strong winds emanating from the valleys on the west side of Sulafjorden, i.e. near Brandal and Hareid. The location of the jets varies, but Kvitneset is in the lee of the mountains while Trælbodneset is at least once located in one of the jets.

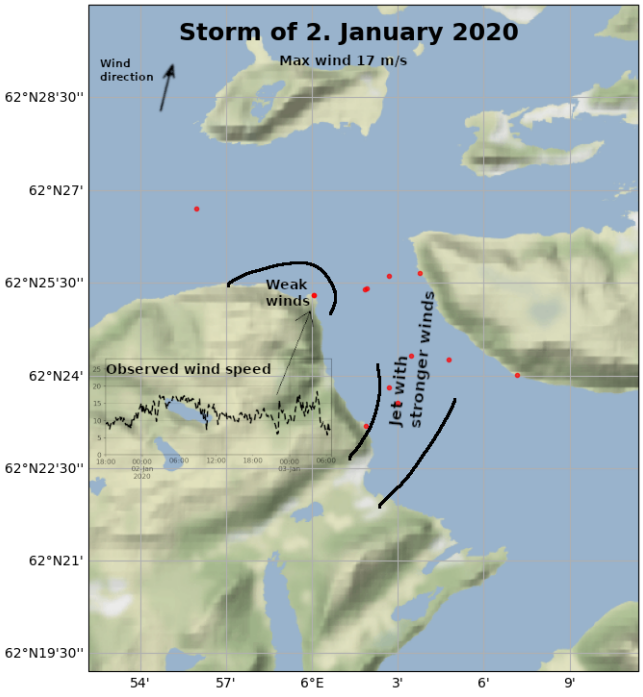

Figure 80: *A schematic summary of important aspects of the storm.*

The event is associated with a deep low pressure system near Jan Mayen and a broad high pressure system centred over the Mediterranean, resulting in a steep pressure gradient over the west coast of Norway.

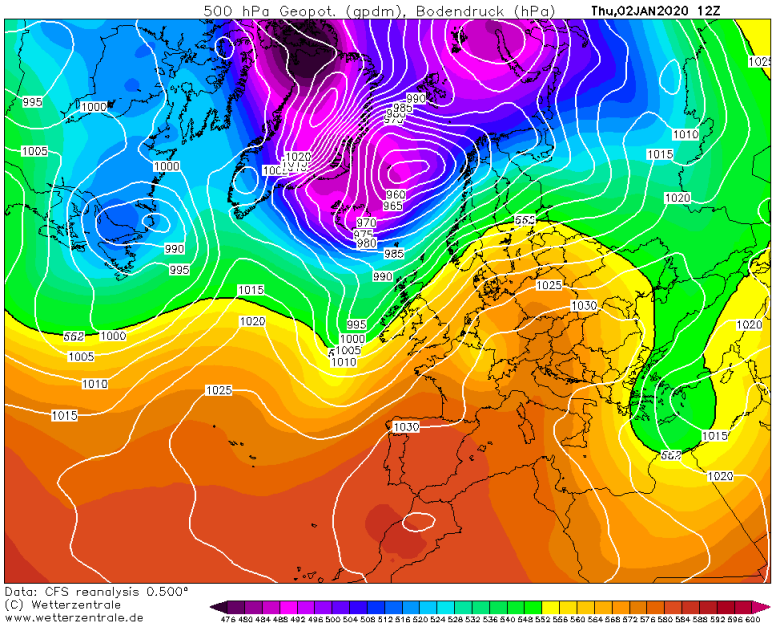

Figure 81: *The analysis from CFS (Climate Forecast System) showing surface pressure and 500 hPa geopotential. Figure is retrieved from Wetterzentale.*

Four masts was recording during the event and we focus on the stations Kvitneset and Trælbodneset. Data is also available from three lidar systems; the vertical lidar at the top of the Kvitneset mast, the buoy lidar, and the scanning lidars. Data is also available from the buoys (4 m asl) in Sulafjorden.

The WRF 500 m x 500 m and the Simra 100 m x 100 m simulated the situation. Data is also available from wave and current model.

3.12.2 Simulated flow - horizontal structure

Simulated winds from Simra show 2-3 wakes formed by the topography on the western side of the fjord. One wake stretches out from near Langeneset to the northern crossing. Kårsteinen is probably also affected by a wake which explains the very low wind there. There are 5 buoys and two masts in the region of enhanced wind in the center of the fjord which mostly confirm the simulated wind field here. Turbulence intensity from Simra (Fig. 84 lower panel) shows increased turbulence associated with the wakes.

3.12.3 Simulated flow - vertical structure

The vertical structure of the flow at the northern section is affected by the wakes (described above) with some variations in wind speed across the fjord (Figure 85 upper pan-

Figure 82: *Simulated (solid lines) and observed (dashed) wind direction (left) and wind speed (right), using simulated data from the WRF-model. The grey envelope indicates the range of the simulated wind speed in the 9 nearest grid points (eq. 1 km x 1 km area). Lower right panel shows wind speed in blue (10 m) and significant wave height (red line) at the center of the outer crossing.*

els). The simulated wind speed in both WRF and Simra is, overall, increasing from west to east which is also the tendency in the observations.

The turbulence intensity is also higher for the northern section as a result of the wake and very low over the southern section (Figure 85 lower panels). The measurements of TI from the masts generally confirm the simulations.

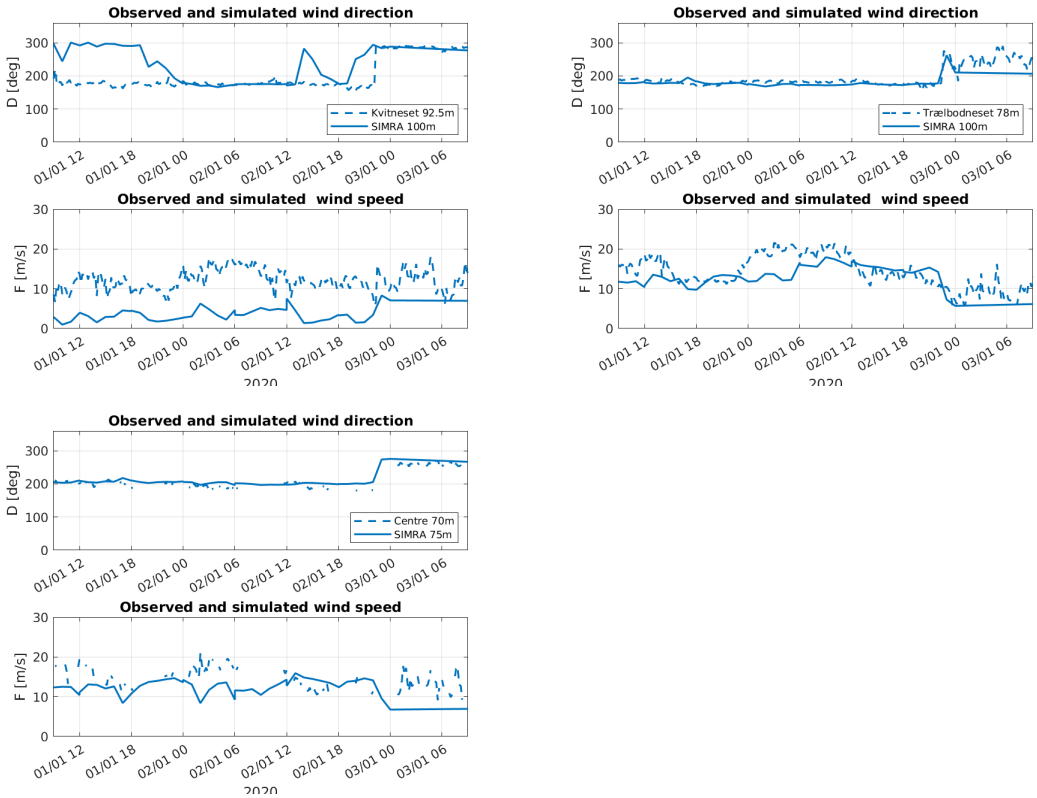

Figure 83: *Observed (dashed lines) and simulated (solid lines) wind direction and wind speed at 100 m from the Simra-model.*

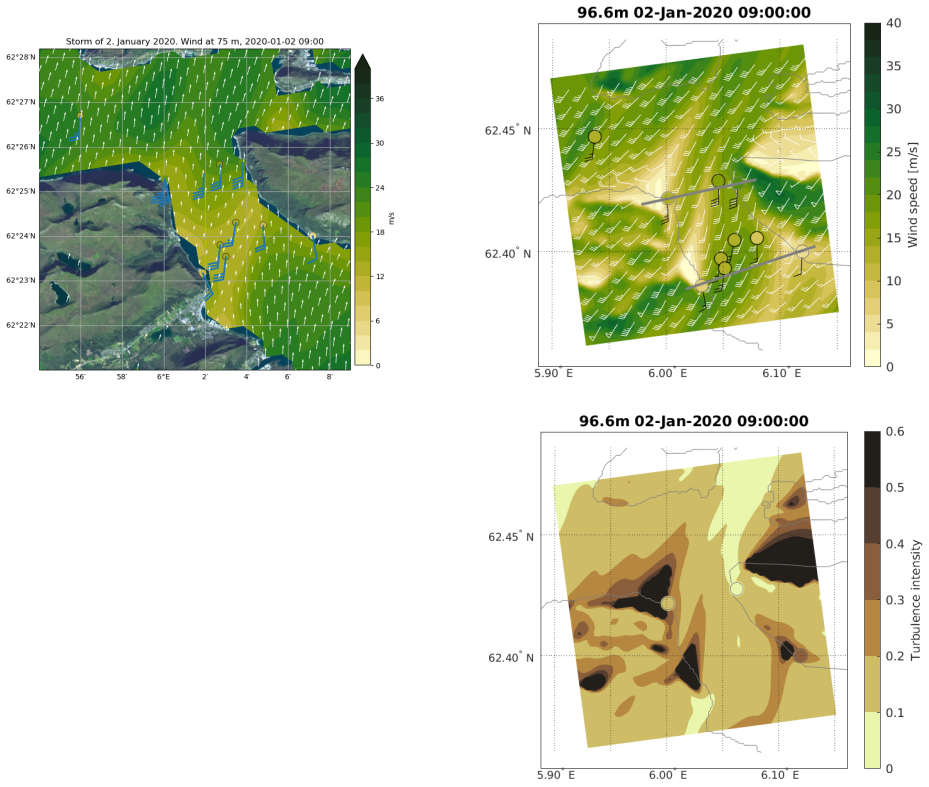

Figure 84: *Upper panels: Simulated wind from WRF at 75 m above sea level (left), and simulated wind from Simra at 97 m above sea level (right), valid when the storm is strongest. Also shown are the observed wind and direction using traditional wind barbs and coloured circles based on the same colour map as the contour plot. Each flag is 5 m/s and a triangle is equivalent to 25 m/s. The direction of the barbs shows the observed horizontal direction. Buoy measurements at 4 m are indicated with a black outline. The grey lines indicate the northern and southern sections. Lower panel: Simulated turbulence intensity from 97 m at Simra.*

3.12.4 Waves

In this southern wind case, which is similar to the previous ones (28 November 2018 and 10 December 2019), we see a split in the observed peak direction at C and C1 versus B and B1 (Figure 86). The buoys (C and C1) near Hareid in the west are sheltered from the incoming waves and thus the wind sea (coming from the south with low peak period) is dominating. This is in agreement with the numerical simulation. The wave height is constant around 2 m during the event (Figure 82). Spectra (figure 87) shows the double peaks at three buoy locations.

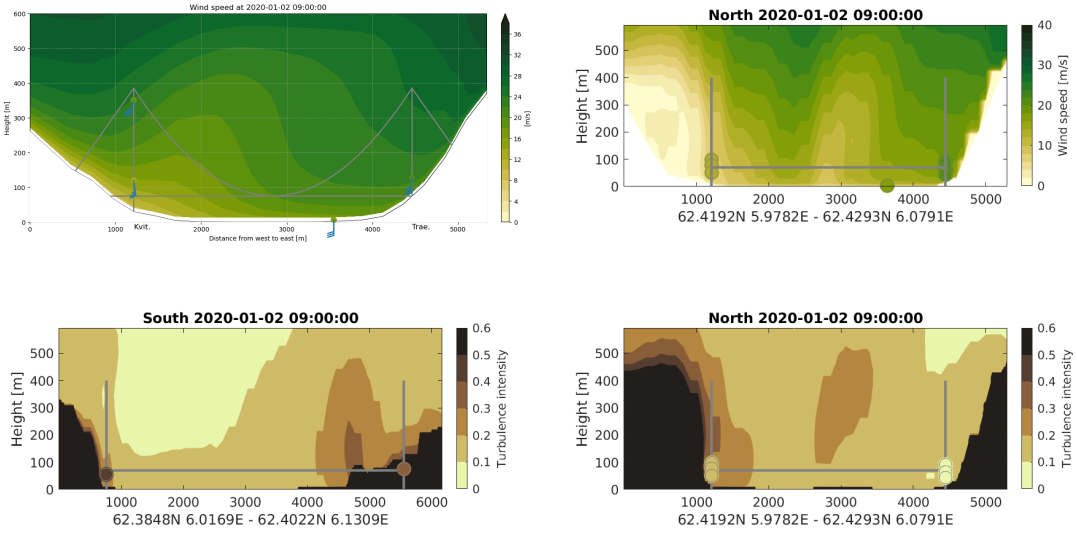

Figure 85: *Simulated wind from WRF (left) and from Simra (right) in a section along the planned crossing, at 9 UTC, 2 January 2020. Bridge location is indicated with grey lines. Also shown are the observed wind and direction using traditional wind barbs and coloured circles based on the same colour map as the contour plot. Each flag is 5 m/s and a triangle is equivalent to 25 m/s. The direction of the barbs shows the observed horizontal direction.*

3.12.5 Currents

Model snapshots of surface currents from the storm show that the response of strong winds from the south are visible in Breisundet as eastward currents and a continuing flow toward south-southeast in Sulafjorden with sharp gradients related to wake effects of land (Figure 88). The maximum current speed is about 60 cm/s in location A, and this location also corresponds to the area with the highest velocities toward the southeast. The time series where observation and model data are compared show that the current speed and direction correspond well most of the time during the main storm event.

Since the long-term average current direction in Sulafjorden is toward the north, the strong surface currents from the west-northwest alter the current pattern in the entire water column (Figure 89). Instead of a 10-15 m thick surface layer with a northward flow and southward currents below down to approximately 100 m, the model sets up a southward flow from the surface down to more than 100 m and northward currents below.

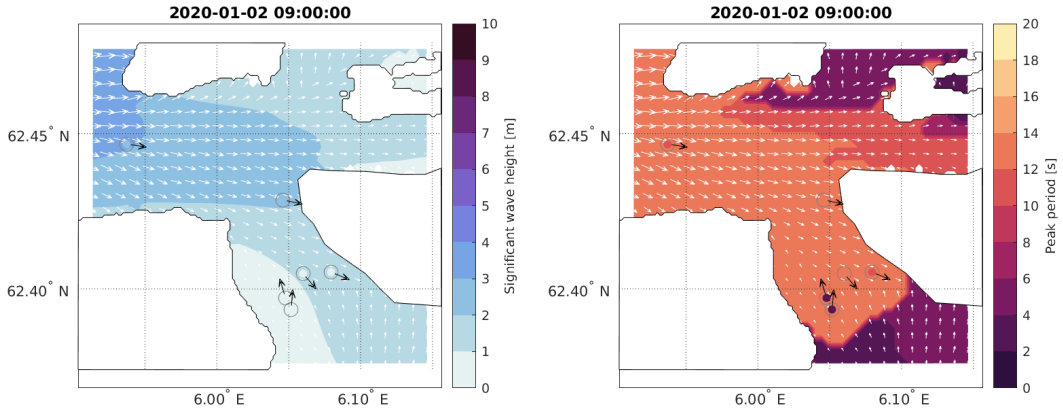

Figure 86: *Significant wave height [m] (left) and peak period (right) from SWAN and observations at the peak of the storm.*

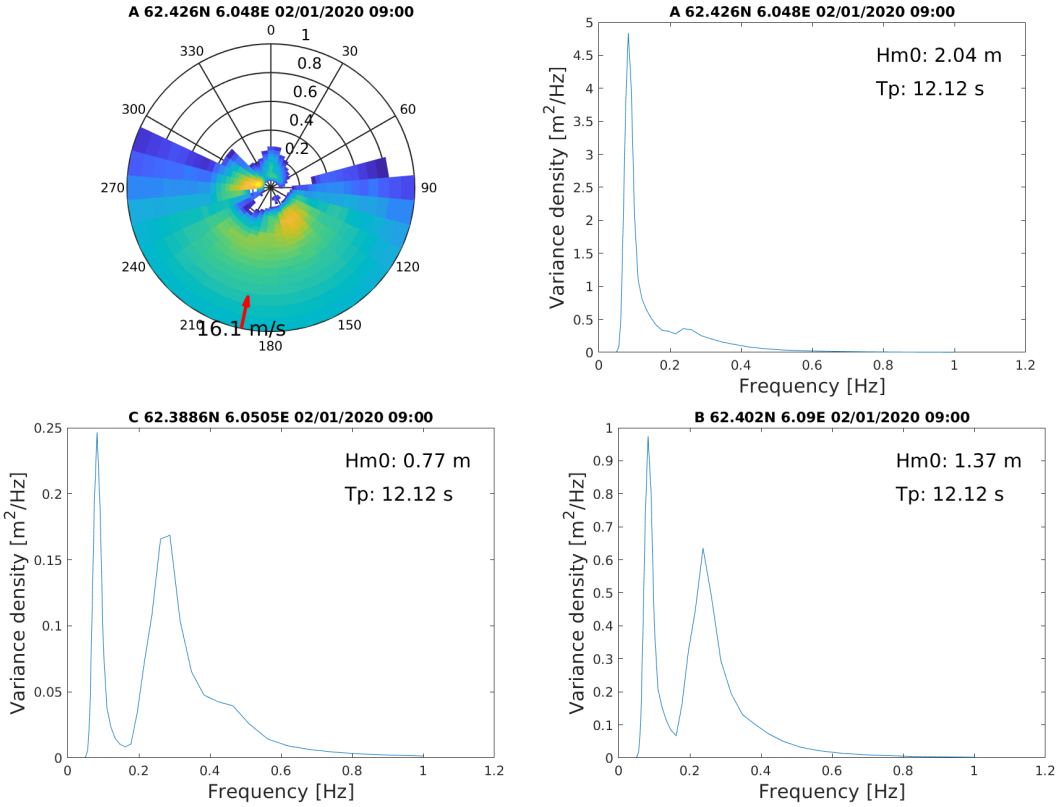

Figure 87: *2D (direction-frequency) wave spectrum from location A (top left panel) and 1D (frequency) wave spectra from locations A (top right panel), B (lower right panel) and C (lower left panel) from SWAN at the storm peak. Please note the different scale on the y-axes. Wind speed and direction (from WRF) is shown in the 2D spectrum. The energy is plotted in the direction the waves come from. Significant wave height (Hm0 or Hs) and peak period (Tp) is indicated for each location in the 1D plots.*

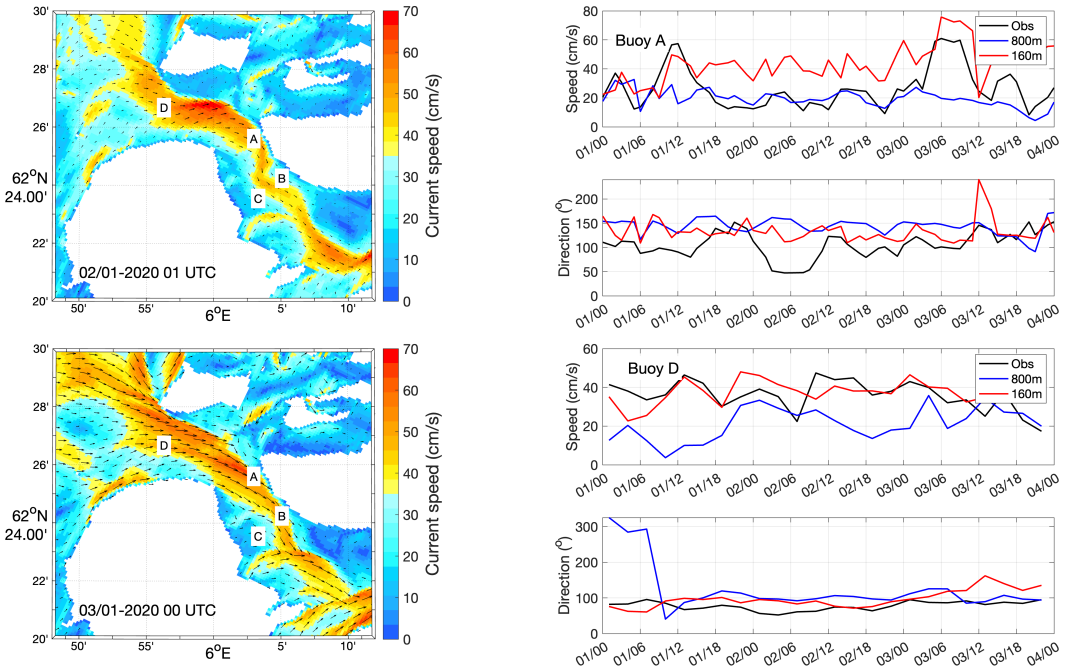

Figure 88: *The maps show instantaneous surface currents from the 160m-model valid at the times indicated in the map (left panels). The observational buoy locations A, B, C and D are denoted in the maps. The graphs to the right show current speed and direction at 1m depth from the two buoy locations A (upper two panels) and D (lower two panels) based on measurements (black line), NorKyst800 (blue) and 160m-model (red). The time stamps are written as day/hour.*

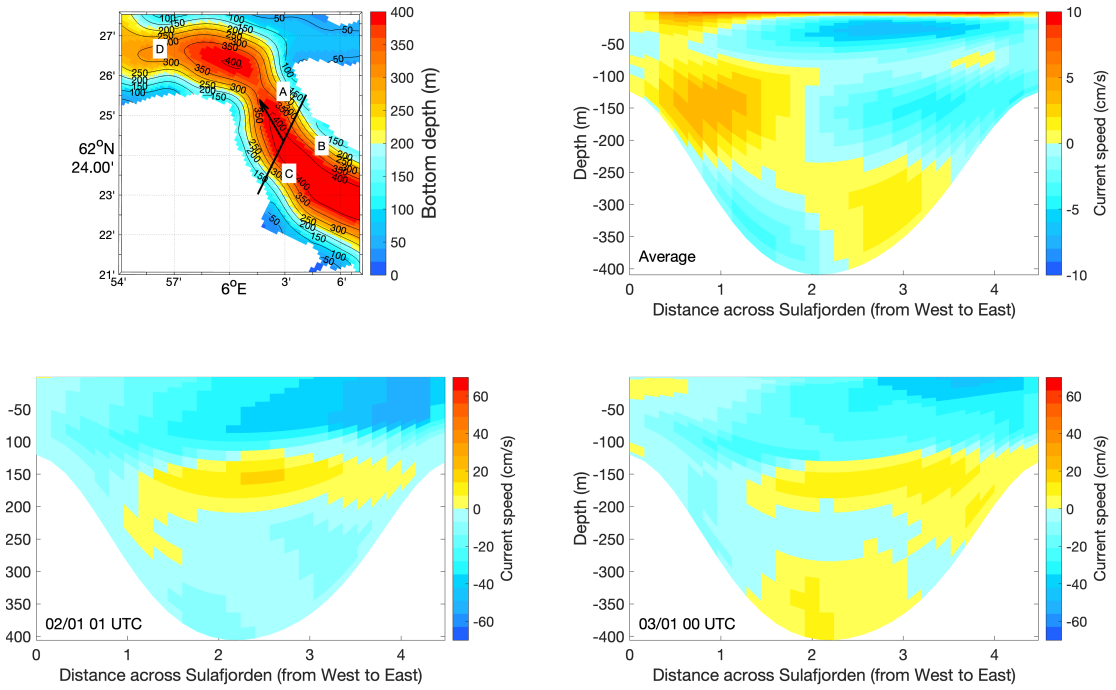

Figure 89: *The upper right panel is retrieved from Ágústsson et al. [2020b] and shows long-term average current speed normal to the transect crossing Sulafjorden denoted as a black line in the bathymetric map (upper left). The lower panels show two snapshots of current speed over the same transect. Red and yellow colors denote currents toward the north in the direction of the arrow in the map, while blue colors denote the opposite southerly currents.*

3.13 The storm of 7 January 2020

3.13.1 General overview

The storm of 7 January is considerably stronger than the latter storm (2 January), see Fig 90 for an overview.

Observed 10-minute winds were from the south and west and showed magnitudes as great as 25 m/s at the masts and at the centre of the fjord. The WRF simulations indicated even stronger winds at the fjord centre and at Trælbodneset.

The observed wind speed and direction are well reproduced by the WRF-model, except that the wind speed is overestimated at Trælbodneset.

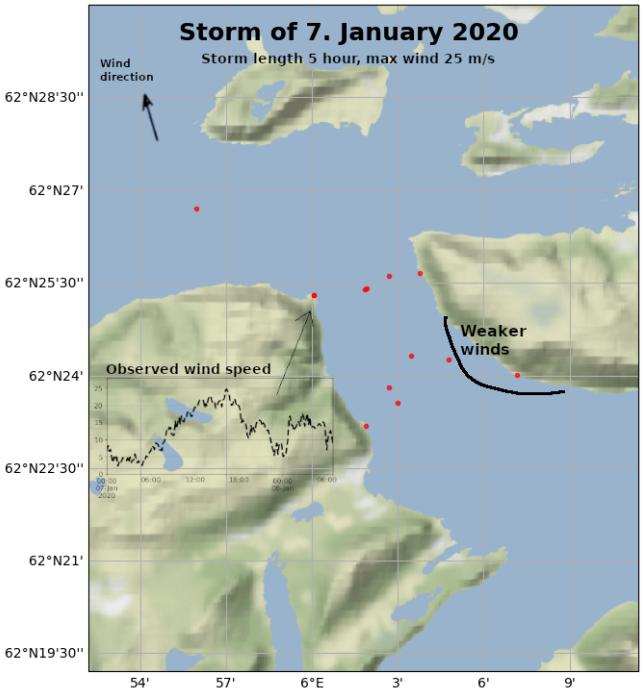

Figure 90: *A schematic summary of important aspects of the storm*

The event is associated with a broad and deep low over East-Iceland and a broad high pressure system stretching from Iberian peninsula towards Belarus, resulting in a steep pressure gradient over the west coast of Norway.

Four masts recorded in Sulafjorden during the storm, and we focus in particular on Kvitneset and Trælbodneset. Data is also available from three lidar systems; 1) the vertical lidars at the top of the Kvitneset mast and 2) on the buoy lidar, as well as from 3) the scanning lidars onshore. Data is also available from the buoys (4 m asl) in Sulafjord.

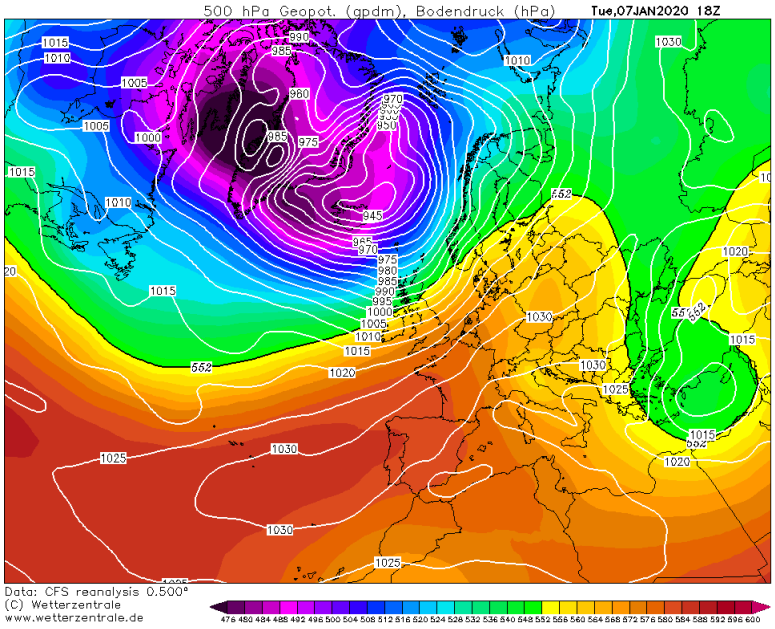

Figure 91: *The analysis from CFS (Climate Forecast System) showing surface pressure and 500 hPa geopotential. Figure is retrieved from Wetterzentale.*

Both model suites were used for this event. Data is also available from wave and current model.

3.13.2 Simulated flow - horizontal structure

The simulated wind field from WRF is rather smooth (see Figure 93), but when comparing to the wind field from Simra, we see a tendency for the same wake structures, similar to the previous cases with southerly wind. The wind direction seems to be in agreement with the observations. The wakes and streaks of enhanced wind speed (jets) are found affecting the crossings as we have seen earlier for southerly situations. The turbulence intensity according to Simra is reduced across the fjord.

3.13.3 Simulated flow - vertical structure

According to the simulations, the southerly wind conditions lead to higher wind at the eastern side of the fjord in the northern section (Figure 94 upper panels). This is not confirmed by the wind speed at Kvitneset, which is very high at all heights. The turbulence intensity according to Simra is moderate but higher for the southern section.

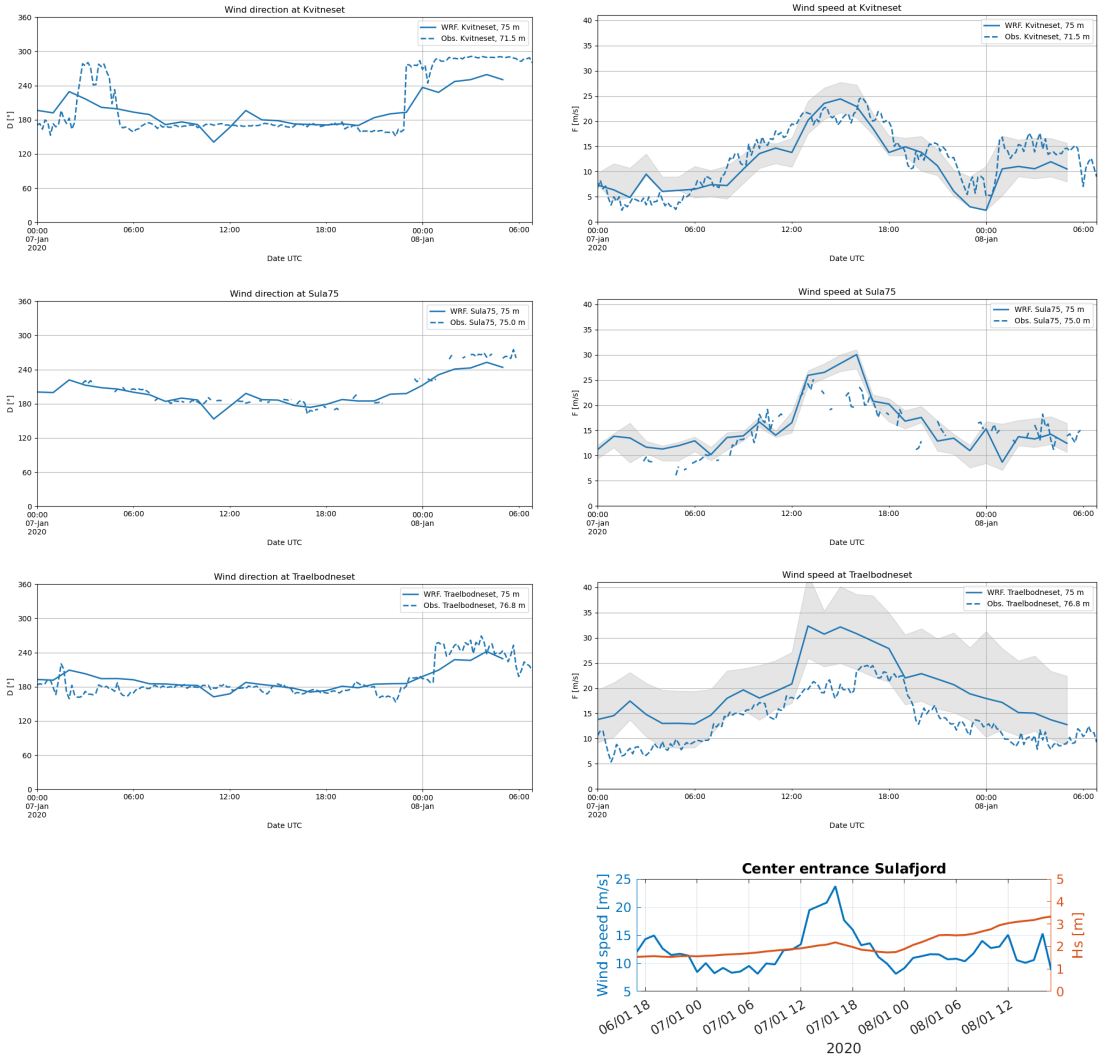

Figure 92: *Simulated (solid lines) and observed (dashed) wind direction (left) and wind speed (right) from the WRF-model. The grey envelope indicates the range of the simulated wind speed in the 9 nearest grid points (eq. 1 km x 1 km area). Lower right panel shows wind speed in blue (10 m) and significant wave height (red line) at the center of the outer crossing.*

3.13.4 Waves

The southerly wind leads to mixed opposing wind sea and swell in Sulafjorden (Figure 95). A wave height at the center of the outer crossing of about 2 m as in many of the storm cases, corresponds to a 95 - 99 percentile situation (Furevik and Aarnes [2021] Figure 22 therein). The swell is slightly lower and the wind is stronger in this case (figure 96

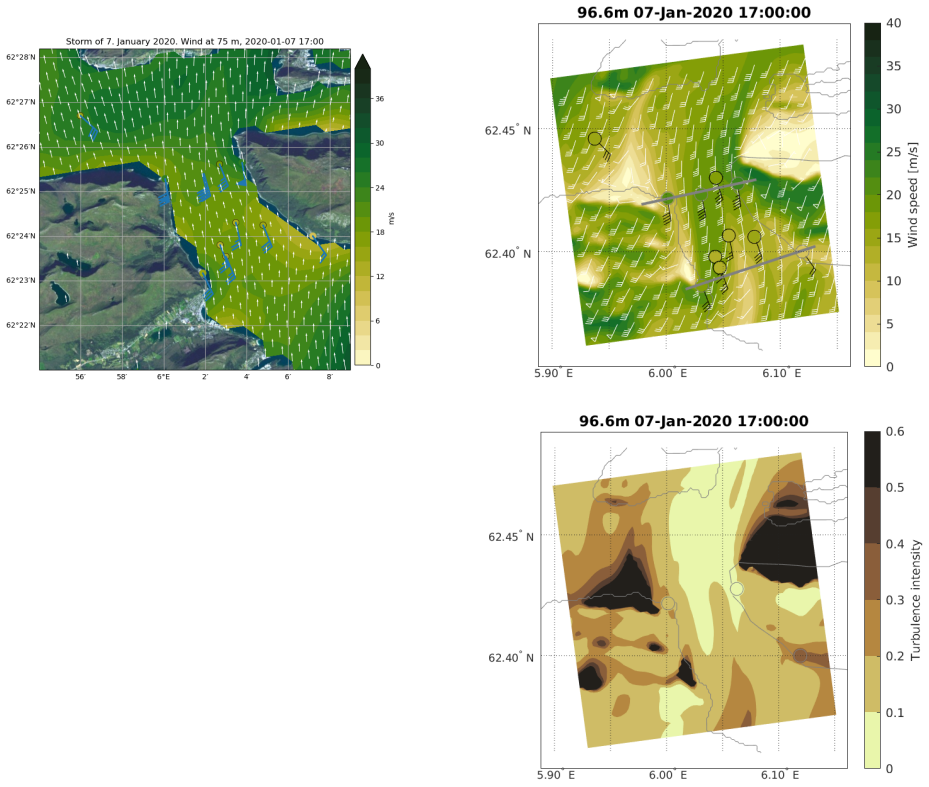

Figure 93: *Simulated wind from WRF at 75 above sea level (left) and at 97 m from Simra (right) when the storm is strongest. Also shown are the observed wind and direction using traditional wind barbs and coloured circles based on the same colour map as the contour plot. Each flag is 5 m/s and a triangle is equivalent to 25 m/s. The direction of the barbs shows the observed horizontal direction. Buoy observations at 4 m are marked with a black circle. Lower panel: Simulated turbulence intensity from Simra at 97 m.*

compared to the previous (2 January 2020)(figure 87). The wind is also aligned along the fjord axis which gives a longer and broader fetch.

3.13.5 Currents

Model snapshots of surface currents from the storm show that the response of strong winds from the south make a complex pattern with flow from the southwest in Breisundet and flow from the south in Sulafjorden and with sharp gradients related to wake effects of land (Figure 97). The maximum current speed is about 70 cm/s in location A, and this location also corresponds to the area with the highest velocities toward the north. The time series where observation and model data are compared show that the current speed

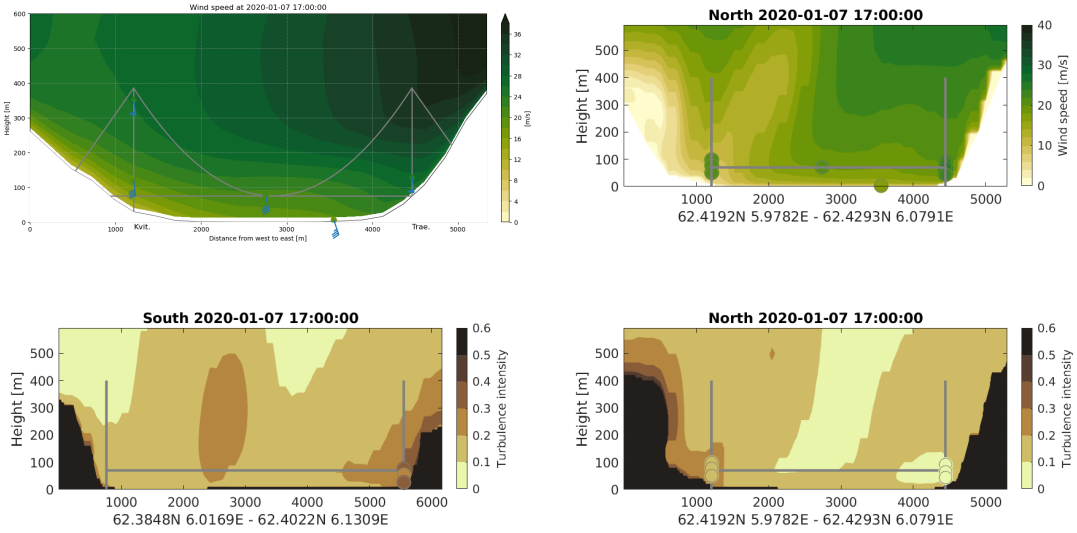

Figure 94: *Simulated wind from WRF (left) and Simra (right) in a section along the planned crossing. Bridge location is indicated with grey lines. Also shown are the observed wind and direction using traditional wind barbs and coloured circles based on the same colour map as the contour plot. Each flag is 5 m/s and a triangle is equivalent to 25 m/s. The direction of the barbs shows the observed horizontal direction. Lower panels: Turbulence intensity from Simra at the southern (left) and northern crossing (right)*

and direction correspond well most of the time during the main storm event.

The long-term average surface current direction in Sulafjorden is toward the north, and the winds from the south extend this layer with northward currents down to 30-40 m depth (Figure 98).

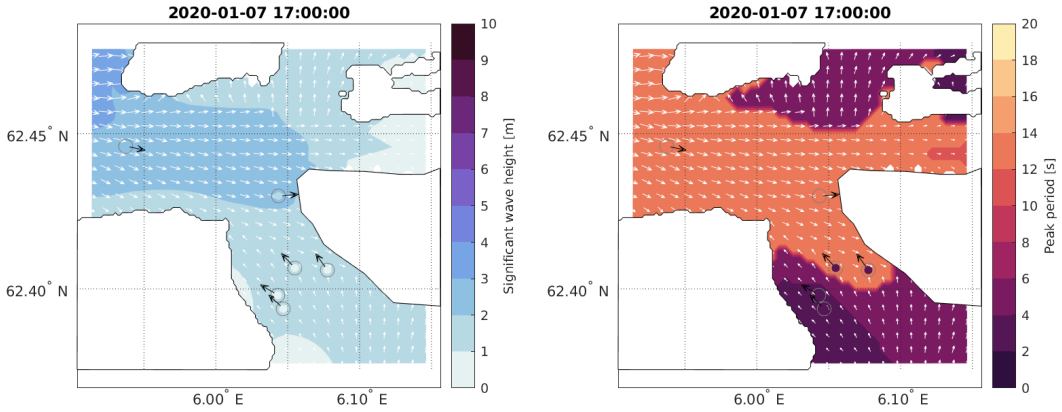

Figure 95: *Significant wave height [m] (left) and peak period (right) from SWAN and observations at the peak of the storm.*

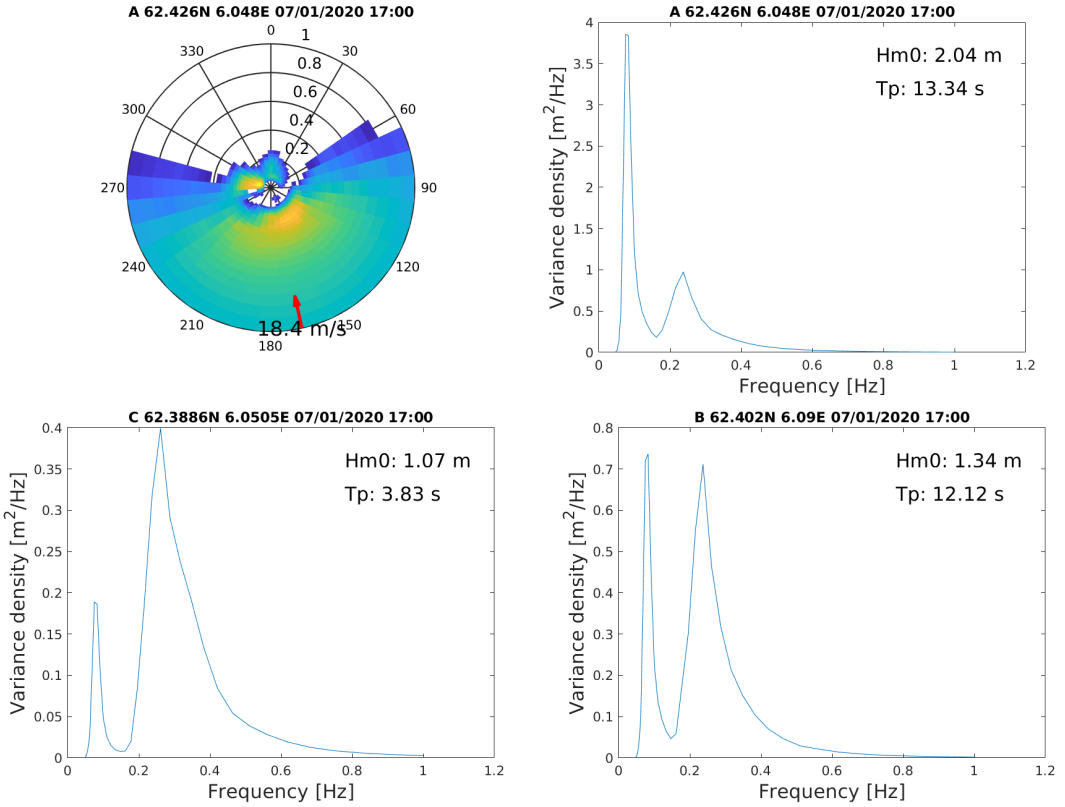

Figure 96: *2D (direction-frequency) wave spectrum from location A (top left panel) and 1D (frequency) wave spectra from locations A (top right panel), B (lower right panel) and C (lower left panel) from SWAN at the storm peak. Please note the different scale on the y-axes. Wind speed and direction (from WRF) is shown in the 2D spectrum. The energy is plotted in the direction the waves come from. Significant wave height (Hm0 or Hs) and peak period (Tp) is indicated for each location in the 1D plots.*

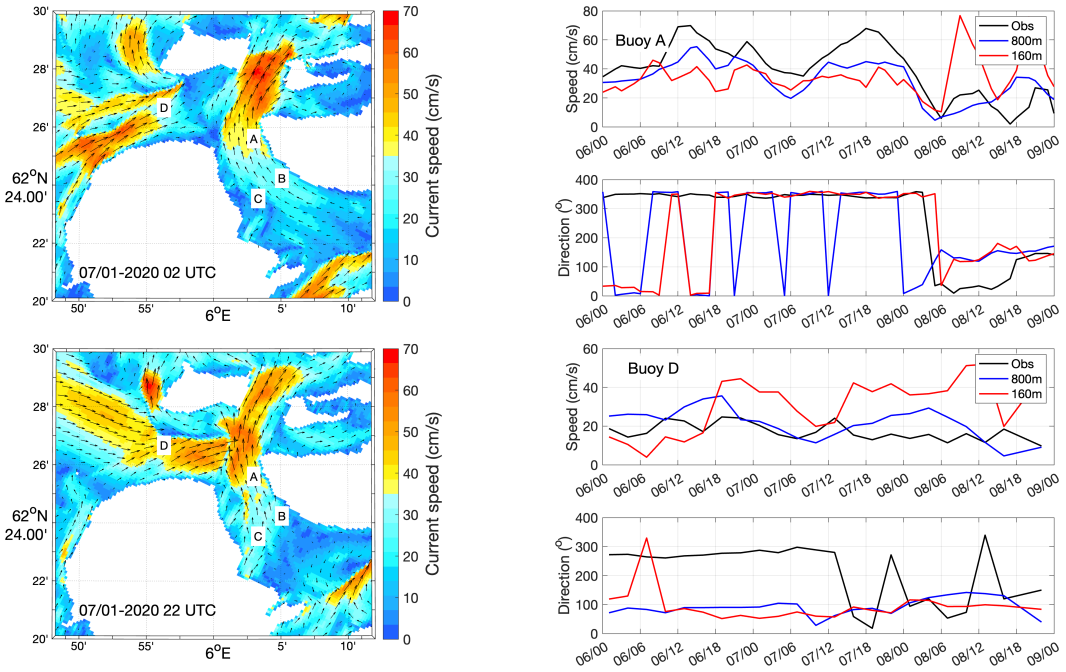

Figure 97: *The maps show instantaneous surface currents from the 160m-model valid at the times indicated in the map (left panels). The observational buoy locations A, B, C and D are denoted in the maps. The graphs to the right show current speed and direction at 1m depth from the two buoy locations A (upper two panels) and D (lower two panels) based on measurements (black line), NorKyst800 (blue) and 160m-model (red). The time stamps are written as day/hour.*

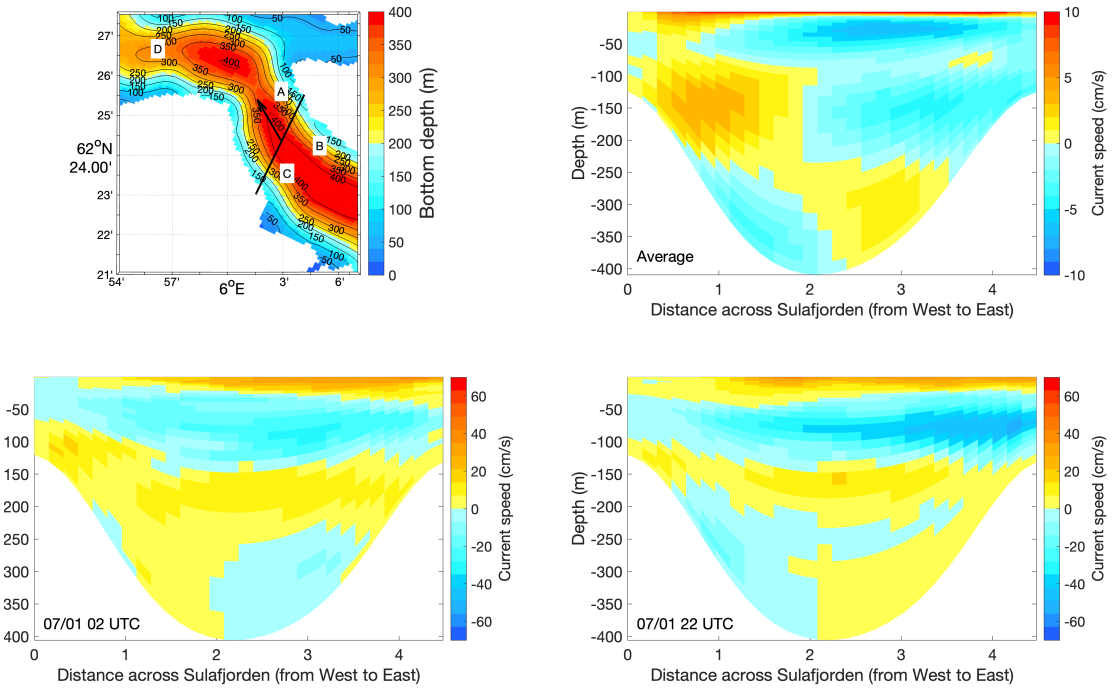

Figure 98: *The upper right panel is retrieved from Ágústsson et al. [2020b] and shows long-term average current speed normal to the transect crossing Sulafjorden denoted as a black line in the bathymetric map (upper left). The lower panels show two snapshots of current speed over the same transect. Red and yellow colors denote currents toward the north in the direction of the arrow in the map, while blue colors denote the opposite southerly currents.*

3.14 The storm of 11 January 2020

3.14.1 General overview

In early January 2020, a series of southerly storms occurred in Sulafjorden. The storm of 11 January is the the third and strongest in this series of storms.

Observed 10-minute winds were from the south and west and up to 25 m/s at the masts, see overview in Fig. 99. The observed wind speed and direction are well reproduced by the WRF-model at Kvitneset, but the wind speed is overestimated at Trælbodneset. The model shows a jet of strong wind emanating from the Hareid valley on the western bank of the fjord.

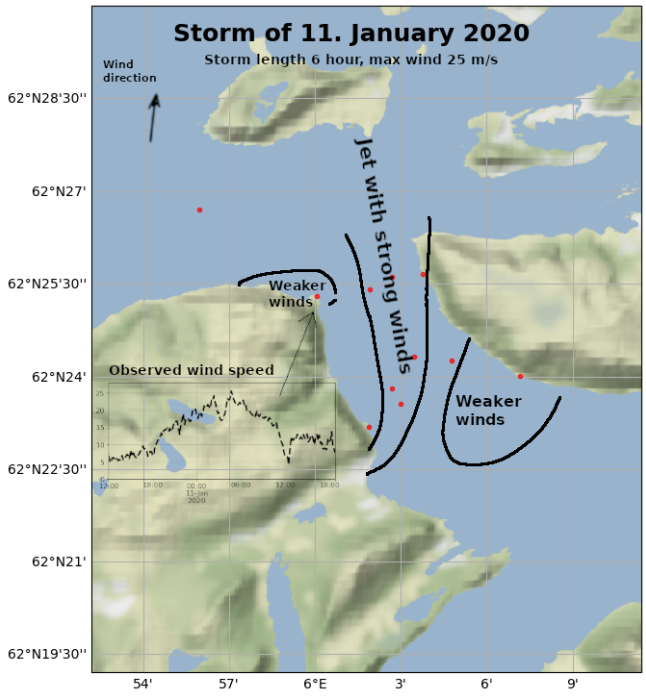

Figure 99: *A schematic summary of important aspects of the storm*

The event is associated with a very deep and broad low pressure system over Iceland and a broad high pressure system extending from Iberian peninsula to central Europe, resulting in a steep pressure gradient over the west coast of Norway.

Four masts were operational and we focus on Kvitneset and Trælbodneset. Data is also available from the buoy lidar at the centre of the fjord, but not from the other lidar systems. Buoy data (4 m asl) is available from the buoys in Sulafjorden.

The WRF 500 m x 500 m and the Simra 100 m x 100 m datasets are both available for the event. Data is also available from wave and current model.

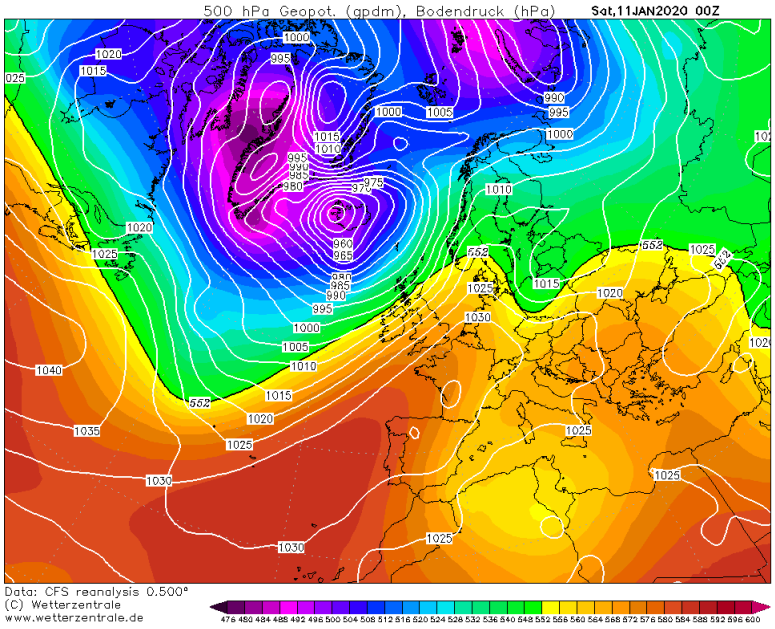

Figure 100: *The analysis from CFS (Climate Forecast System) showing surface pressure and 500 hPa geopotential. Figure is retrieved from Wetterzentale.*

3.14.2 Simulated flow - horizontal structure

As shown in Fig. 101, the wind direction is well reproduced by WRF-model at Kvitneset and Trælbodneset. The wind speed tends to be a bit low late in the event at Kvitneset, but we see that the model grossly overestimates the wind speed at Trælbodneset.

In this case the wind direction is more southerly and a clear wake is formed in the WRF simulation south of Langeneset radiating towards Sula and north of Kvitneset (Figure 102 upper panels). The simulations from Simra have similar features, but more pronounced. The observations largely confirm the picture. The turbulence intensity from Simra is moderate in the fjord, but higher turbulence is indicated at Langeneset and Kårsteinen than at the other masts (lower panel).

3.14.3 Simulated flow - vertical structure

As for previous cases with southerly wind, WRF shows generally increasing wind from Kvitneset to Trælbodneset, while results from Simra have alternating weak and strong winds up to large altitudes, due to the topographic effects described above (Figure 103 upper panels). Higher turbulence is found related to the wakes and close to terrain (lower panels).

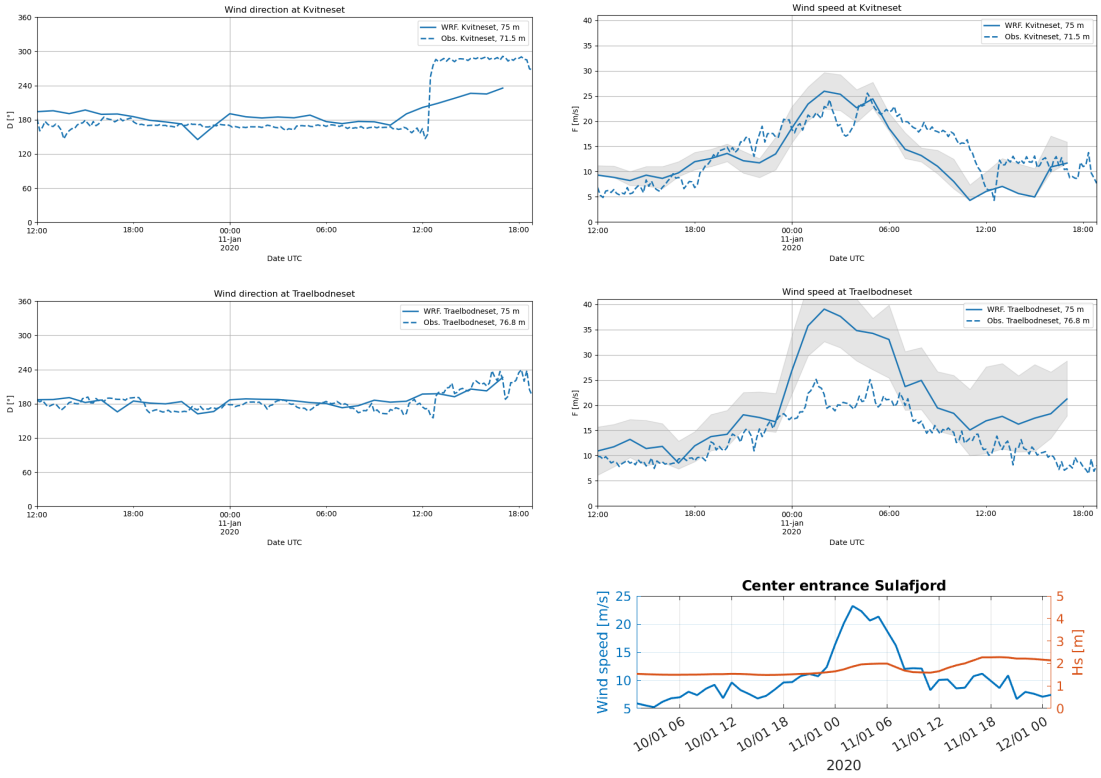

Figure 101: *Simulated (solid lines) and observed (dashed) wind direction (left) and wind speed (right) from the WRF-model. The grey envelope indicates the range of the simulated wind speed in the 9 nearest grid points (eq. 1 km x 1 km area). Lower right panel shows wind speed in blue (10 m) and significant wave height (red line) at the center of the outer crossing.*

3.14.4 Waves

The wave conditions in this case (Figures 104, 105 and 101 lower right panel) is similar to previous south-southwesterly cases e.g. during January 2020. The fjord is subject to two wave systems, the swell entering from Breisundet and the wind sea locally generated in Sulafjord.

3.14.5 Currents

Model snapshots of surface currents from the storm show that the response of strong winds from the south are visible in the entire Sulafjorden fjord system with northward currents with sharp gradients related to wake effects of land (Figure 106). The maximum current speed is about 80 cm/s in location A, and this location also corresponds to the

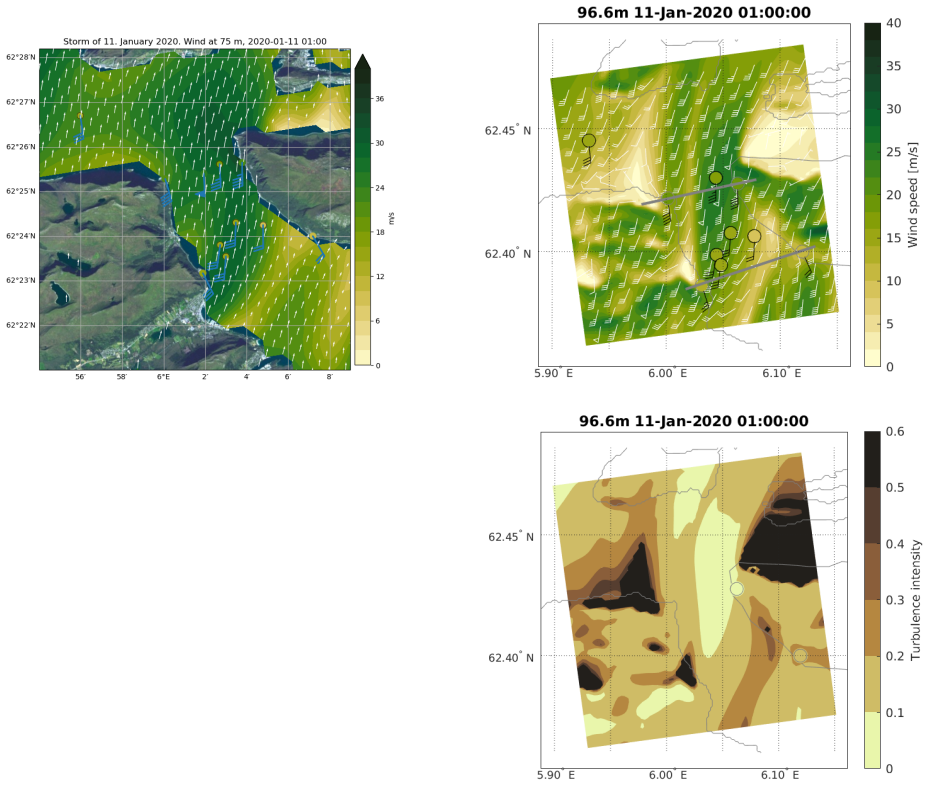

Figure 102: *Simulated wind from WRF at 75 m above sea level (left) and from 97 m in Simra (right) valid when the storm is strongest. Also shown are the observed wind and direction using traditional wind barbs and coloured circles based on the same colour map as the contour plot. Each flag is 5 m/s and a triangle is equivalent to 25 m/s. The direction of the barbs shows the observed horizontal direction. Buoy observations at 4 m are indicated with a black circle. Lower panel: Simulated turbulence intensity from Simra at 97 m.*

area in the northern part of Sulafjorden and inner part of Breisundet that is exposed to the highest velocities toward the north. The time series where observation and model data are compared show that the current speed and direction correspond well most of the time during the main storm event.

The long-term average surface current direction in Sulafjorden is toward the north, and the winds from the south extend this layer with northward currents down to 30-40 m depth (Figure 107).

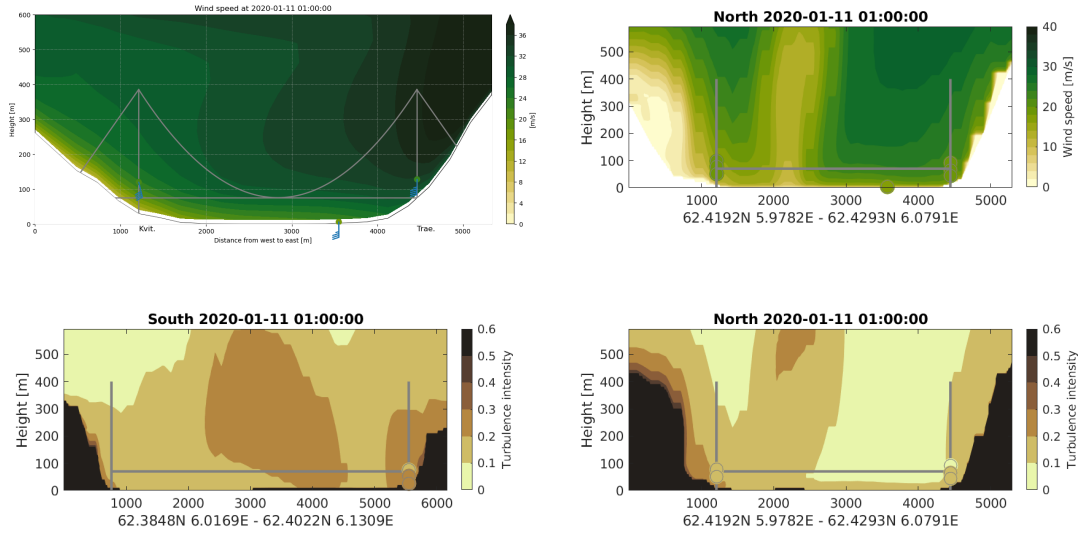

Figure 103: *Simulated wind from WRF (left) and from Simra (right) in a section along the planned crossing. Bridge location is indicated with grey lines. Also shown are the observed wind and direction using traditional wind barbs and coloured circles based on the same colour map as the contour plot. Each flag is 5 m/s and a triangle is equivalent to 25 m/s. The direction of the barbs shows the observed horizontal direction. Lower panels: Turbulence intensity from Simra at the southern (left) and northern crossing (right).*

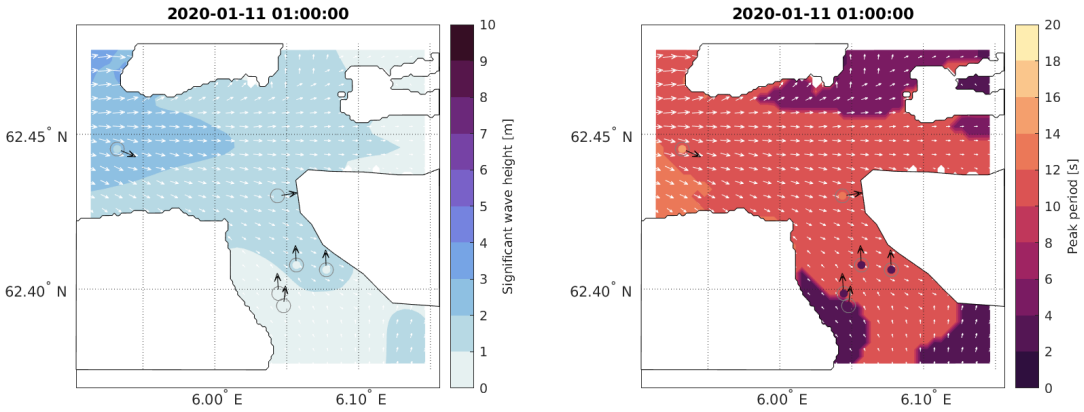

Figure 104: *Significant wave height [m] (left) and peak period (right) from SWAN and observations at the peak of the storm.*

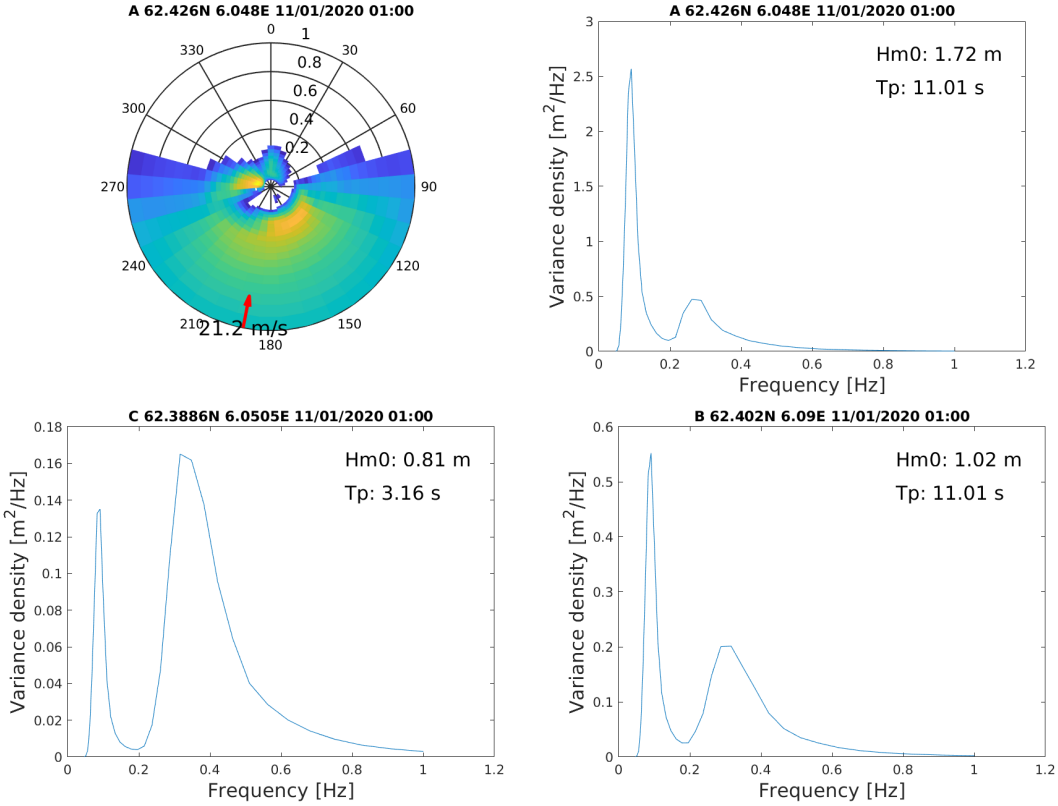

Figure 105: *2D (direction-frequency) wave spectrum from location A (top left panel) and 1D (frequency) wave spectra from locations A (top right panel), B (lower right panel) and C (lower left panel) from SWAN at the storm peak. Please note the different scale on the y-axes. Wind speed and direction (from WRF) is shown in the 2D spectrum. The energy is plotted in the direction the waves come from. Significant wave height (Hm0 or Hs) and peak period (Tp) is indicated for each location in the 1D plots.*

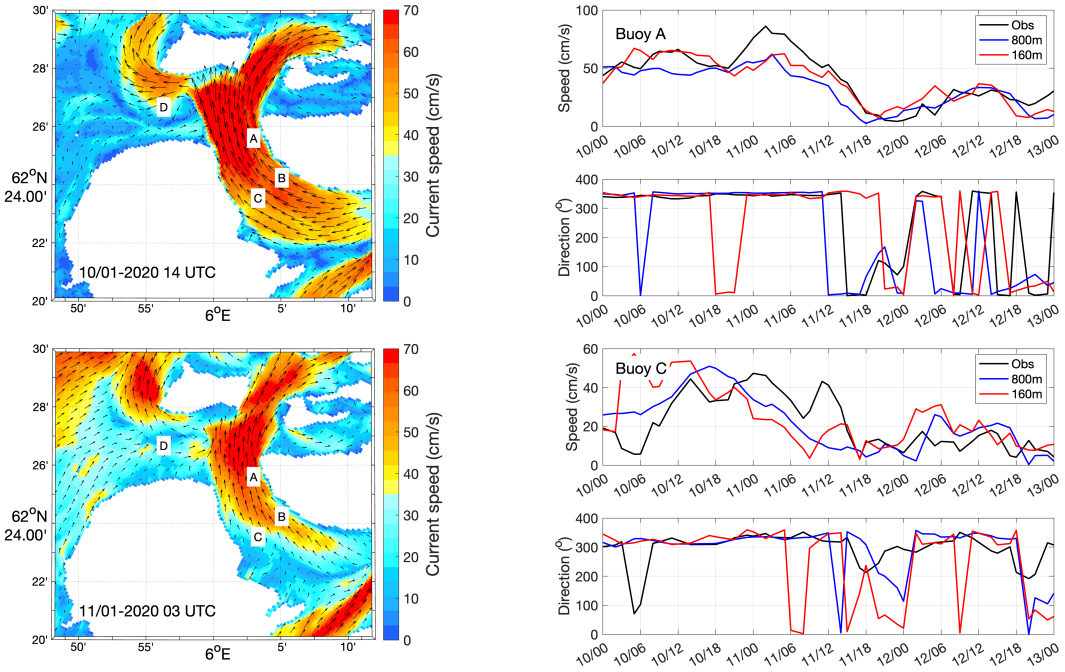

Figure 106: *The maps show instantaneous surface currents from the 160m-model valid at the times indicated in the map (left panels). The observational buoy locations A, B, C and D are denoted in the maps. The graphs to the right show current speed and direction at 1m depth from the two buoy locations A (upper two panels) and C (lower two panels) based on measurements (black line), NorKyst800 (blue) and 160m-model (red). The time stamps are written as day/hour.*

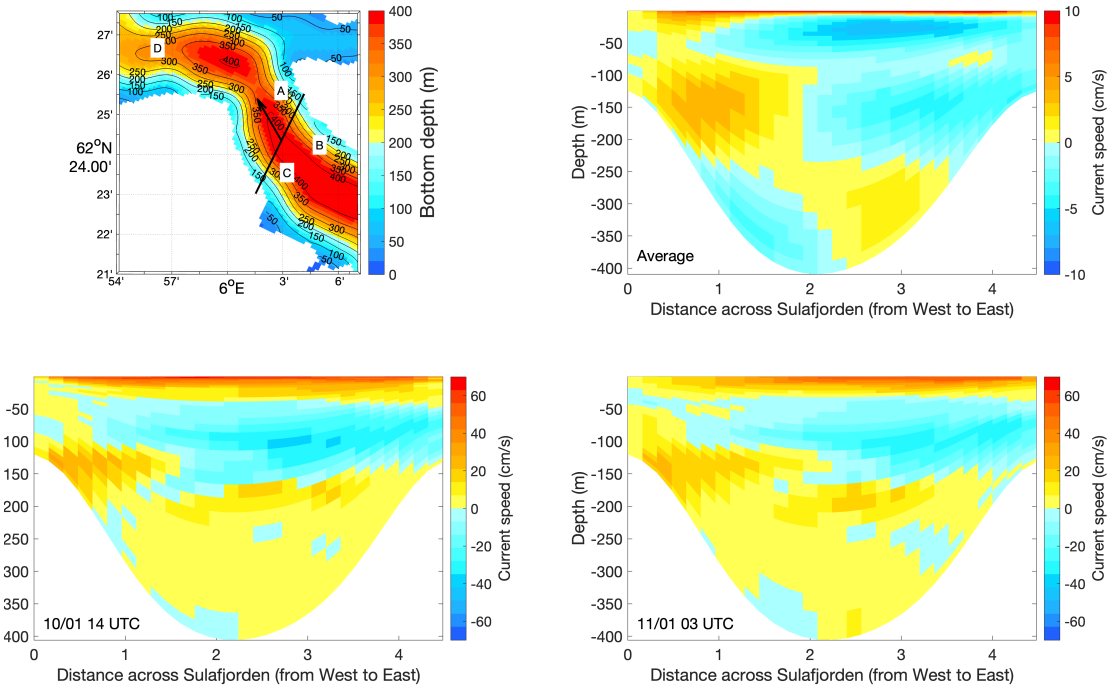

Figure 107: *The upper right panel is retrieved from Ágústsson et al. [2020b] and shows long-term average current speed normal to the transect crossing Sulafjorden denoted as a black line in the bathymetric map (upper left). The lower panels show two snapshots of current speed over the same transect. Red and yellow colors denote currents toward the north in the direction of the arrow in the map, while blue colors denote the opposite southerly currents.*

3.15 The storm of 12 April 2020

3.15.1 General overview

Observed 10-minute winds reached 24 m/s at Kvitneset but were slightly weaker at Trælbodneset and at the fjord centre. The observed wind speed and direction are well reproduced by the WRF-model at Kvitneset, but the wind speed is overestimated at Trælbodneset. The simulations, in particular the Simra model, show a wake behind Godøya which at times reaches the fjord crossing, but its spatial extent varies considerably. See an overview of the situation in Fig. 108.

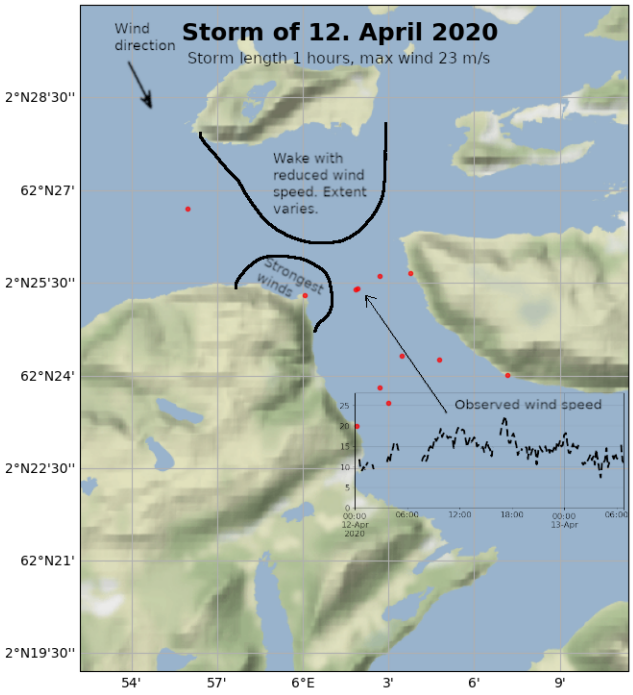

Figure 108: *A schematic summary of important aspects of the storm*

A northerly and northwesterly storm occured on 12 April 2020, see figure for synoptic situation, Fig. 109. The event is associated with a deepening low pressure system moving in from the southwest late on the 11 April. There were relatively weak southerly winds in advance of the low, which then quickly turned to close to 20 m/s from the northwest during the following day.

During the event, four masts in Sulafjorden were operational. We choose to focus on Kvitneset and Trælbodneset. Data is also available from lidar systems; the scanning lidars, the buoy lidar and the lidar at the top of the Kvitneset mast. Data is also available from the buoys in Sulafjorden at 4 m asl.

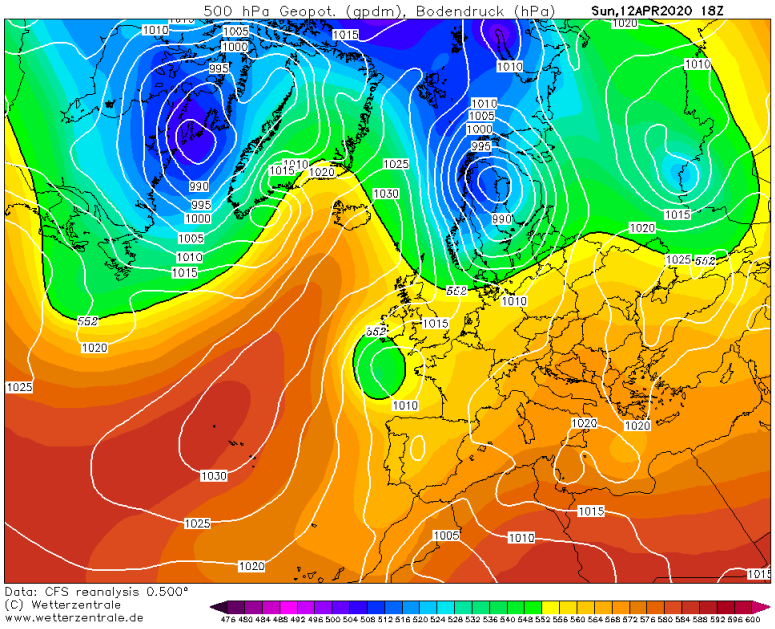

Figure 109: *The analysis from CFS (Climate Forecast System) showing surface pressure and 500 hPa geopotential. Figure is retrieved from Wetterzentale.*

WRF 500 m x 500 m and Simra 100 m x 100 m simulated the event. Data is also available from the current model.

3.15.2 Simulated flow - horizontal structure

From Fig. 110, we see that the WRF-model captures the wind direction well and the wind speed reasonably well. There seems to be a little disturbance appearing in the early afternoon which the models do not capture.

Simulations from both WRF and Simra show the generation of a wake behind Godøy in this northerly event. The wake seems to reach as far as the northern section (Figure 111). The position of the wake is not directly confirmed from the observations, since we should see lower wind at Kvitneset than at the lidar, while the opposite is the case. However, if the wind direction is actually slightly more westerly (Simra) than the simulations (notice the difference in wind direction at most observation sites), the wake is possibly directly in the centre of the fjord. This may explain the lower wind observations at the lidar than at Kvitneset and Trælbodneset.

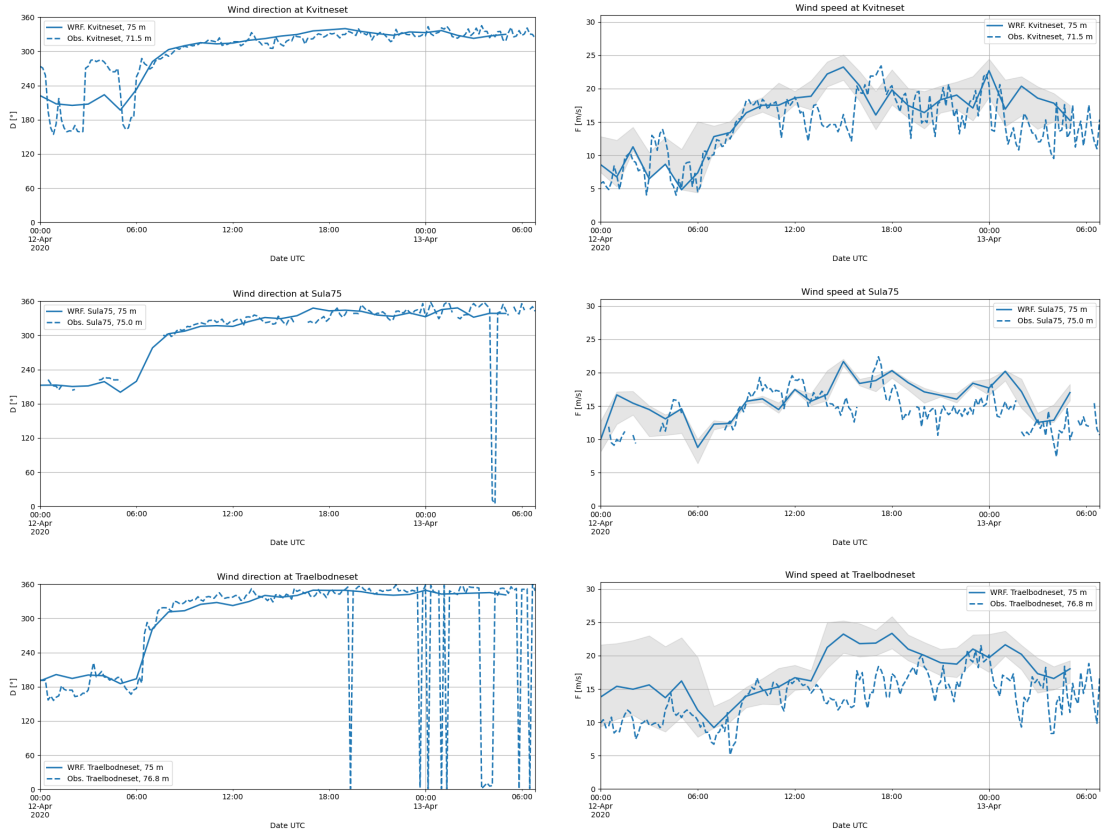

Figure 110: *Simulated (solid lines) and observed (dashed) wind direction (left) and wind speed (right) from the WRF-model. The grey envelope indicates the range of the simulated wind speed in the 9 nearest grid points (eq. 1 km x 1 km area).*

3.15.3 Simulated flow - vertical structure

Vertical sections are extracted from WRF and Simra along the two possible fjord crossings at the peak of this event (Figure 112). In WRF the wind speed is lower on the western side of the fjord, due to the wake from Godøy. The same is the case from Simra, but with more details in the flow structure. We have also included the turbulence intensity from Simra along both sections. Simulated TI is low except in the wake region and at the eastern side of the southern section. All the sensors at Kvitneset measure a higher wind speed and lower TI at this time. This may be due to incorrect incoming wind direction, as discussed above, or wake meandering.

Turbulence intensity from Simra over the domain is shown in Figure 113 with a section from Godøy towards the northern proposed crossing. Moderate to high turbulence affect the sea area between Godøy and Sula up to 5-600 m but the effect is very much reduced

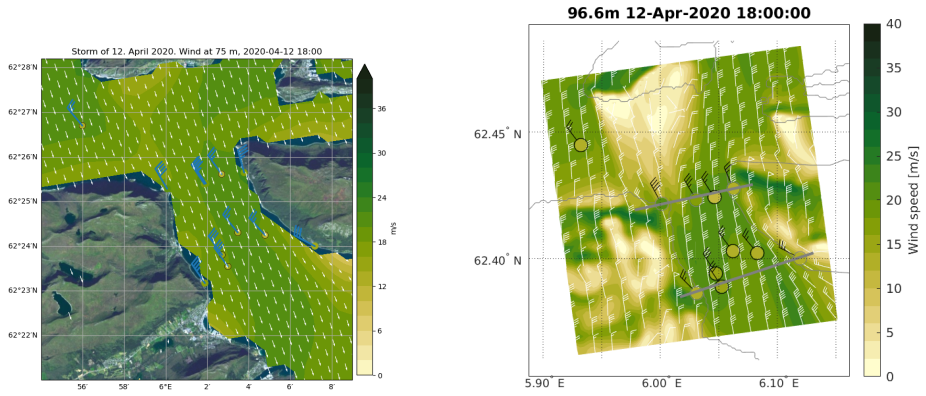

Figure 111: *Simulated wind from WRF at 75 m above sea level (left) and from Simra at 97 m (right), valid when the storm is strongest. Also shown are the observed wind and direction using traditional wind barbs and coloured circles based on the same colour map as the contour plot. Each flag is 5 m/s and a triangle is equivalent to 25 m/s. Buoy observations at 4 m are marked with a black circle. The direction of the barbs shows the observed horizontal direction.*

when reaching the northern crossing.

3.15.4 Currents

Model snapshots of surface currents from the storm show that the response of strong winds from the north-northwest are strong currents into Breisundet from the west and southward currents in Sulafjorden with sharp gradients and a complex current pattern related to wake effects of land (Figure 114). The maximum current speed is about 60 cm/s in location B, and this location also corresponds to the area with the highest velocities toward the south. The time series where observation and model data are compared show that the current speed and direction correspond well most of the time during the main storm event.

Since the long-term average current direction in Sulafjorden is toward the north, the strong surface currents from the north alter the current pattern in the entire water column (Figure 115). Instead of a 10-15 m thick surface layer with a northward flow and southward currents below down to approximately 100 m, the model sets up a southward flow from the surface down to about 80m and northward currents below.

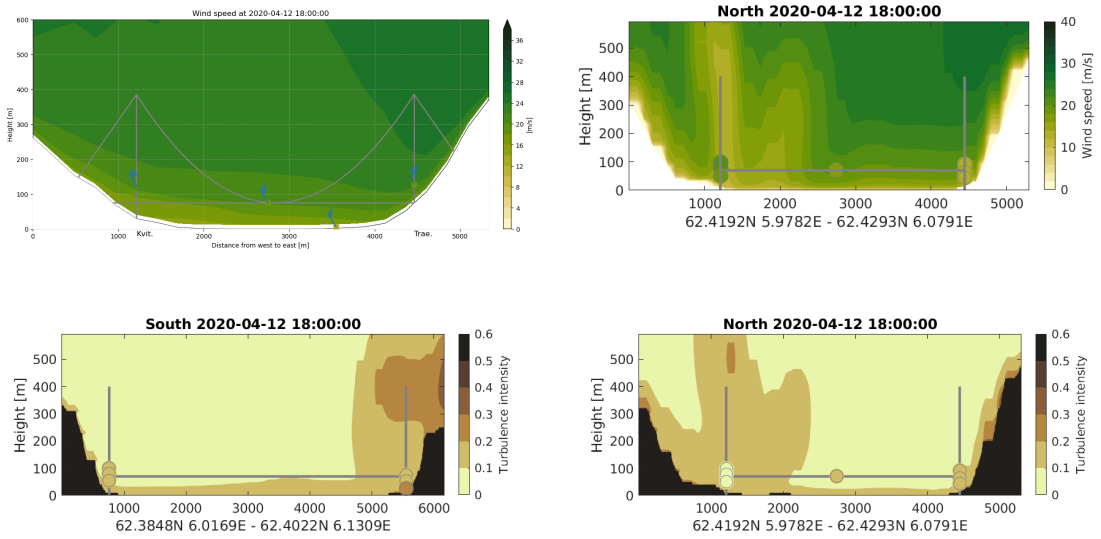

Figure 112: *Simulated wind from WRF (left) and from Simra (right) in a section along the planned crossing. Bridge location is indicated with grey lines. Also shown are the observed wind and direction using traditional wind barbs and coloured circles based on the same colour map as the contour plot. Each flag is 5 m/s and a triangle is equivalent to 25 m/s. The direction of the barbs shows the observed horizontal direction. Lower panels: Simulated turbulence intensity from Simra at 97 m at the southern (left) and northern (right) section.*

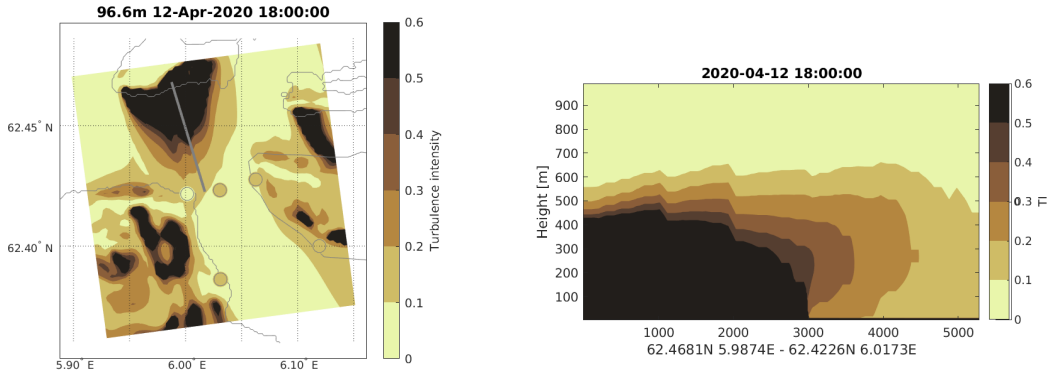

Figure 113: *Turbulence intensity from Simra at 97 m. The line in the map (left) indicates the location of the vertical transect (right).*

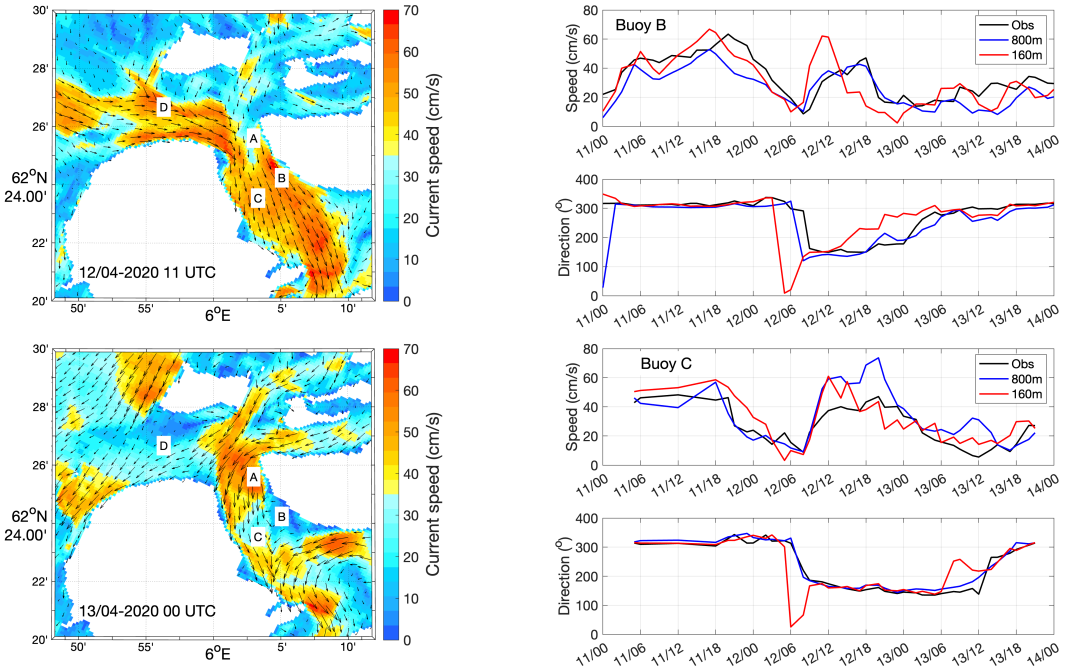

Figure 114: *The maps show instantaneous surface currents from the 160m-model valid at the times indicated in the map (left panels). The observational buoy locations A, B, C and D are denoted in the maps. The graphs to the right show current speed and direction at 1m depth from the two buoy locations B (upper two panels) and C (lower two panels) based on measurements (black line), NorKyst800 (blue) and 160m-model (red). The time stamps are written as day/hour.*

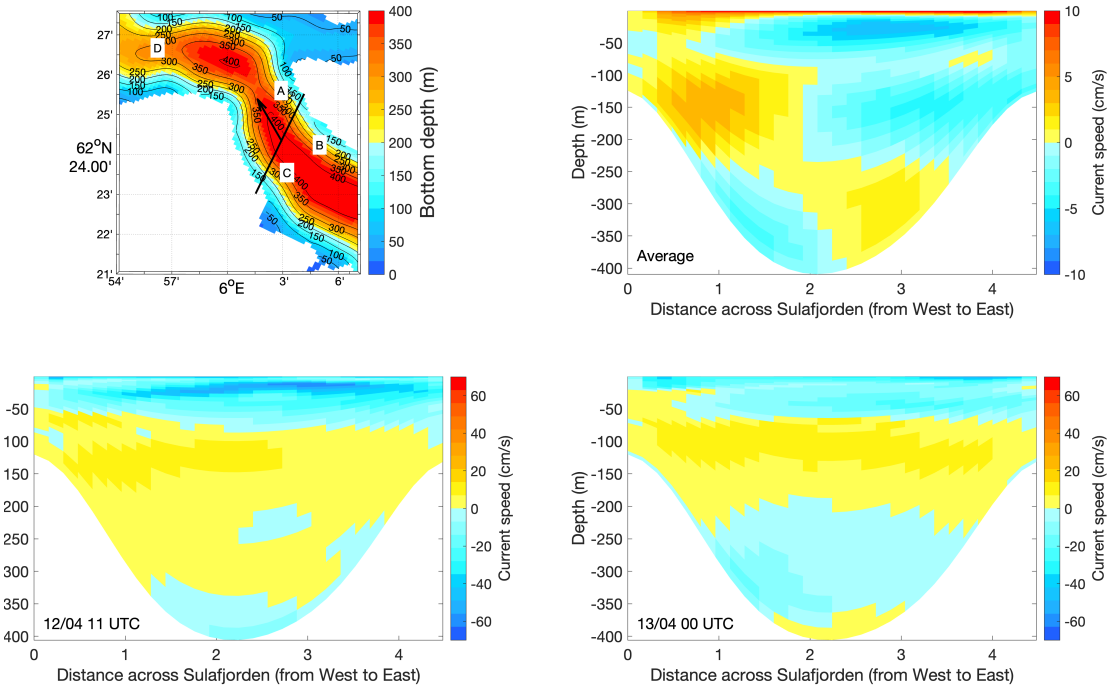

Figure 115: *The upper right panel is retrieved from Ágústsson et al. [2020b] and shows long-term average current speed normal to the transect crossing Sulafjorden denoted as a black line in the bathymetric map (upper left). The lower panels show two snapshots of current speed over the same transect. Red and yellow colors denote currents toward the north in the direction of the arrow in the map, while blue colors denote the opposite southerly currents.*

3.16 The westerly event of 23 September 2020

3.16.1 General overview

On 22 and 23 of September, winds were westerly in Sulafjorden, and not particularly strong. The event is included as observations from the buoy lidar show a very strong vertical wind shear, i.e. a strong increase in wind speed from roughly bridge deck level to further aloft (see an overview in Fig. 116).

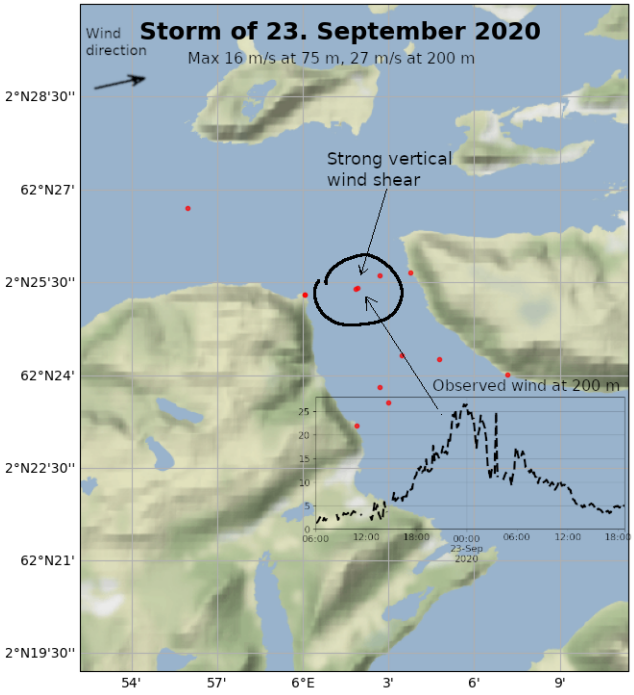

Figure 116: *A schematic summary of important aspects of the storm*

Observed 10-minute winds were westerly and up to 15 m/s at the masts and the scanning lidar at the fjord centre. The buoy lidar measured 26 m/s from the west at the same time, with indications of a layer with very strong vertical wind shear. At the same time, the lidar at the top of the Kvitneset mast measured roughly 18 m/s, but many samples were missing due to unfavourable sampling conditions.

The observed wind speed and direction are generally reproduced by the WRF-model at the bridge deck level, except that the wind speed is overestimated at Trælbodneset. The model fails to reproduce the strong increase in wind speed with height, as seen in the buoy lidar data. It seams plausible that this may be at least explained by the limited horizontal and vertical resolution of the WRF model, where the upstream mountains are not steep enough.

The event is associated with a relatively small-scale low just off the west coast of Norway, see Fig. 117.

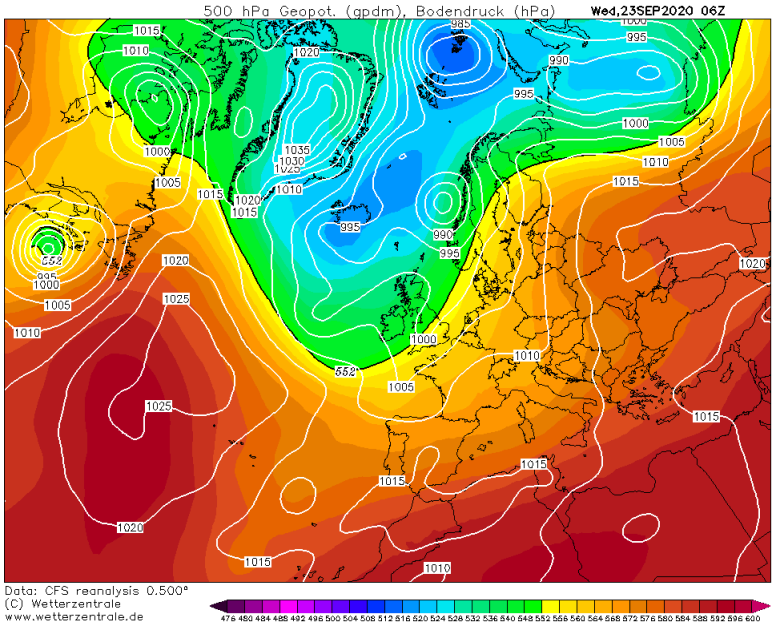

Figure 117: *The analysis from CFS (Climate Forecast System) showing surface pressure and 500 hPa geopotential. Figure is retrieved from Wetterzentale.*

During the storm, there are observational data available from the 4 masts in Sulafjorden, and we focus on Kvitneset and Trælbodneset. Data is also available from three lidar systems; the vertical lidar at the top of the Kvitneset mast, the buoy lidar, and from the scanning lidars. Data is also available from the buoys in Sulafjorden (4 m asl).

The WRF 500 m x 500 m model and Simra 100 m x 100 m were used to simulate the event. Data is also available from the current model.

3.16.2 Model validation at observation sites

We see that the WRF-model overestimates the wind speed slightly at bridge deck level, in particular at Trælbodneset (Fig. 118). The strong wind shear at the centre of the fjord is not reproduced, as the observed wind speed from the buoy lidar at 200 m is underestimated. The wind direction is well reproduced for all the station considered.

3.16.3 Simulated flow - horizontal structure

The horizontal flow structure and wind speed simulated by WRF and Simra compare well with the observations at, respectively, the 75 and 100 m levels (Figure 120 two upper

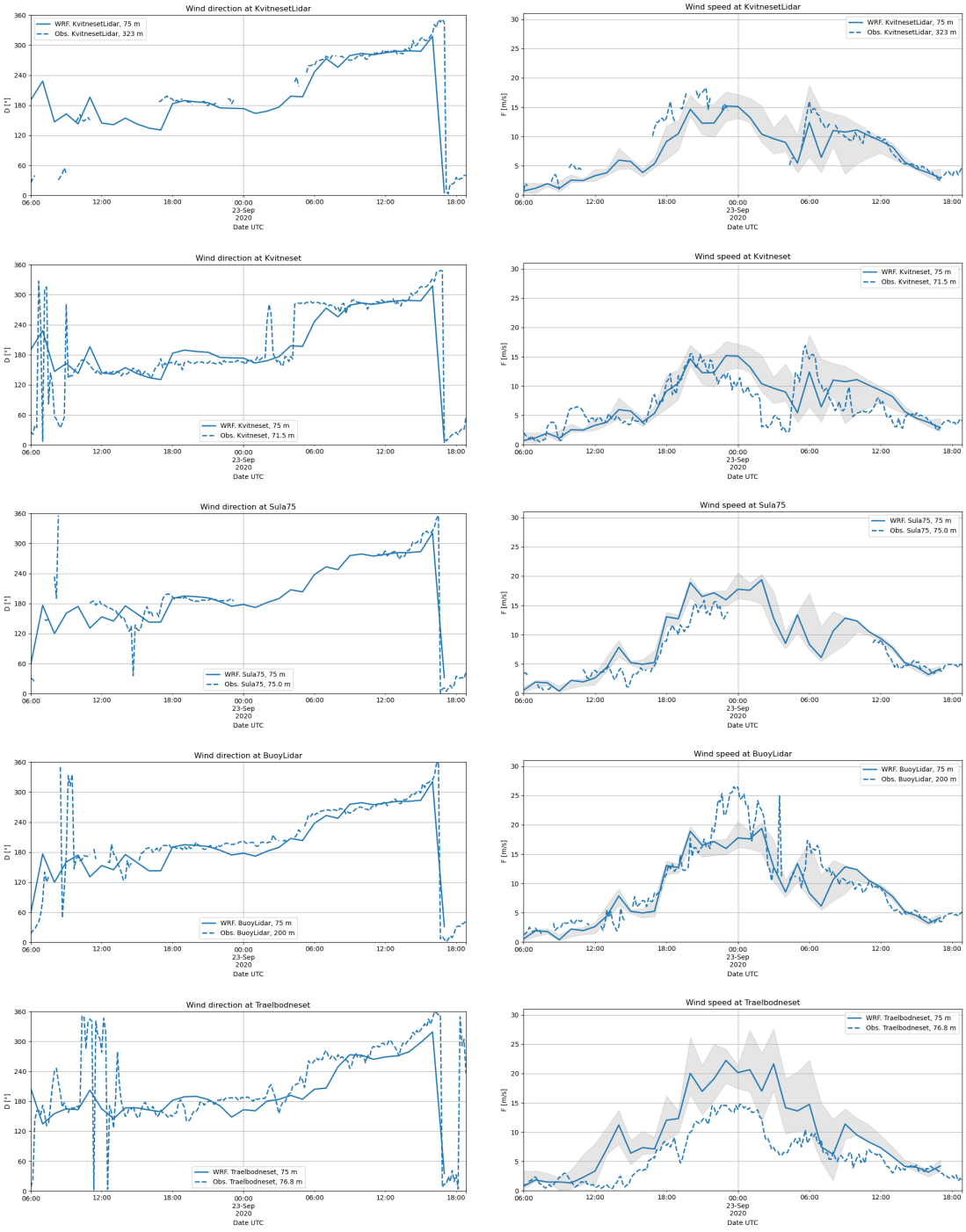

Figure 118: *Simulated (solid lines) and observed (dashed) wind direction (left) and wind speed (right) from the WRF-model. The grey envelope indicates the range of the simulated wind speed in the 9 nearest grid points (eq. 1 km x 1 km area).*

right panels). Around midnight the wind was southerly, then turning westerly during the morning. This is in good agreement to the many of the observation points. Ørsta/Volda

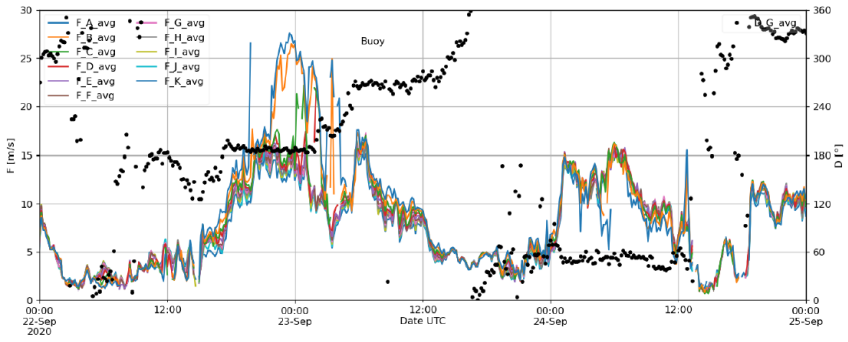

Figure 119: *Observed wind from all levels up to 200 m in the buoy lidar.*

airport had 4 m/s when the nearby mountain station Eitrefjell had 18.8 m/s at 03 UTC the 23rd. This corroborates the findings regarding vertical shear found in Sulafjorden.

3.16.4 Currents

Model snapshots of surface currents from the storm show that the response of strong winds from the south are visible in the entire Sulafjorden fjord system with northward currents with sharp gradients related to wake effects of land (Figure 122). The maximum current speed is nearly 100 cm/s, as seen in location A, but the entire Sulafjorden is exposed to velocities above 70cm/s during the evening of 22 September 2020. The time series where observation and model data are compared show that the current speed and direction correspond well most of the time during the main storm event.

The long-term average surface current direction in Sulafjorden is toward the north, and the winds from the south extend this layer with northward currents down to about 20 m depth (Figure 123).

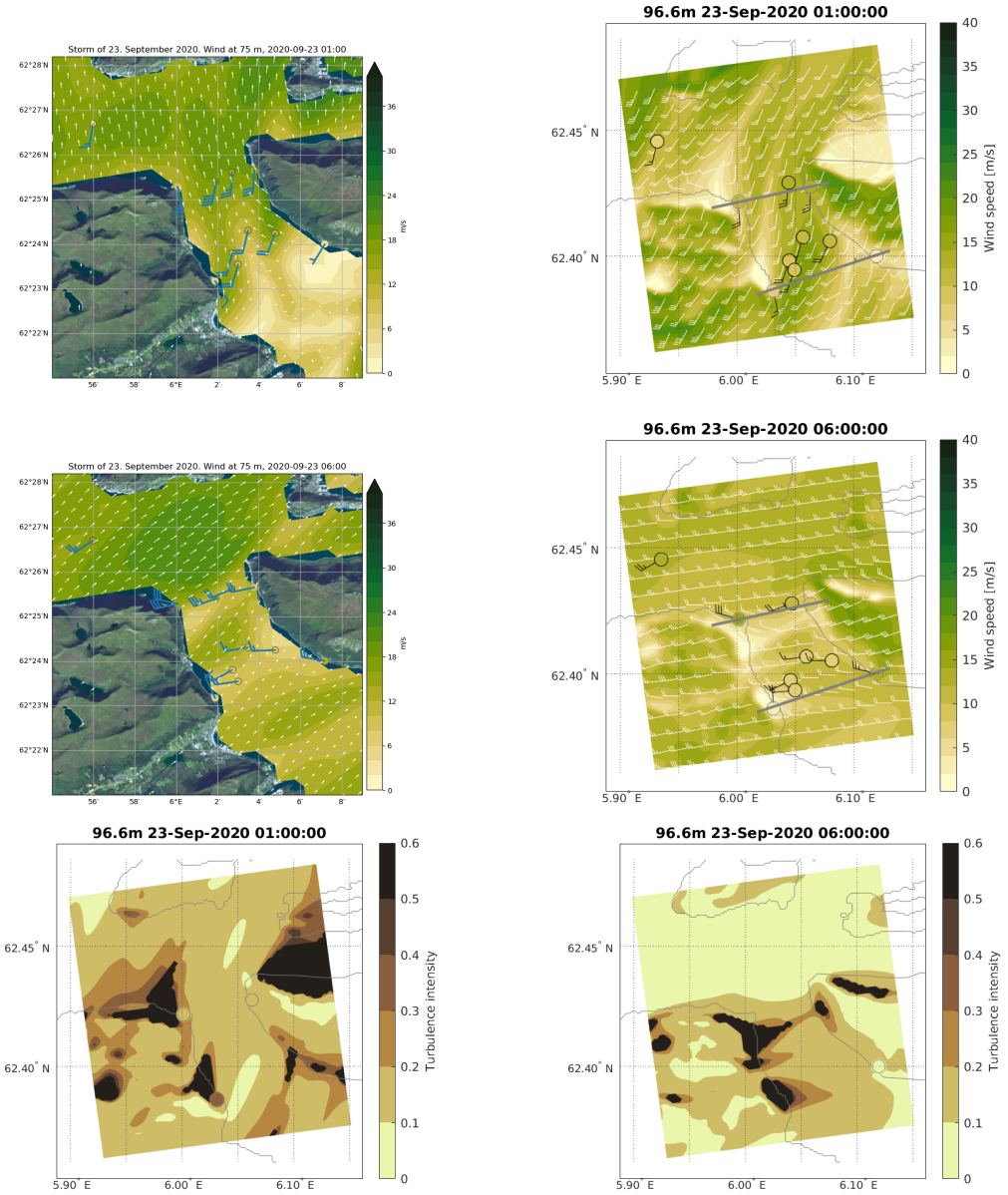

Figure 120: *Simulated wind from WRF (left), and from Simral (right). Also shown are the observed wind and direction using traditional wind barbs and coloured circles based on the same colour map as the contour plot. Each flag is 5 m/s and a triangle is equivalent to 25 m/s. The direction of the barbs shows the observed horizontal direction. Buoy observations at 4 m are marked with a black circle. The two lower panels: Turbulence intensity from Simra at 01 and 06 UTC, 23 September 2020.*

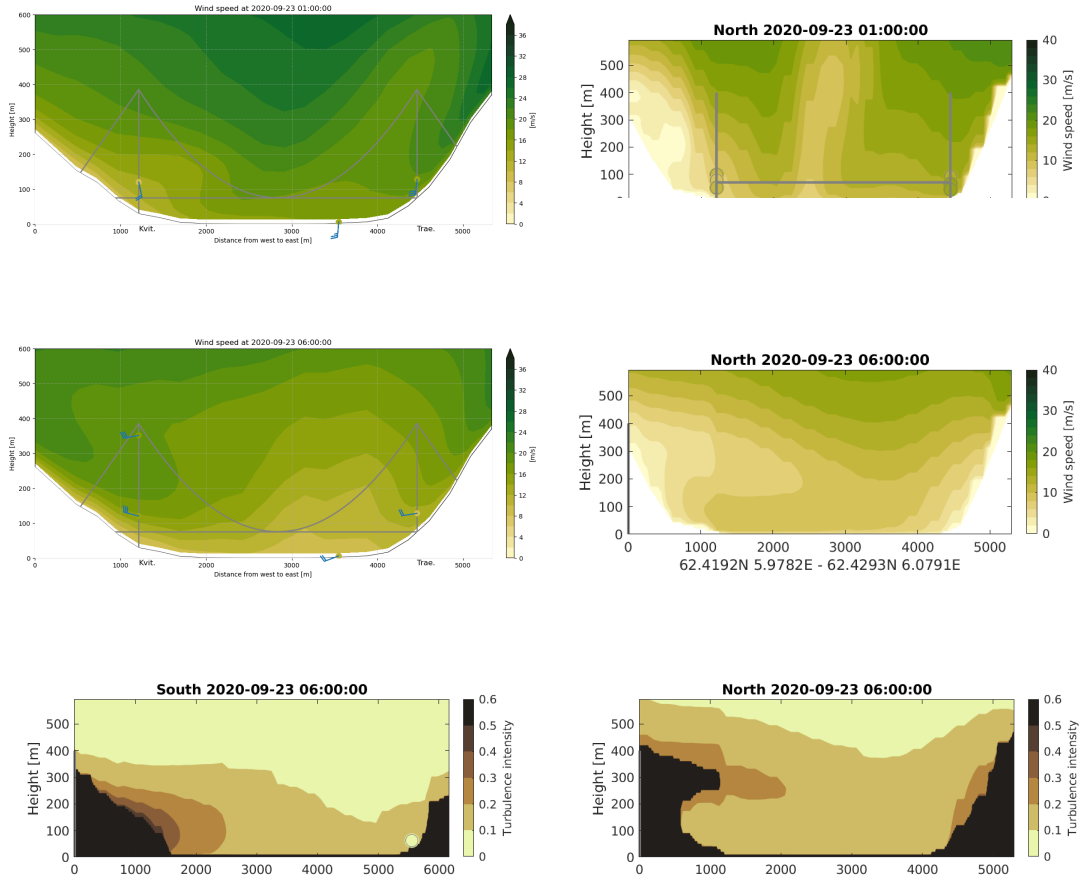

Figure 121: *Simulated wind from WRF (left) and from Simra (right) in a section along the planned crossing. Bridge location is indicated with grey lines. Also shown are the observed wind and direction using traditional wind barbs and coloured circles based on the same colour map as the contour plot. Each flag is 5 m/s and a triangle is equivalent to 25 m/s. The direction of the barbs shows the observed horizontal direction. The two lower panels: Turbulence intensity from Simra at the southern (left) and northern crossing (right).*

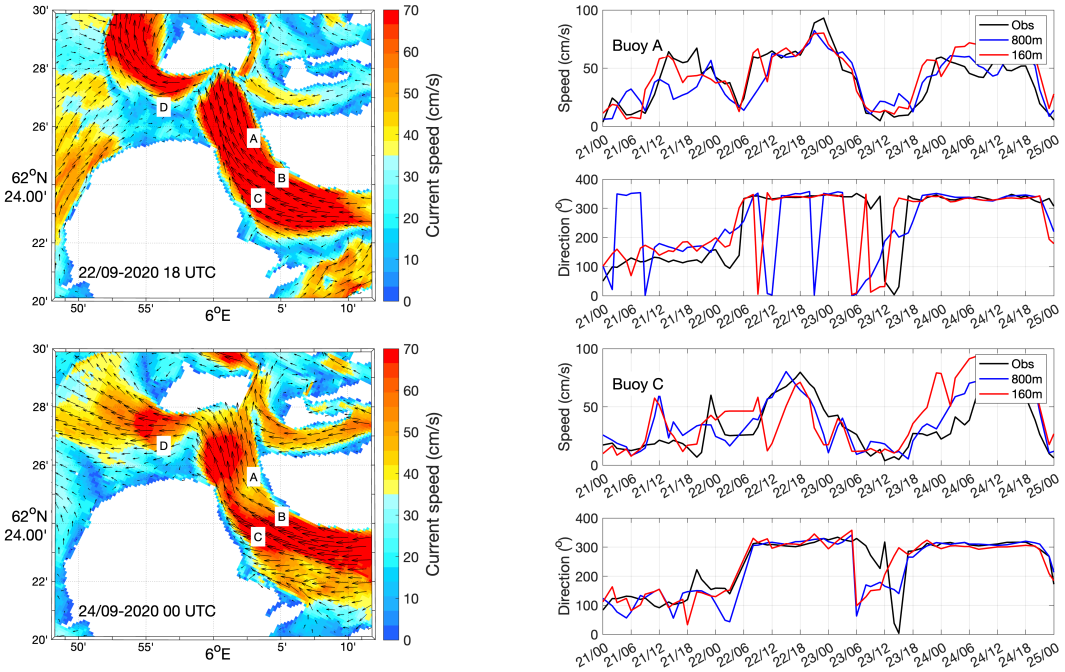

Figure 122: *The maps show instantaneous surface currents from the 160m-model valid at the times indicated in the map (left panels). The observational buoy locations A, B, C and D are denoted in the maps. The graphs to the right show current speed and direction at 1m depth from the two buoy locations A (upper two panels) and C (lower two panels) based on measurements (black line), NorKyst800 (blue) and 160m-model (red). The time stamps are written as day/hour.*

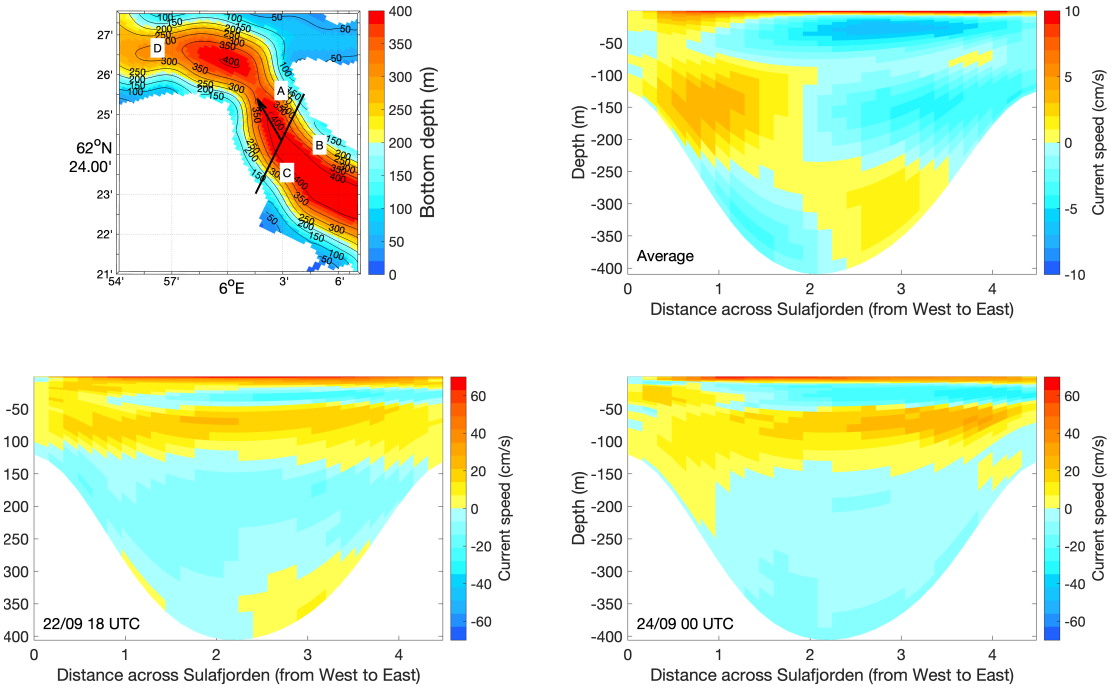

Figure 123: *The upper right panel is retrieved from Ágústsson H (2020a) and shows long-term average current speed normal to the transect crossing Sulafjorden denoted as a black line in the bathymetric map (upper left). The lower panels show two snapshots of current speed over the same transect. Red and yellow colors denote currents toward the north in the direction of the arrow in the map, while blue colors denote the opposite southerly currents.*

3.17 The storm of 19 November 2020

3.17.1 General overview

Observed 10-minute winds reached 29 m/s at Kvitneset but were slightly weaker at Trælbodneset and at the fjord centre. See overview in Fig. 124. The observed wind speed and direction are well reproduced by the WRF-model at Kvitneset and at the fjord centre, but the wind speed is slightly overestimated at Trælbodneset. The simulations, in particular the Simra model, show a wake behind Godøya, extending to the southeast, but not in the proximity of the planned fjord crossing.

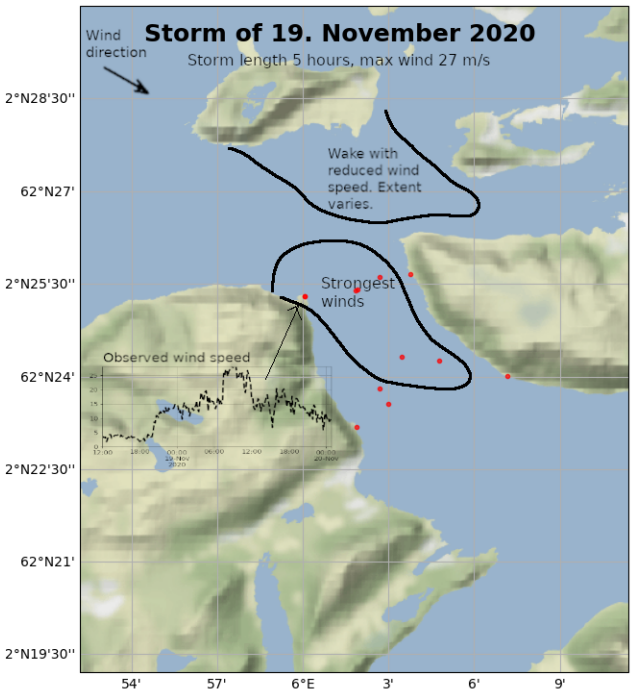

Figure 124: *A schematic summary of important aspects of the storm*

A northwesterly storm occurred on 19 November 2020. As the low passed the area, cold air was drawn down from the Arctic and a small-scale low was formed in our area, see synoptic overview in Fig. 125. This is seen in the rapid change of wind direction around midnight the 19th. There were relatively weak winds in advance of the low, but the winds rose quickly to 29 m/s from the northwest in the first part of the day.

During the storm, there are observational data available from the 4 masts in Sulafjorden, we focus in particular on Kvitneset and Trælbodneset. Data is also available from lidar systems; the scanning lidars, the buoy lidar, and the lidar at the top of the Kvitneset mast. Data is also available from the buoys in Sulafjorden, but only at 4 m asl.

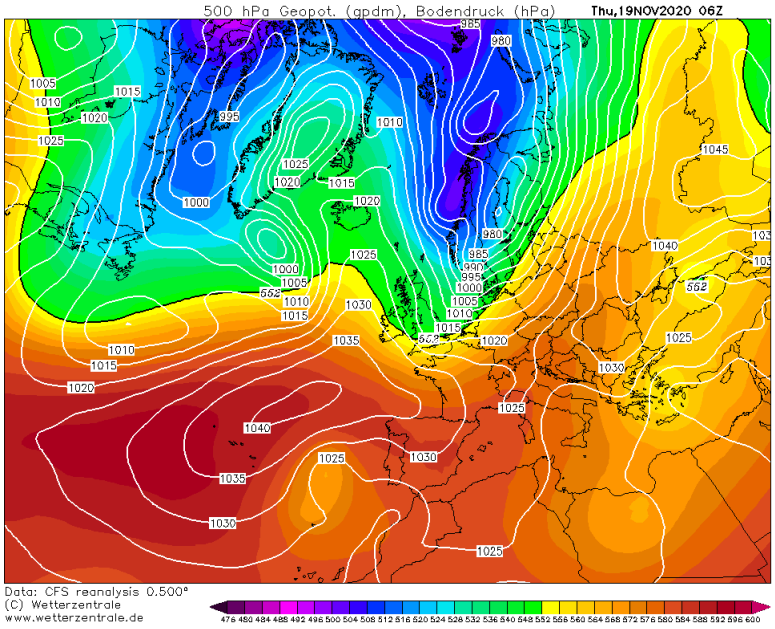

Figure 125: *The analysis from CFS (Climate Forecast System) showing surface pressure and 500 hPa geopotential. Figure is retrieved from Wetterzentale.*

The WRF 500 m x 500 m dataset and the Simra 100 m x 100 m datasets are both available for the event. Data is also available from the current model.

3.17.2 Model performance looking at the time series

The WRF-model did reasonably well in reproducing the wind direction the 19 November, see Fig. 126. Also the wind speed was good, but again the maximum at Trælbodneset was overestimated. Simra did well reproducing direction and wind speeds, except for the strongest peak at Kvitneset and Trælbodneset which was underestimated by Simra.

3.17.3 Simulated flow - horizontal structure

Looking at the plain view wind speed Figure 128 from WRF and Simra, we see that the northwesterly flow coming in Breisundet has little small scale details in the area where the buoys are. Enhanced winds are the shores in Sulafjorden is apparent in the models and in the observations. The additional small-scale details in Simra cannot be verified by the observation for this directions.

3.17.4 Simulated flow - vertical structure

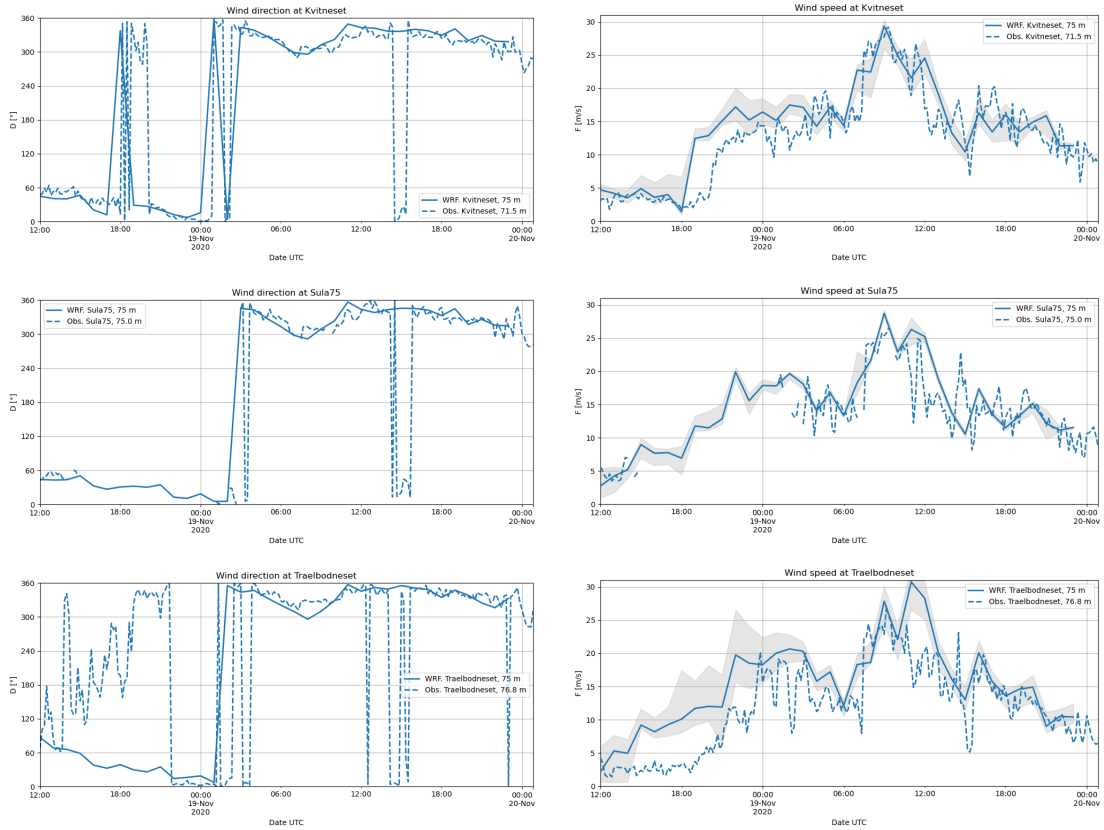

Figure 126: *Simulated (solid lines) and observed (dashed) wind direction (left) and wind speed (right) from the WRF-model. The grey envelope indicates the range of the simulated wind speed in the 9 nearest grid points (eq. 1 km x 1 km area).*

Sections across the fjord (129 strong wind across the fjord and from the sea surface and upwards in WRF, while in Simra the winds weaken towards Trælbodneset. The turbulence intensity from Simra is strongest in the wake behind Godøy and downstream of Kvitneset, as previously seen for northerly events (Figs. 130 and 131).

3.17.5 Currents

Model snapshots of surface currents from the storm show that the response of strong winds from the north-northwest are strong currents into Breisundet from the north and southward currents in Sulafjorden with sharp gradients and a complex current pattern related to wake effects of land (Figure 132). The maximum current speed is about 50cm/s in location A, but the periods with high velocities are short and variable due to the complex current pattern. The time series where observation and model data are compared show that the

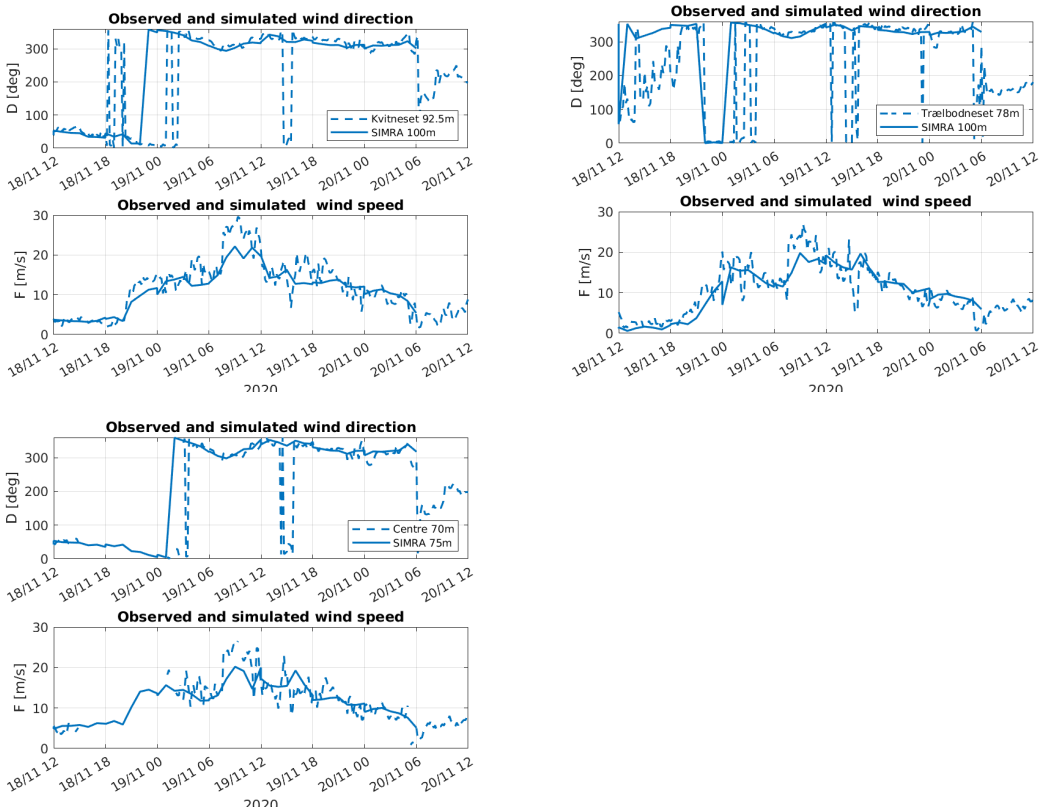

Figure 127: *Observed (dashed lines) and simulated (solid lines) wind direction and wind speed from 100 m in the Simra-model.*

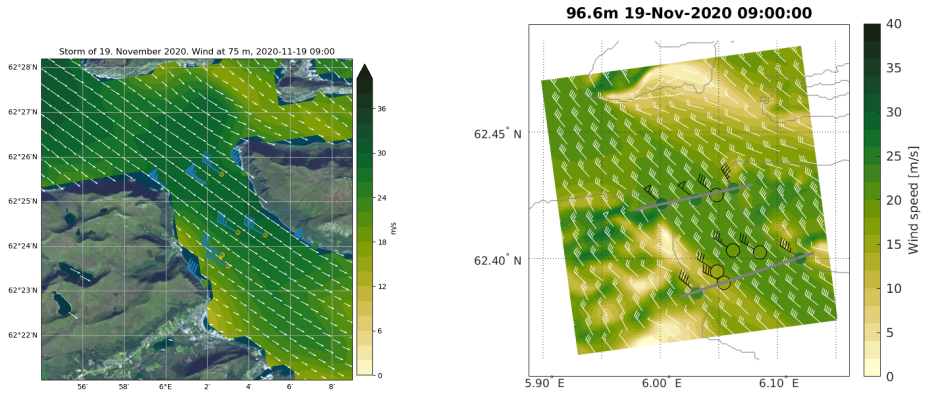

Figure 128: *Simulated wind from WRF at 75 m above sea level (left), and at 97 m from Simra (right), valid when the storm is strongest. Also shown are the observed wind and direction using traditional wind barbs and coloured circles based on the same colour map as the contour plot. Each flag is 5 m/s and a triangle is equivalent to 25 m/s. Buoy observations at 4 m are indicated with a black circle. The direction of the barbs shows the observed horizontal direction.*

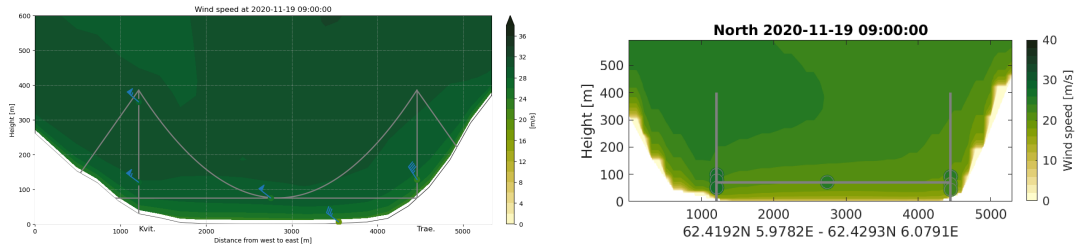

Figure 129: *Simulated wind from WRF at 75 m above sea level (left) and from Simra at 97 m (right) in a section along the planned crossing. Bridge location is indicated with grey lines. Also shown are the observed wind and direction using traditional wind barbs and coloured circles based on the same colour map as the contour plot. Each flag is 5 m/s and a triangle is equivalent to 25 m/s. Buoy observations at 4 m are shown with a black circle. The direction of the barbs shows the observed horizontal direction.*

current speed and direction correspond well most of the time during the main storm event.

Since the long-term average current direction in Sulafjorden is towards the north, the strong surface currents from the north alter the current pattern in the entire water column (Figure 133). Instead of a 10-15 m thick surface layer with a northward flow and south-

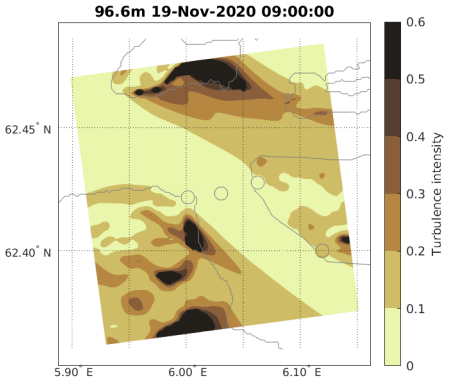

Figure 130: *Turbulence intensity from Simra at 97 m.*

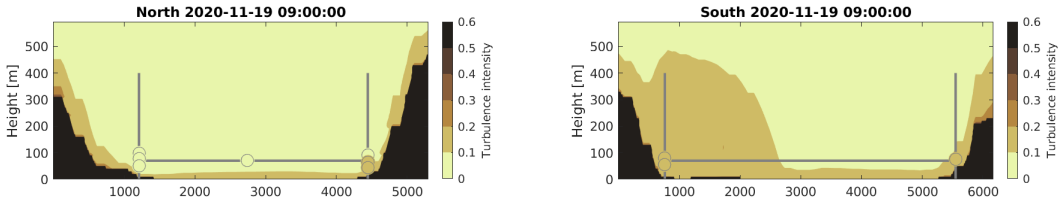

Figure 131: *Turbulence intensity from Simra at the northern (left) and southern crossing (right). Bridge tower and deck locations are indicated with grey lines.*

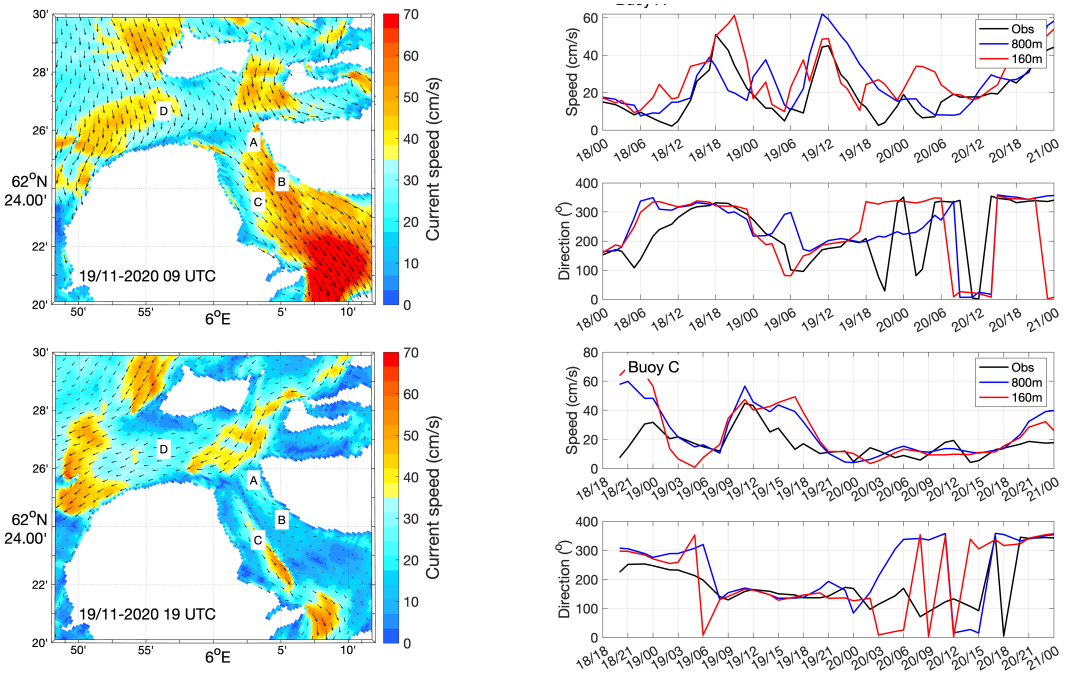

Figure 132: *The maps show instantaneous surface currents from the 160m-model valid at the times indicated in the map (left panels). The observational buoy locations A, B, C and D are denoted in the maps. The graphs to the right show current speed and direction at 1m depth from the two buoy locations A (upper two panels) and C (lower two panels) based on measurements (black line), NorKyst800 (blue) and 160m-model (red). The time stamps are written as day/hour.*

ward currents below down to approximately 100 m, the model sets up a southward flow in a thin surface layer down to about 10 m, northward currents below down to about 80 m and a southward flow below down to about 200 m. Note especially that the model suggests a southward flow of water in the centre of Sulafjorden with velocities up to 60 cm/s at 100-150 m depth.

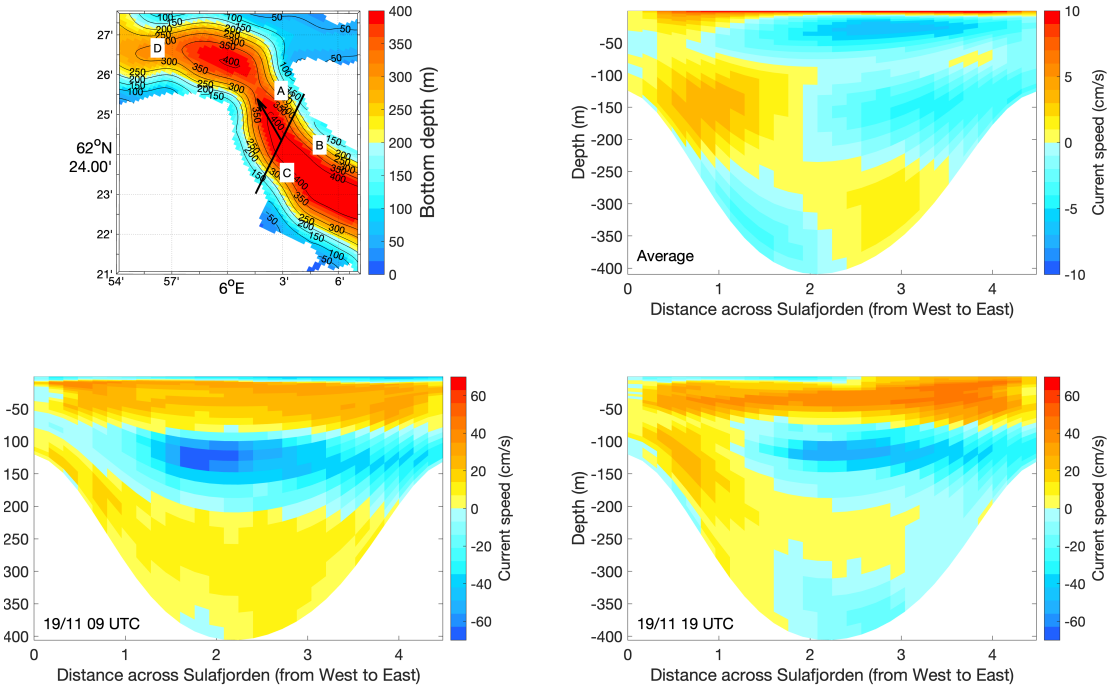

Figure 133: *The upper right panel is retrieved from Ágústsson et al. [2020a] and shows long-term average current speed normal to the transect crossing Sulafjorden denoted as a black line in the bathymetric map (upper left). The lower panels show two snapshots of current speed over the same transect. Red and yellow colors denote currents toward the north in the direction of the arrow in the map, while blue colors denote the opposite southerly currents.*

4 Summary and concluding remarks

Detailed and extensive observations of atmospheric flow, waves and currents in Sulafjorden, simulated waves and currents, as well as long series of high-resolution atmospheric simulations have been used to investigate the flow conditions during strong wind events in Sulafjorden.

A simple storm climatology based on correlated observed and modelled wind data indicates that most storms in Sulafjorden are either northerly or southerly. We have investigated a series of storms, both present in the observational dataset as well as several historic storms that hit the region, all of which in some way have had the potential of creating strong-wind events in Sulafjorden.

4.1 Common features in storms in Sulafjorden

If we use Vigra airport measurements which is a station representing this area well, we see that most storms in the region had maximum wind for a southwesterly direction, i.e. 200 – 240°. This indicates that the terrain along the coastline of Møre og Romsdal typically acts as a barrier for which a low-level barrier flow enhancement may occur along the coast. For these winds, Sulafjorden is mostly in the lee of the Hareid mountains. Small changes in the background flow seem to shift shallow wake zones (wind shadows generated by local terrain) along the shores in Sulafjorden. A complementary strong wind area is typically found on the opposite side of the fjord. With the right background direction, a small jet radiates out from just south of Langeneset and into the fjord centre. The jet is elevated; the surface flow is not accelerated while there is typically a core of stronger winds at some elevation below mountain top level.

For some cases where the wind at Vigra comes from the western sector, the low pressure system is typically in a late stage of the development cycle and a back-bent occluded front can be identified. This may lead to re-intensification of lows and sharp pressure gradients on the backside of the lows. Many of extreme events along the coast in this region have been of this type. However, they are generally not associated with wind extremes at low levels in Sulafjorden. Occasionally, cold air breakout can happen on the backside of a passing low. Embedded in this, polar lows may form in the cool arctic air flowing southward. In the analysis presented here, no polar low has impacted the area of interest. The strongest winds are, most likely, not associated with polar lows.

In northerly flows, observations and model results indicate that Godøy may create a wake downstream which, in some cases, extends as far as Trælbodneset at low levels. Wakes extending further or oriented more into the fjord centre could probably be formed during weaker winds and stronger stability. The wind in the wakes is weaker and more turbulent than the stronger flow at the wake boundaries. The vertical extension of the wake is unclear but model results indicate a considerable speed reduction in at least the lowest several hundred metres. For the northerly events, the wind is typically strongest at Kvitneset, however, small variations in wind direction can shift the wind speed maxima into the centre of the fjord and even closer to Trælbodneset. When the wind direction is close to northwesterly during storms there is typically strong wind through Breisundet and into the full width of Sulafjorden, as the wake is absent from the fjord in such directions. A large-scale deceleration due to the downstream topography may occur during northerly flow but appears not to be a particularly strong or frequent feature of the flow in the outer part of Sulafjorden during the storms studied. This is however difficult to quantify.

Looking at the atmospheric models performance, we see that the main features are well reproduced and the model synchronizes relatively well with the available observations during the events. The high-resolution (500 m x 500 m) mesoscale WRF-model obviously smooths the flow features in Sulafjorden due to the reduced terrain representation in the model. However, the wind speed strength and direction are surprisingly well reproduced. Abrupt changes in weather can sometimes be too smooth and short-lived disturbances may be missed. The very high-resolution CFD-model Simra does a good job reproducing features such as wakes and jets in Sulafjorden. It has an obvious problems with getting the correct wind speed strength and sometimes the wind direction is a bit off. This may be related to some tuning issues, problems with the representation of surface characteristics or inflow at the model boundaries. It can not be expected that the model correctly reproduces small scale terrain-induced features in the flow at all when the wind direction is not correct.

In the WRF-model, we see that Trælbodneset has larger variations in wind speed than for instance Kvitneset for southerly flows. This indicates that the area on the eastern and outer side of Sulafjorden has lesser terrain control on the flow. In the area from Langeneset to Kvitneset, the terrain steers the flow to a higher degree producing a more steady flow picture.

We have indicated that violent rotors set up by the mountains of Hareid may form in Sulafjorden in westerly flows. There are, however, no clear signal from the observations

that this is the case. There are observations of strong and turbulent winds at e.g. Kvitneset during westerly flow, but they have not been associated with particularly strong flow at the surface elsewhere in the fjord. On that basis, we conclude that such rotors is most likely not formed in this area. Very strong forward shear has been observed above the centre of the fjord during strong westerly synoptic flow, indicating the vertical extent of the terrain sheltering. It is presumably the relatively short horizontal distance across Sulafjorden, i.e. between the high mountains at Sula and Hareid, that hinders the full development of accelerated flow to descend all the way down to the surface. This is reminiscent of the results in Ágústsson and Ólafsson [2007], where in somewhat similar terrain an atmospheric wave aloft would no longer reach the surface of the earth when the downstream distance across a narrow fjord was reduced.

4.2 Wave and currents in Sulafjorden during storms

The waves in Sulafjorden during storm situations are strongly affected by the swell penetrating into the fjord through Breisundet. During northwesterly winds, Hs is further enhanced by the local wind from the same direction, while at southerly or southwesterly winds, opposing wind waves are building up in the fjord. Of the buoy locations in Sulafjorden (excluding D) the highest Hs is found in location A.

The wave model SWAN has been used to model the waves in Sulafjorden. The simulations are described and validated in Furevik and Aarnes [2021]. It was shown that SWAN models the waves well at location A where the maximum Hs is around 4 m from both the model and observations. Further into the fjord, the model typically overestimates Hs which may be caused by too strong wind input from the WRF-model during storm situations. It was also found that pure wave propagation without wind forcing is not able to reproduce the measured Hs and mean wave periods at any of the buoy locations.

The waves in Sulafjord during storm conditions are a combination of "swell" and local wind sea. The term "swell" is somewhat misleading as the oceanic waves propagating into the fjord are seldom independent swell arriving from a distant storm. Usually they are ocean waves penetrating into the fjord and their maximum is directly related to the general wind conditions in the area and thus correlated with the local wind sea in the fjord. The combined maximum in wind and waves is expected during northwesterly winds.

The average currents in Sulafjorden are characterised by a northward flow in a surface layer (10 - 15 m deep). Below, down to about 100 m, there is a south going flow in most of the fjord, but strongest in the eastern part. Between 100 - 250 m the flow is northward

along Hareid and weakly southward along Sula. This flow pattern changes significantly during storm conditions.

At the surface, the currents in storm situations are dominated by the wind and show strong gradients related to lee effects, wind enhancements, coastlines and bathymetry. Maximum current velocities reach typically 70 - 80 cm/s, but with high variability related to the sharp gradients in current speed. The vertical pattern is also altered during storm conditions with dominating inflow in the upper 100 m during northwesterly winds and outflow during southerly wind. After decrease of strong or northwesterly wind, the water masses that are pressed into the fjord system flows out with relatively high speed in an intermediate layer.

Model performance of the current model during storm events shows very good results. The ocean model used is not primarily designed for extreme events, and deviations that already exist in the atmosphere model will also be transferred to the ocean model. Our validation of currents during wind storm events indicates that extreme current analysis previously conducted with the same ocean model system are realistic.

References

H. Ágústsson. E39, Sulafjorden, Møre og Romsdal, Norway: Analysis of lidar derived wind measurements, September 2018 - March 2021. Technical Report KVT/2021/R093/HÁ Rev1, Kjeller Vindteknikk, 2021.

H. Ágústsson, J. Albretsen, S. Grini, and B. R. Broe. Sulafjorden, Vartdalsfjorden og Halsafjorden, Møre og Romsdal - Kart for ekstremstrøm og validering av modellert strøm. Technical Report KVT/HÁ/2019/R100, Kjeller Vindteknikk, 2019.

H. Ágústsson, A. S. Haslerud, and J. Albretsen. Ekstremverdier for modellert strøm i Sulafjorden, Møre og Romsdal - Transekter langs to mulige rørbrutraséer. Technical Report KVT/2020/R132/HÁ, Kjeller Vindteknikk, 2020a.

H. Ágústsson, A. S. Haslerud, and J. Albretsen. Langtidskorrigering av strøm i Sulafjorden og Halsafjorden - Ekstremstrømberegninger. Technical Report KVT/2020/R127/ASH, Kjeller Vindteknikk, 2020b.

H. Ágústsson and H. Ólafsson. Simulating a severe windstorm in complex terrain. *Met. Zeit.*, 16(1):111–122, 2007.

I. Barstad and S. Grønås. Southwesterly flows over southern norway—mesoscale sensitivity to large-scale wind direction and speed. *Tellus A: Dynamic Meteorology and Oceanography*, 57(2):136–152, 2005.

I. Barstad and S. Grønås. Dynamical structures for southwesterly airflow over southern norway: the role of dissipation. *Tellus A: Dynamic Meteorology and Oceanography*, 58(1):2–18, 2006.

L. Bengtsson, U. Andrae, T. Aspelien, Y. Batrak, J. Calvo, W. de Rooy, E. Gleeson, B. Hansen-Sass, M. Homleid, M. Hortal, K.-I. Ivarsson, G. Lenderink, S. Niemelä, K. P. Nielsen, J. Onvlee, L. Rontu, P. Samuelsson, D. S. Muñoz, A. Subias, S. Tijm, V. Toll, X. Yang, and M. Ødegaard Køltzow. The harmonie–arome model configuration in the aladin–hirlam nwp system. *Monthly Weather Review*, 145(5):1919 – 1935, 2017. doi: 10.1175/MWR-D-16-0417.1. URL `https://journals.ametsoc.org/view/journals/mwre/145/5/mwr-d-16-0417.1.xml`.

K. Christakos, G. Varlas, J. Reuder, P. Katsafados, and A. Papadopoulos. Analysis of a low-level coastal jet off the western coast of norway. *Energy Procedia*, 53:162–172, 2014. ISSN 1876-6102. doi: https://doi.org/10.1016/j.egypro.2014.07.225. URL https://www.sciencedirect.com/science/article/pii/S1876610214011023. EERA DeepWind' 2014, 11th Deep Sea Offshore Wind R&D Conference.

K. Christakos, B. R. Furevik, O. J. Aarnes, Ø. Breivik, L. Tuomi, and Ø. Byrkjedal. The importance of wind forcing in fjord wave modelling. *Ocean Dynamics*, 70:57–75, 2020. doi: 10.1007/s10236-019-01323-w.

J. D. Doyle, V. Grubišić, W. O. Brown, S. F. De Wekker, A. Dörnbrack, Q. Jiang, S. D. Mayor, and M. Weissmann. Observations and numerical simulations of subrotor vortices during t-rex. *Journal of the atmospheric sciences*, 66(5):1229–1249, 2009.

B. R. Furevik and O. J. Aarnes. Wave conditions in Sulafjorden, Vartdalsfjorden, Halsafjorden and Julsundet - Fjordcrossing E39. Technical Report 3, Norwegian Meteorological Institute, Oslo (Norway), 2021.

B. R. Furevik, H. Ágústsson, A. L. Borg, Z. Midjiyawa, F. Nyhammer, and M. Gausen. Meteorological observations in tall masts for the mapping of atmospheric flow in norwegian fjords. *Earth System Science Data*, 12(4):3621–3640, 2020. doi: 10.5194/essd-12-3621-2020. URL https://essd.copernicus.org/articles/12/3621/2020/.

S. Grønås. The seclusion intensification of the new year's storm 1992. *Tellus A*, 47A: 733–746, 1995.

H. Haakenstad, Ø. Breivik, B. R. Furevik, M. Reistad, P. Bohlinger, and O. J. Aarnes. Nora3: A nonhydrostatic high-resolution hindcast of the north sea, the Norwegian sea, and the barents sea. *Journal of Applied Meteorology and Climatology*, 60(10), 2021. ISSN 15588432. doi: 10.1175/JAMC-D-21-0029.1.

K. Harstveit. Sulafjorden og vartdalsfjorden, møre og romsdal: Analyse av modellert vind, strøm og bølger for 2007 - 2017. Kvt/2018/r105/kh, Kjeller Vindteknikk, 2018.

A. S. Haslerud. Analysis of wind measurements form 6 masts at sulafjorden, 24.11.2016 - 31.03.2021. Technical Report KVT/2021/R063/ASH, Kjeller Vindteknikk, 2021.

K. H. Midtbø, B. Furevik, and L. Østvand. Finskala modellering av vind i fjorder. sulafjorden og vartdalsfjorden 2018. Technical report, METreport - Research report 05/2020, 2020a. URL https://www.met.no/publikasjoner/met-report/.

K. H. Midtbø, B. Furevik, and L. Østvand. Finskala modellering av vind i fjorder. halsafjorden 2018. Technical report, METreport - Research report 10/2020, 2020b. URL https://www.met.no/publikasjoner/met-report/.

J. E. Overland and N. A. Bond. Observations and scale analysis of coastal wind jets. *Monthly Weather Review*, 123(10):2934–2941, 1995.

M. Reistad, O. Breivik, H. Haakenstad, O. J. Aarnes, and B. R. Furevik. A high-resolution hindcast of wind and waves for The North Sea, The Norwegian Sea and The Barents Sea. *Journal of Geophysical Research, Oceans.*, 116, 2011. doi: 10.1029/2010JC006402. C05019.